



Thesis for the degree of Licentiate of Technology, Sundsvall 2008

## **BONDING ABILITY DISTRIBUTION OF FIBERS IN MECHANICAL PULP FURNISHES**

**Sofia Reyier**

Supervisors:  
Professor Hans Höglund  
Professor Per Engstrand  
M.Sc. Olof Ferritsius

FSCN - Fibre Science and Communication Network  
Department of Natural Science  
Mid Sweden University, SE-851 70 Sundsvall, Sweden

ISSN 1652-8948  
Mid Sweden University Licentiate Thesis 31  
ISBN 978-91-85317-90-5



Akademisk avhandling som med tillstånd av Mittuniversitetet i Sundsvall framläggs till offentlig granskning för avläggande av teknologie licentiatexamen i kemiteknik med inriktning mot mekanisk fiberteknologi, onsdagen den 18 juni, 2008, klockan 10.00 i sal "Granen" på Stora Enso Kvarnsvedens Pappersbruk, Borlänge. Seminariet kommer att hållas på svenska.

Ett förseminarium hålls fredagen den 9 maj klockan 10.30, sal N109 på Mittuniversitetet i Sundsvall.

## **BONDING ABILITY DISTRIBUTION OF FIBERS IN MECHANICAL PULP FURNISHES**

**Sofia Reyier**

© Sofia Reyier, 2008

The figure on the cover page shows the BIN-distributions (Bonding Indicator) for fibers of three different mechanical pulps, of fiber length 0.7-2.3 mm, predicted from optical measurement raw data on whole pulps.

FSCN - Fibre Science and Communication Network  
Department of Natural Sciences  
Mid Sweden University, SE-851 70 Sundsvall, Sweden  
Telephone: +46 (0)771-975 000

Printed by Kopieringen Mittuniversitetet, Sundsvall, Sweden, 2008

# **BONDING ABILITY DISTRIBUTION OF FIBERS IN MECHANICAL PULP FURNISHES**

**Sofia Reyier**

FSCN - Fibre Science and Communication Network, Department of Natural Sciences, Mid Sweden University, SE-851 70 Sundsvall, Sweden  
ISSN 1652-8948, Mid Sweden University Licentiate Thesis 31; ISBN 978-91-85317-90-5

## **ABSTRACT**

This thesis presents a method of measuring the distribution of fiber bonding ability in mechanical pulp furnishes. The method is intended for industrial use, where today only average values are used to describe fiber bonding ability, despite the differences in morphology of the fibers entering the mill. Fiber bonding ability in this paper refers to the mechanical fiber's flexibility and ability to form large contact areas to other fibers, characteristics required for good paper surfaces and strength.

Five mechanical pulps (Pulps A-E), all produced in different processes from Norway spruce (*Picea Abies*) were fractionated in hydrocyclones with respect to the fiber bonding ability. Five streams were formed from the hydrocyclone fractionation, Streams 1-5. Each stream plus the feed (Stream 0) was fractionated according to fiber length in a Bauer McNett classifier to compare the fibers at equal fiber lengths (Bauer McNett screens 16, 30, 50, and 100 mesh were used).

Stream 1 was found to have the highest fiber bonding ability, evaluated as tensile strength and apparent density of long fiber laboratory sheets. External fibrillation and collapse resistance index measured in FiberLab™, an optical measurement device, also showed this result. Stream 5 was found to have the lowest fiber bonding ability, with a consecutively falling scale between Stream 1 and Stream 5. The results from acoustic emission measurements and cross-sectional scanning electron microscopy analysis concluded the same pattern. The amount of fibers in each hydrocyclone stream was also regarded as a measure of the fibers' bonding ability in each pulp.

The equation for predicted Bonding Indicator (BIN) was calculated by combining, through linear regression, the collapse resistance index and external fibrillation of

the P16/R30 fractions for Pulps A and B. Predicted Bonding Indicator was found to correlate well with measured tensile strength. The BIN-equation was then applied also to the data for Pulps C-E, P16/R30, and Pulp A-E, P30/R50, and predicted Bonding Indicator showed good correlations with tensile strength also for these fibers.

From the fiber raw data measured by the FiberLab™ instrument, the BIN-equation was used for each individual fiber. This made it possible to calculate a BIN-distribution of the fibers, that is, a distribution of fiber bonding ability.

The thesis also shows how the BIN-distributions of fibers can be derived from FiberLab™ measurements of the entire pulp without mechanically separating the fibers by length first, for example in a Bauer McNett classifier. This is of great importance, as the method is intended for industrial use, and possibly as an online-method. Hopefully, the BIN-method will become a useful tool for process evaluations and optimizations in the future.

**Keywords:** Fiber, mechanical pulp, bonding ability, fiber characterization, Bonding Indicator, BIN, acoustic emission, hydrocyclone, Fiberlab, collapse resistance, fibrillation

## SAMMANDRAG

Den här studien presenterar en metod för att mäta fördelning av fiberbindning i mekaniska massor. Metoden hoppas kunna användas industriellt, där i dagsläget enbart medelvärden används för att mäta fiberbindnings-fördelning, trots råvarans (fibrernas) morfologiska skillnader.

Fem mekaniska massor (Massa A-E) från olika massaprocesser men från samma råvara, norsk gran (*Picea Abies*), har fraktionerats i hydrocykloner med avseende på fiberbindningsförmåga. Från hydrocyklon-fraktioneringen bildades fem strömmar, Ström 1-5. Varje ström plus injektet (Ström 0) fraktionerades också med avseende på fiberlängd i en Bauer McNett för att kunna jämföra fibrerna vid samma fiberlängd (Bauer McNett silplåtarna 16, 30, 50 och 100 mesh användes).

Fiberbindningsförmåga i den här studien härrör till fiberns flexibilitet och förmåga att skapa stora kontaktytor med andra fibrer, vilket bidrar till papprets yt- och styrkeegenskaper.

Ström 1 visade sig ha den högsta fiberbindningsförmågan, utvärderat som dragstyrka och densitet av långfiberark, samt yttre fibrillering och kollaps resistans index mätt i den optiska analysatorn FiberLab™. Akustisk emission och tvärsnittsanalyser visade samma resultat. Ström 5 visade sig ha den lägsta fiberbindningsförmågan, med en avtagande skala från Ström 1 till Ström 5. Andelen fibrer från injektet som gick ut med varje hydrocyklon-ström ansågs också vara ett mått på fibrernas bindningsförmåga i varje massa.

Genom att kombinera fiberegenskaperna kollaps resistans och yttre fibrillering från den optiska mätningen på varje fiber genom linjär regression, kunde Bindnings Indikator (BIN) predikteras. Medelvärdet av Bindnings Indikator för varje hydrocyklon-ström korrelerar med dragstyrka för långfiber-labark.

Det visade sig att predikterad Bindnings Indikator inte bara fungerade för Massa A och Massa B P16/R30 fraktionen, som var de fraktioner som användes i den linjära regressionen, utan även för Massa C-E, P16/R30, och Massa A-E P30/R50 som också visade goda korrelationer med långfiber-dragstyrka när de sattes in i BIN-formeln.

BIN-formeln användes sedan för varje enskild fiber, i den rådata som levererats från FiberLab™. Detta gjorde det möjligt att få en BIN-distribution av fibrerna, d.v.s. en fördelning av fiberbindningsförmåga.

Den här rapporten visar också hur det går att få BIN-distributioner också från mätningar på hela massan, för valbara fiberlängder, utan att först mekaniskt separera massan efter fiberlängd. Det är viktigt, då metoden är tänkt att användas som en industriell metod, och eventuellt som en online-metod. Förhoppningsvis kommer BIN-metoden att bli ett användbart verktyg för processutveckling- och optimering i framtiden.

**Nyckelord:** Fiber, mekanisk massa, bindningsförmåga, fiber karakterisering, Bindnings Indikator, BIN, akustisk emission, hydrocyklon, Fiberlab, kollaps resistans, fibrillering

## TABLE OF CONTENTS

ABSTRACT .....	ii
SAMMANDRAG .....	iv
LIST OF PAPERS .....	viii
PREFACE .....	xii
1. INTRODUCTION .....	1
2. BACKGROUND .....	5
2.1 FIBERS.....	5
2.1.1 <i>Fiber morphology and geometry</i> .....	5
2.1.2 <i>Fiber chemistry</i> .....	8
2.2 FIBER BONDING .....	11
2.2.1 <i>The notation fiber bonding</i> .....	11
2.2.2 <i>Fines</i> .....	12
2.3 THE MECHANICAL AND CHEMIMECHANICAL PROCESSES .....	13
2.3.1. <i>Groundwood pulp (GW)</i> .....	13
2.3.2 <i>Thermomechanical pulp (TMP)</i> .....	14
2.3.3 <i>Chemithermomechanical pulp (CTMP)</i> .....	16
2.4 FIBER QUALITY .....	18
2.4.1 <i>Measuring fiber quality today</i> .....	18
2.4.2 <i>Fibers in printing paper</i> .....	19
2.4.3 <i>Distribution of fiber bonding ability</i> .....	22
3. MATERIALS AND METHODS .....	25
3.1 HYDROCYCLONE FRACTIONATION .....	25
3.2 BAUER MCNETT FRACTIONATION.....	27
3.3 PHYSICAL PROPERTIES OF LABORATORY SHEETS.....	29
3.4 FIBER GEOMETRY BY CROSS-SECTIONAL SEM-MICROGRAPHS.....	30
3.5 ACOUSTIC EMISSION.....	31
3.6 MEASUREMENT OF FIBER PROPERTIES IN FIBERLAB <sup>TM</sup> .....	32
3.7 BONDING INDICATOR - BIN .....	34
4. RESULTS AND DISCUSSION .....	35
4.1 HYDROCYCLONE FRACTIONATION – WEIGHT PERCENT PER STREAM .....	35
4.2 FRACTIONATION BY FIBER LENGTH IN THE BAUER MCNETT CLASSIFIER .....	37

4.3 PHYSICAL PROPERTIES OF LABORATORY SHEETS.....	40
4.4 FIBER GEOMETRY BY CROSS-SECTIONAL SEM-MICROGRAPHS.....	43
4.5 ACOUSTIC EMISSION.....	45
4.6 MEASUREMENT OF FIBER PROPERTIES IN FIBERLAB™.....	48
4.6.1 External fibrillation.....	48
4.6.2 Fiber wall thickness .....	49
4.6.3 Fiber width.....	51
4.6.4 Collapse resistance index (CRI).....	52
4.7 BONDING INDICATOR – BIN.....	53
4.7.1 Prediction of average Bonding Indicator.....	53
4.7.2 Distributions of Bonding Indicator .....	55
4.7.4 Identifying all fibers in the BIN-distributions.....	58
4.7.5 BIN-distributions for fibers – without fiber length fractionation .....	59
<b>5. FINAL DISCUSSION.....</b>	<b>63</b>
<b>6. CONCLUSIONS.....</b>	<b>65</b>
<b>7. FUTURE WORK.....</b>	<b>65</b>
<b>8. ACKNOWLEDGEMENTS .....</b>	<b>67</b>
<b>9. REFERENCES .....</b>	<b>71</b>
<b>APPENDIX .....</b>	<b>75</b>
APPENDIX 1. PHYSICAL PARAMETERS OF LONG FIBER LABORATORY SHEETS.....	75
APPENDIX 2. DISTRIBUTIONS OF FIBER PROPERTIES FROM FIBERLAB™ .....	79
APPENDIX 3. BIN-DISTRIBUTIONS (BONDING INDICATOR) .....	82
BIN-distributions from whole pulps for fiber length intervals .....	83
Average BIN for fiber length intervals .....	85
Amount negative BIN-fibers (low bonding fibers) for fiber length intervals.....	85
APPENDIX 4. SEM-IMAGES .....	87
Cross-sectional micrographs from fiberlength fraction P16/R30.....	87
Long fiber laboratory sheets, fiberlength fraction P16/R30. ....	88

## LIST OF PAPERS

This thesis is mainly based on the following two papers, herein referred to by their Roman numerals:

- |          |   |
|----------|---|
| Paper I  | <b>Ways to measure the bonding ability distribution of fibers in mechanical pulps</b><br>Reyier, S., Ferritsius, O., Shagaev, O.<br>Manuscript, accepted for publication in TAPPI Journal (2008)                              |
| Paper II | <b>BIN – a method of measuring the distribution of Bonding Indicator of fibers in mechanical pulp furnishes</b><br>Reyier, S., Ferritsius, O.<br>Manuscript, to be submitted to Nordic Pulp and Paper Research Journal (2008) |

## AUTHOR'S CONTRIBUTION TO THE REPORTS

The author's contributions to the papers in the thesis are as follows:

- |          |  |
|----------|--|
| Paper I  | Experimental work, interpretation of results together with Olof Ferritsius; paper written together with Olof Ferritsius and Oleg Shagaev. Results regarding acoustic emission measurements were interpreted together with professor Per Gradin, Mid Sweden University, and Anders Hansson, Stora Enso Research Centre Falun. |
| Paper II | Experimental work, interpretation of results together with Olof Ferritsius; paper written together with Olof Ferritsius.   |

## **RELATED MATERIAL**

Results related to this work have been published or presented at international conferences as follows:

### **Ways to measure the bonding ability distribution of fibers in mechanical pulps**

Reyier, S., Ferritsius, O., Shagaev, O.

Proceedings of International Mechanical Pulping Conference, Minneapolis, USA, May 6-9, 2007, CD-ROM

### **Some aspects of fiber bonding ability in mechanical pulps**

Reyier, S., Ferritsius, O., Shagaev, O.

Presented at PIRA International Refining & Mechanical Pulping Conference, Arlanda, Sweden, December 12-13, 2007, CD-ROM

### **BIN - A method to measure the distribution of fiber bonding ability in mechanical pulps**

Reyier, S., Ferritsius, O.

Presented and extended abstract, 6th Fundamental Pulp Research Seminar, Espoo, Finland, May 21-22, 2008

“En droppe droppad i livets älv har ingen kraft till att flyta själv  
Det ställs ett krav på varenda droppe, hjälp till att hålla de andra oppe”

(Tage Danielsson, Swedish writer 1928-1985 “Organisations-söndagen”, Tage Danielssons postilla, 1965)

Swedish poem that to some extent mirrors how each individual fiber contributes to paper quality, the general hypothesis of this study.



## PREFACE

If it wasn't love at first sight, it was at least total fascination at first sight.

I saw my first paper machine in Sundsvall, Sweden, in 2001, during a visit to a nearby mill during my first year of the master's program. I remember staring at paper rolling onto the tambour, with my mouth partly open and my eyes as big as tennis balls, not believing what I saw. How could the wood logs we just saw entering the mill now have transformed into a broad web of white, thin paper, traveling at an incredible speed without breaking? Looking next to me at my friend Ylva, I met the same tennis ball sized eyes and staring look.

Not being able to forget the sight of the paper sweeping by, I did some Google-research and soon realized that the thing holding the paper together was wood fibers. This was amazing in itself but my amazement only grew when I also learned how the fibers were singled out one by one from wood chips, only by feeding the chips into a refiner, basically two large rotating steel plates. Was this really possible? Now I know that it is possible. I have also learnt that refiners are incredibly advanced systems that we know very little about but that the refiners still - in some miraculous way combined with extensive mill-personnel experience - actually treat the fibers more or less to the quality we desire.

I have finally realized that I am doomed to a lifelong fascination with the pulp and paper process in general and with fibers in particular. The more I learn about the process, the less I realize I know and the more I want to know. The mechanisms of fiber bonding ability is one area I have had the privilege to dig deeper into. The first year student's vivid curiosity about the fundamental fiber properties that hold paper together is still very much alive.



## 1. INTRODUCTION

In a global perspective, the Swedish pulp and paper industry is a large net exporter of both pulp and paper. The export of pulp and paper alone amounts to 72.2 Gkr a year (about 7 GEuro). The pulp and paper industry in Sweden alone employs directly about 27,500 people and indirectly about the double that number (source: Swedish Bureau of Statistics, 2007).

A large proportion, about 30%, of all pulp produced are mechanical or chemimechanical pulps (source: [www.skogsindustrierna.nu](http://www.skogsindustrierna.nu)). Mechanical pulps are mainly used for printing papers such as newsprint and magazine paper grades. High yield, high opacity, low production costs, and high bulk are some of the advantages compared to chemical pulps. The electric energy consumption is the main disadvantage. As the asset to raw material might become an issue in the future, the use of about 97% of the tree in mechanical pulping (compared to about 50 % in chemical pulping) is also of importance.

In the northern hemisphere, coniferous tree fibers entering the mill for mechanical pulp production are inhomogeneous. Fibers that have grown in spring have different properties than fibers that have grown in summer, for example in diameter and fiber wall thickness. These fibers will give in different surface and strength properties in the printing paper.

Homogeneous paper quality is vital to the end user, *i.e.* the printing houses. Surface properties, paper strength, and paper structure must be the same for printing to be optimal. One important factor for both paper surface and runnability is the fiber bonding ability. Despite the inhomogeneous raw material (wood fibers of different density) and the knowledge of the importance of how the fibers' bonding ability influences printing paper quality, currently fiber bonding is measured only as average values, *e.g.*, average values of tensile strength, density, or porosity of sheets from the entire pulp.

This study aims to develop a method of measuring the distribution of fiber bonding ability in mechanical pulp furnishes and it is hoped that this method will mirror the produced paper's surface and runnability properties. The study has been carried out from an industrial perspective. Fiber bonding ability is defined here as the fibers' ability to form a paper structure with a high strength and good surfaces. In the future the method will also hopefully be used in online measurement applications.

A method to measure the distribution of fiber bonding ability could be used for process evaluation and as a tool for process optimization. The degree of fiber treatment should be neither higher nor lower than the desired level when the fiber leaves the pulping process. Fibers with too low a treatment are disadvantageous to the surface and paper furnish. Fibers of too high a treatment may result in unnecessary strong paper which is unfavourable for both energy efficiency and economy.

This study is based on trials performed on pilot plant scale with samples from different grades of mechanical pulps. The mechanical pulps were fractionated with respect to fiber bonding ability into five parts, in respect of fiber bonding ability. Each of the five parts was then fractionated into three new parts each, in respect of fiber length, using a Bauer McNett classifier. These fifteen parts were further separated into 30,000 parts each, every part being one fiber, using a FiberLab™ optical analyzer. The fibers were analyzed one by one in the optical analyzer.

The working hypothesis of this study is that an average value of the entire pulp might not tell the whole truth about the pulp's fiber quality. It is therefore believed that more fundamental fiber properties are needed to fully characterize the mechanical pulp.

## **1.1 Objective**

Some years ago, Stora Enso employee Luigi Alfonsetti asked the question "How many of our fibers have too low bonding?" The aim of this entire study has been to develop a method to later on be able to answer Luigi's relevant question, that is, to develop a method that can be used for measuring the distribution of fiber bonding ability in mechanical pulp furnishes.

As the method is hoped to be implemented for industrial use, fiber bonding ability is characterized with respect to surface and strength properties. The fibers entering the mill have inhomogeneous properties that are today only measured as average values. As fibers themselves seldom are the weakest link in the paper, but rather the interactions between the fibers, it is assumed that high fiber bonding ability is advantageous for surface, structure, and runnability properties.

Hopefully, the proposed method presented in this thesis will be able to predict the fiber bonding ability in mechanical pulps without the making and evaluation of laboratory sheets, as is the case today.

## 1.2 Contents description

Below is given a short description of the contents of this thesis:

Section 2 presents a background to the research presented in this thesis. Some of the more general reasons are given as to why fiber properties, even within the same tree, are inhomogeneous (Section 2.1). Fiber bonding, which is a concept yet to be completely defined, is discussed and fiber bonding ability as referred to in this thesis is defined (Section 2.2). The three main processes for producing high-yield pulp are briefly described (Section 2.3) and some aspects of fiber quality and how it is measured today are discussed (Section 2.4).

Section 3 presents and discusses the equipment and methods used in this study. Hydrocyclones were used to fractionate the mechanical fibers with respect to mainly specific surface area and fiber wall density (Section 3.1). Fiber length fractionation in the Bauer McNett classifier is also discussed (Section 3.2) as well as the production and testing of long fiber laboratory sheets (Section 3.3). Scanning electron microscopy (SEM) micrographs were used to measure fiber geometry and the results were compared with the results obtained by optical measurements (Section 3.4). Acoustic emission (Section 3.5) was used to further evaluate the mechanisms of fiber bonding ability during tensile testing. Optical measurements to determine the geometry (*e.g.* fiber width, fiber wall thickness, external fibrillation) of each individual fiber were performed in FiberLab™ (Section 3.6). Based on the optical measurements, a definition of Bonding Indicator, BIN is presented and discussed (Section 3.7).

Section 4 presents the results of the study in which five different mechanical pulps were evaluated. The way the fibers fractionated in the hydrocyclones (Section 4.1) gives an indirect measure of the fiber bonding ability of the different pulp furnishes. The results of the Bauer McNett fractionation (Section 4.2) are then discussed, as are results from the testing of tensile strength and apparent density of long fiber laboratory sheets (Section 4.3). Some of the fiber properties that were measured in the cross-sectional SEM micrographs are evaluated (Section 4.4) after which differences in fiber bonding mechanisms during strain are evaluated from acoustic emission measurements (Section 4.5). The results of individual fiber properties, including external fibrillation, fiber wall thickness, and fiber width from FiberLab™ measurements are presented and discussed (Section 4.6). Finally in this section Bonding Indicator, BIN, is defined as a measure of the fiber's bonding ability in a sheet structure (Section 4.7) and it is shown that BIN-distributions can be used to describe the distribution of fiber bonding ability in mechanical pulp furnishes. It is further emphasized that neither the bonding ability

of fines nor the chemical interactions as such are evaluated in this study and that only pure mechanical pulp furnishes was examined.

Section 5 contains a lengthy final discussion combining the results of the previous section.

Section 6 gives a brief summary of the conclusions of the research described in this thesis.

Section 7 is a short list of some of the activities included in future work.

An appendix containing additional figures of interest for the study is also included to the thesis.

## 2. BACKGROUND

*As wood fibers are the main raw material in most modern pulp and paper processes, a deepened knowledge of their properties can only improve quality and cost-efficient pulping. This background section gives a general background to fibers in the pulp and paper process.*

*As the study has been performed on mechanical pulps from Norway spruce from northern growing conditions only, the focus is on softwoods and mechanical and chemimechanical pulping.*

### 2.1 Fibers

All trees, and also non-wood such as grasses, consist of fibers that provide for both stability and the transport of water and nutrition.

#### 2.1.1 Fiber morphology and geometry

Two main fiber groups, hardwood and softwood can be distinguished, where hardwood generally speaking is from deciduous trees and softwood from conifers. As the name suggests, hardwoods generally have a higher density than softwoods. The fibers of softwoods are biologically named tracheids (libri-form fibers for hardwoods). The common name however is fibers, which is also the term used in this thesis for the softwood tracheids.

A typical native spruce fiber is cylinder-shaped, 1.1-6.0 mm long and 21-40 micrometers wide (Tables 1a and 1b). In this specific study, Norway spruce, *Picea Abies*, has been used exclusively as the raw material. Tables 1a and 1b show averages and ranges of fiber length and width for some wood species. [24, 25].

Table 1a. Length and width of typical softwood tracheids [24].

Wood species	Tracheid length(mm)		Tracheid width (μm)	
	Mean	Range	Mean	Range
<i>Picea Abies</i> (Norway spruce)	3.4	1.1-6.0	31	21-40
<i>Pinus sylvestris</i> (Scots pine)	3.1	1.8-4.5	35	14-46
<i>Sequoia sempervirens</i> (Californian redwood)	7.0	2.9-9.3	50-65	

Table 1b. Length and width of some typical Swedish hardwood libriform fibers. Modified from [25].

Wood species	Fiber length (mm)		Fiber width ( $\mu\text{m}$ )	
	Mean	Range	Mean	Range
<i>Betula verrucosa</i> (Syn. <i>Betula Pendula</i> ) (European white birch)	1.3	0.8-1.8	25	18-36
<i>Fagus sylvatica</i> (European beech)	1.2	0.5-1.7	21	14-30
<i>Fraxinus excelsior</i> (European ash)	0.9	0.4-1.5	22	12-32

The more or less cylinder-shaped softwood fiber consists of a cell wall around an inner space called the lumen, used for water and nutrition transport. The fiber cell wall consists of not only one but several layers with different chemical compositions and fibril angles for maximal strength.

In the wood, the fibers lie embedded in parallel in the middle lamella (ML) which functions as a kind of glue between the fibers (Figure 1). The fiber wall consists of the primary wall (P) and the secondary wall (S). The secondary wall in turn consists of three different layers, the S1, S2, and S3 walls, where the S2 wall is by far the thickest, about ten times thicker than the S1 and S3 wall (Figure 1).

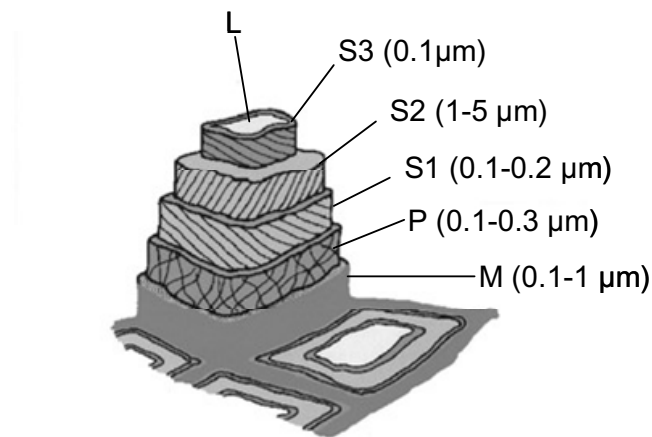


Figure 1. Softwood tracheid showing the different layers of the fiber wall and the middle lamella that keep the fibers together in the wood [19].

Even within the same wood species, the fibers differ in morphology, geometry, and chemical composition. The largest variation is that between early- and latewood,

fibers that have grown in spring and summer, respectively. For example, average fiber wall thickness in earlywood fibers is  $2.3\ \mu\text{m}$  and  $4.5\ \mu\text{m}$  in latewood fibers [16].

The earlywood fibers start growing when the length of daylight increases, to meet the tree's demand for water and nutrition. These fibers are therefore large in diameter, have a large lumen (the inner space in the middle of the fiber), and thin fiber walls. During summer, growth rate decreases and the fibers' most important task is to reinforce the wood. These latewood fibers will have a smaller diameter, thicker walls, and smaller lumens and can be seen in the wood as dark areas in annual rings, for example in a stump. Naturally, the early- and latewood fibers behave differently in the pulp and paper processes. A cross-section image of fibers in wood is shown in Figure 2 below [20] and shows the differences in geometry of early- and latewood.

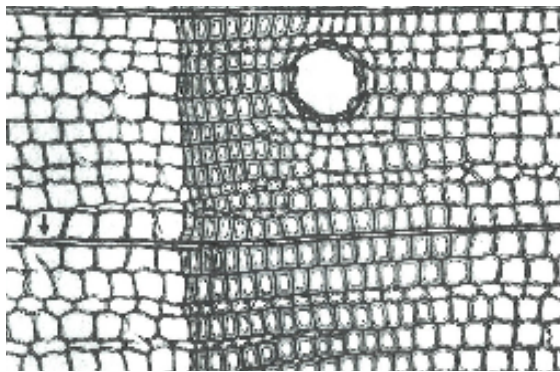


Figure 2. Cross-section of softwood from Ilvessalo-Pfäffli [20]. The earlywood fibers to the left in the figure have a large lumen and thin fiber walls, the latewood fibers in the middle have small lumens, are smaller in diameter and have thicker fiber walls.

Other differences in fiber geometry and chemistry come from growth conditions, the latitude of the growing area, the growth rate and age of the tree, the tree's surroundings, access to water and nutrition, access to sunlight, angle of ground where the tree is growing etc. To keep the tree upright, fibers in a tree growing in a slope adapt by changing its shape and chemical composition. In softwoods, this is done by the creation of compression wood that contains almost circular fibers with a higher amount of lignin [27]. The fibers in a tree, even in the same tree, also differ both in chemical composition and geometry, depending on where in the tree they are found [24]. Fibers from the "living" part of the tree, the sapwood, will provide higher strength papers than the "dead" part of the tree, the heartwood in the middle of the tree.

The tangential cut of the spruce tree below (Figure 3) shows that the tree has grown both on a slope and close to another tree, making the log shape non-circular, probably due to both reaction wood and a lack of sun from one side. The annual rings, the latewood fibers, are also visible.

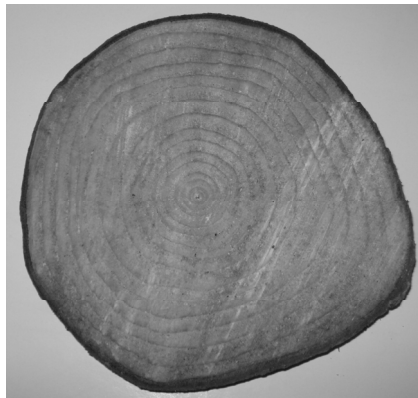


Figure 3. Tangential cut of Norway spruce stem. The latewood fibers with a smaller diameter and a thicker fiber wall than the earlywood fibers are the cause of the annual rings that can be seen. The asymmetry is probably caused both by reaction wood and the blockage of sun from one side. *Planted by Henrik Reyier 1986, harvested by Anders Reyier 2006.*

To be able to make paper, the fibers in the tree need to be separated from each other without too much fiber breakage (fiber breakage causes strength reduction in the paper). This can either be done chemically, by dissolving the middle lamella until the fibers separate, or mechanically, by exposing the wood to repeated impulses in a refiner or a grinder, until the middle lamella releases the fibers. In the mechanical pulping processes, steam is also used to preheat and soften the wood and middle lamella, to facilitate the separation of the fibers.

In this thesis, only fibers from mechanical and chemimechanical pulping has been studied. The long, slender fibers of Norwegian spruce growing in the northern hemisphere are specifically suited to producing high-quality printing paper, for example magazine paper grades. However, there will always be differences in raw material and therefore the produced pulp will always consist of fibers of different quality. The aim of this study is to develop a method to measure differences in fiber quality in the pulp.

### **2.1.2 Fiber chemistry**

Not only the appearance of the leaves, the barks, and the fiber geometry (Tables 1a and 1b) differs between different trees species – the chemical composition also

differs. Wood fibers consist mainly of cellulose, hemicellulose, lignin, and extractives that have different compositions depending on the species the wood has come from. To provide a general background to this study which only covers Norway spruce, a short, very general overview of the chemical composition of some of the components is given below.

Figure 4 from [22] below shows the distribution of cellulose, hemicellulose, and lignin in a softwood fiber. It can be seen how the highest amount of lignin can be found in the middle lamella and the lowest in the S3 wall. When producing mechanical pulp, almost all components in the native fiber are maintained in the pulp, as compared to chemical pulp where almost all lignin is removed.

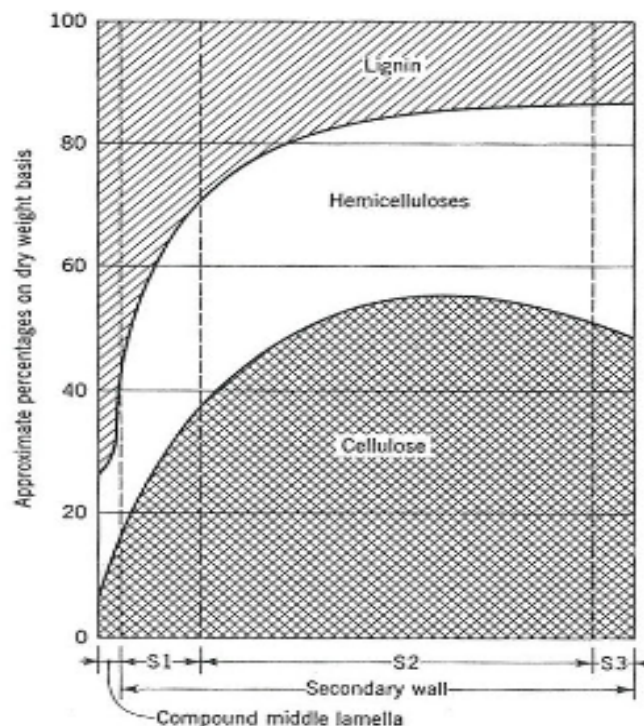


Figure 4. Composition of cellulose, hemicelluloses and lignin for the different fiber wall layers compound middle lamella, S1 wall, S2 wall, and S3 wall [22].

**Cellulose** chains are built from cellobiose units, as shown in Figure 5 below [28]. Cellulose is a homopolysaccharide composed of  $\beta$ -D-glucopyranose units that are linked together by (1 $\rightarrow$ 4)-glycosidic bonds [28, 40]. Cellulose I, which is the native cellulose, is a completely linear molecule with a strong tendency to form intra- and intermolecular bonds. Bundles of cellulose molecules are aggregated together in the form of microfibrils. These microfibrils have both highly ordered (crystalline)

and less ordered (amorphous) areas. The microfibrils form fibrils that form cellulose fibers.

In the cellobiose chain, every second cellobiose unit is rotated  $180^\circ$  [28, 40]. The smallest repeating unit of cellulose is therefore in reality two cellobiose units. The softening temperature of cellulose is about  $200^\circ\text{C}$ .

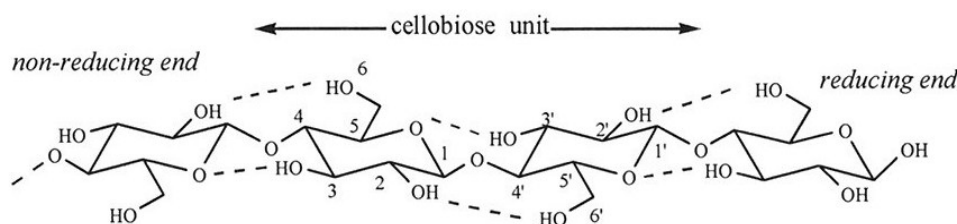


Figure 5. The molecular structure of a segment of a cellulose chain, showing the internal hydrogen bonds and the reducing and non-reducing ends [28].

**Hemicelluloses** found in softwoods are *e.g.*, arabinoglucuronoxylan and glucomannan [41]. The hemicelluloses are believed to function as glue between cellulose and lignin, and also give some flexibility to the wood [40]. Hemicelluloses are amorphous structures and absorb water easier than cellulose, something that results in low softening temperatures.

**Lignin** is a large, three-dimensional, optically inactive molecule that, just as for cellulose and hemicellulose, has different chemical composition in softwoods and hardwoods. In chemical pulps, most of the lignin is removed, which is not the case for mechanical pulps where everything but the tree bark (that is removed, pressed, and burnt for energy) is used in the paper. Lignin is the reason for yellowing of wood-containing printing papers by heat, air-pollutions, or sunlight, and lignin's high softening temperature (about  $120^\circ\text{C}$  at 10 Hz, [30]) is also the reason why high process temperatures are needed in the mechanical and chemimechanical pulping processes.

**Extractives**, or resins, can be described as the tree's chemical defence, protecting it from insects and fungi. Some extractives are soluble in water and for pulp and paper production applications, extractives are mainly a problem. For example, extractives consume large quantities of bleaching chemicals. A large amount of the extractives are found in the bark, which is removed from the wood logs before pulping but the extractives remaining in the wood entering the mill can cause problems in water systems of the paper machines, which are becoming increasingly closed.

## 2.2 Fiber bonding

### 2.2.1 The notation fiber bonding

The bonds acting between the fibers have traditionally been suggested in the literature to be hydrogen bonds [31]. Also van der Waal forces and electrostatic interactions may play a large role between fiber surfaces. Capillary forces between surfaces are suggested as a driving force to create close-contact between the fibers. Torgnysdotter *et al.* refers to the bonds between the fibers as “joints” and refers to micro or even nano scale bonding properties [34]. The modification reported by Wågberg *et al* of fiber surfaces to improve bonding shows great potential both in process applications and in tailor-made applications [35].

This thesis is about fiber bonding ability in mechanical pulp furnishes, and a method to measure the distribution of fiber bonding ability is developed. However, the notation fiber bonding ability has yet to be defined. Fiber bonding ability in a paper structure formed from mechanical pulp fibers can refer to both chemical and physical interactions between fiber surfaces as well as to long fiber quality (flexibility and shape). The fiber bonding ability will be reflected in the fibers’ ability to form printing papers of good surfaces and high runnability (mainly mechanical pulps).

Mechanical pulp fibers have generally a high strength. However in sheets from mechanical pulps, the bonds between the fibers are relatively weak. Therefore, Forgacs in 1963 evaluated the bonding potential of long fibers as tensile strength [1]. Mohlin wrote in 1989 about the importance of the long fiber bonding ability of mechanical fibers in printing papers [6]. Strand [2] and Ferritsius and Ferritsius [3-5, 33] have used factor analysis to illustrate the phenomena fiber bonding in mechanical pulps. Huusari [26] describes that “Mechanical pulp with long, slender fibers with good bonding ability is favored for the best combination of runnability and printability of paper.” These references are just a few examples of some of the work which show that the long fiber bonding ability affect the quality of printing paper surface and the runnability.

It is probable that rather strong surface interactions are present also in mechanical pulp fibers. However to form bonds of *e.g.*, hydrogen bridges or van der Waal forces, the distance between the fiber surfaces and the contact area between the fibers are vital. The fibers in chemical pulps are lignin-free and therefore have more accessible HO· groups on the surface than mechanical pulp fibers to form bonds [31]. For the fairly stiff mechanical fibers especially at room temperature, to be able to form any kinds of fiber bonds, fiber flexibility, contact area, and external

fibrillation are believed to be important. Figure 6 below shows some fiber-fiber and fiber-fibrils interactions in a thermomechanical pulp.

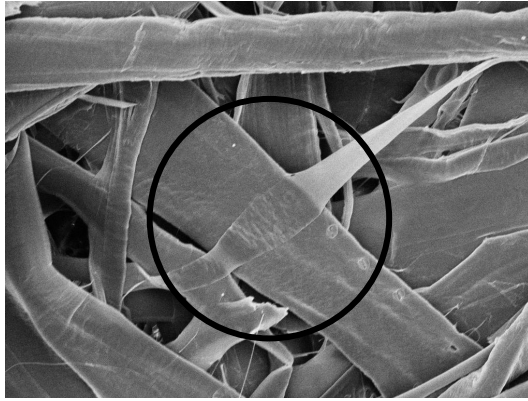


Figure 6. SEM-image of not yet defined fiber-fiber interaction of thermomechanical pulp, Bauer McNett long fiber fraction P16/R30.

In summary, it has to be remembered that fiber “bonding” may be referred to both micro bonds (joints) and the quality of mechanical long fibers. Fiber bonding in mechanical pulping refers mainly to the fiber’s ability to create strong sheets with good surface properties, to some extent the ability to form large contact areas. The external fibrillation of the fiber is also believed to enhance fiber bonding in mechanical pulps.

### 2.2.2 Fines

One other raw-material parameter affecting the strength and to some extent the surface properties of printing paper is the amount and quality of fines, *e.g.*, small pieces of fibers, fibrils that have been peeled off from fiber surfaces in the process, or pieces of the middle lamella or ray cells.

The fines, about 30 weight% of the pulp, function as putty between the fibers in the paper and increase the paper strength. Fines are also important for optical properties (discussed in Section 2.3). Fines and fibers differ a lot in size, morphology, specific surface, and chemical composition. The mechanisms of fiber bonding ability of fines and fibers can therefore not be expected to be the same. There will, however, be no in-depth discussions of the quality or properties of fines included in this thesis, as it deals exclusively with long fiber bonding ability, as defined in Section 2.2.1.

## **2.3 The mechanical and chemimechanical processes**

Mechanical pulp is mainly used to make printing paper, news or magazine grades, where the demands on optical properties are high. Printing paper has generally low basis weights, about 40 grams per square meter. Mechanical fibers as compared to chemical fibers contribute to a high light-scattering coefficient and thereby opacity (higher opacity means lower transparency), making it possible to print on the thin paper without print-through. Generally, the demands on brightness are lower for newsprint and magazine paper than for wood-free fine paper (*e.g.*, copy paper) produced by chemical pulp, but the trend is towards higher and higher brightness also for magazine and news grade paper. The strength of printing paper must be high enough for the paper to manage the high forces in the paper machines and in the printing presses without breaking. Chemical reinforcement fibers are traditionally used in some grades of wood containing printing paper. The strength of the paper increases but the reinforcement fibers are disadvantageous for the printing paper surface and opacity.

The mechanical separation of fibers, defibration, and the treatment to get the right properties of the fibers can primarily be performed in two ways; either by refining or by grinding.

### **2.3.1. Groundwood pulp (GW)**

Grinding was reported to have been used for mechanical pulping to manufacture groundwood pulp (GW), as early as 1844 [32]. Friedrich Keller was the first to press wood logs against a rotating stone together with water, to achieve a pulp for paper production. The process works by the same principles today and when logs are pressed against the rotating grindstone with hot water, the fibers are torn out from its middle lamella matrix. This can be done either at atmospheric or pressurized conditions. Pressurized groundwood pulp (PGW) gives a pulp of higher strength than atmospheric groundwood. Figure 7 below shows how the groundwood process works, with logs pressed against a rotating grindstone.

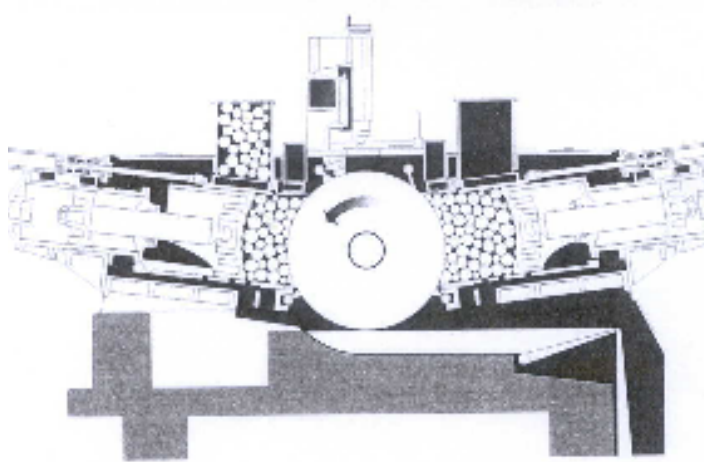


Figure 7. The groundwood process is one of the mechanical pulping processes. Atmospheric Valmet grinder [23].

In general, compared to other pulping processes, groundwood pulp contains fibers with a high degree of treatment and a high amount of fines, providing a high light-scattering coefficient (high opacity). The grinding temperature is usually around 75 degrees centigrade in the process water, with higher temperatures of the wood logs close to the grinding zone. Increasing the grinding temperature makes defibration easier, but causes the pulp to darken. The advantage of GW pulping is the high degree of fiber treatment, being an advantage for generating good surface properties, opacity and printability. The disadvantages are low paper strength due to many broken fibers, high amounts of shives (fibers not separated from each other) and low production capacity on each grinder unit. The low energy consumption in manufacturing compared to thermomechanical pulp (Section 2.3.2) is weighted against the lower value of recovered heat, *i.e.*, hot water instead of steam high pressure.

### 2.3.2 Thermomechanical pulp (TMP)

The second method of producing mechanical pulp is refiner pulping. In 1931, the Swedish engineer Arne Asplund built a pressurized refiner that would become the Asplund Defibrator, the precursor of the refiners used today. In thermomechanical pulping, pre-steamed and washed wood chips are fed into a pressurized, narrow space between two metal discs with grooved patterns. Either one [single disc (SD) refiner] or both [double disc (DD) refiner] plates rotate. A conical disc (CD) refiner has both a plane zone and a conical zone to prolong the retention time of the fiber compared to a single disc refiner with just a flat zone. Double disc refiners are more energy efficient to the same degree of fiber treatment than the conical disc refiners that are more difficult to steer to the right fiber properties. The double disc

refiner fibers have also been found to have a higher degree of external fibrillation and fiber flexibility. Figure 8 below shows a sketch of a 68" double disc refiner (cf. also Figure 9b)

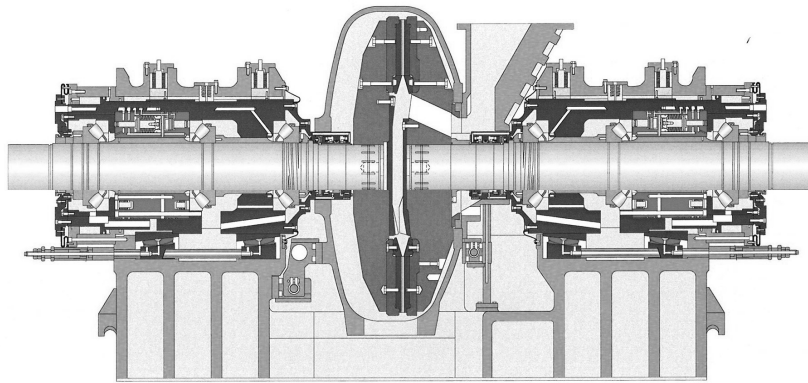
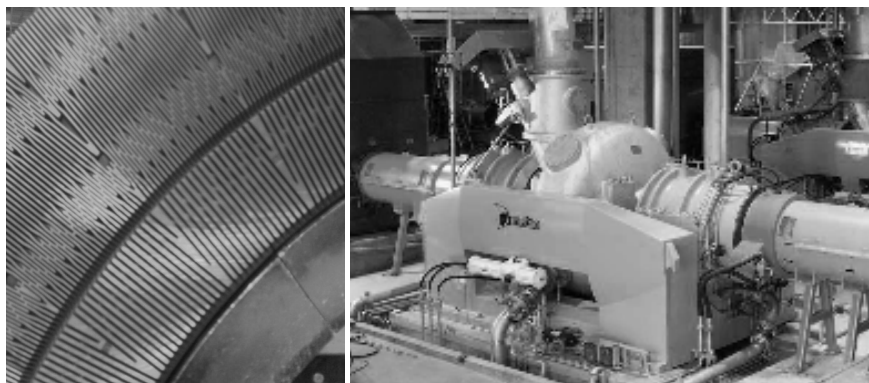


Figure 8. Metso double disc RGP DD68. The preheated wood chips enter the refiner in the middle. The fibers are transported to the periphery where singled out fibers and fines exits.

The refining discs are large, today up to 82" in diameter (208 cm, CD82" refiner), and the normal rotational speed is 1500-1800 rpm. The plate gap between the rotating discs is about 0.6 – 0.8 mm (DD), 0.6-0.9 mm (plane zone CD), and 0.9-1.2 mm (conical zone CD), thus making vast demands on refiner vibrations and process equipment accuracy.

Steaming at high pressure and frictional heating make the lignin in the middle lamella soften and the fibers can be released from the matrix by shearing forces. The chips are fed into the middle of the refiner and transported to the periphery by centrifugal forces. Segments in the refiner plates with patterns narrowing towards the periphery, give the fibers the treatment required. Inside the steam-filled refiner, the fibers are exposed to repeated pulses by the bars of the refiner plates, thus forming the fiber properties. The design of refiner plates is an important area of development in the mechanical pulping industry, with continuously suggested improvements and changes. Figure 9a shows the design of a refiner segment.



Figures 9a and 9b. Refiner segments (left) are grooved patterns where the fibers pass towards the periphery and (right) the Metso RGP DD68 refiner.

The advantages of TMP are the high content of long, strong, slender fibers, which, compared to groundwood pulps, gives a strong printing paper without or with a decreasing need of chemical reinforcement pulp. Different kinds and designs of refiners and refiner segments produce mechanical fibers of different strengths, with different optical and surface properties, depending to a large extent on the energy used during refining. A higher energy input gives a higher degree of fiber treatment, but the consumption of electrical energy is also the main disadvantage of the TMP process.

### **2.3.3 Chemithermomechanical pulp (CTMP)**

The CTMP process is similar to the TMP process, but before refining, the wood chips are exposed to sodiumsulphite that soften the middle lamella surrounding the fiber. This sulphonation makes the rupture of the fiber occur in the primary wall/middle lamella interface, rather than in the S1/S2-wall as in the thermomechanical pulp (Figure 10). CTMP is typically used for the middle layer in paper board, where fibers of high bulk (inverse of density) are needed.

RMP, refiner mechanical pulp, mentioned in Figure 10, is a forerunner of today's thermomechanical pulping process, where no pressurized chip preheating is performed.

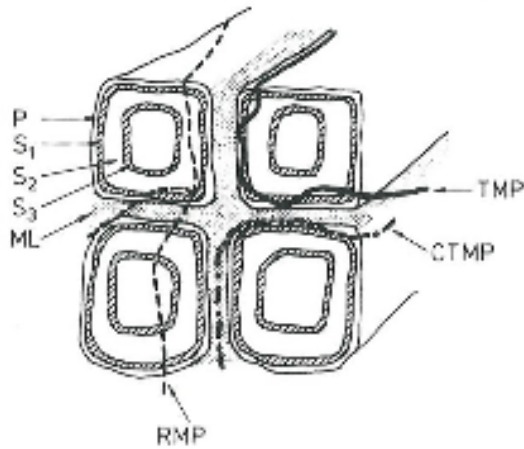


Figure 10. During defibration, the fiber rupture occurs at different places depending on the pulping method used. The TMP (thermomechanical pulp) process results in fiber rupture at the S1/S2 interface in the secondary (S) wall, the CTMP (chemithermomechanical pulp) process in rupture in the middle lamella (ML)/primary wall (P) and the RMP (refiner mechanical pulp) process in rupture across the fiber [22].

For the CTMP process, the rupture of the fiber in the middle lamella/primary wall region makes the fiber stay well intact, without the surface peeling that occurs (and that is desirable) in thermomechanical or groundwood pulping processing. Figure 11 below shows CTMP fibers intended for carton middle layer application.

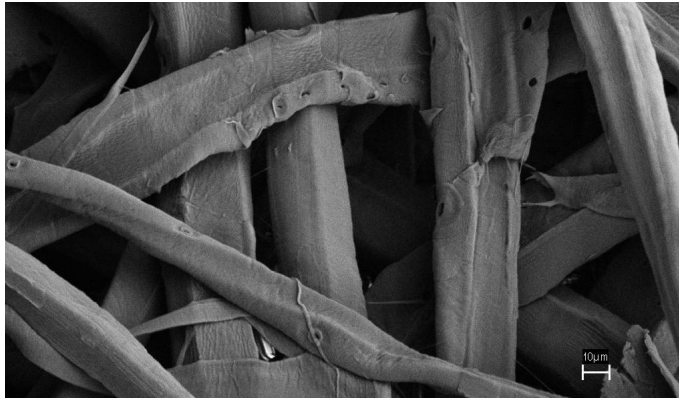


Figure 11. Scanning electron micrograph of chemithermomechanical pulp fibers intended for carton middle layer. The fiber rupture has occurred in the middle lamella/primary wall region, making the fiber bulky and the fiber wall relatively undamaged compared to thermomechanical and groundwood fibers.

## **2.4 Fiber quality**

### **2.4.1 Measuring fiber quality today**

Forgacs (1963) suggested that to characterize the physical properties of a mechanical pulp, at least two parameters were needed: the S-factor, shape, defined as the specific surface of the P48/R100 Bauer McNett fiber length fraction and the L-factor, length, the fiber length fraction retained on a 48-mesh screen [1].

In 1987, Strand then presented a paper on the use of multivariate data analysis to combine physical parameters of laboratory sheets into two factors: fiber bonding (Factor 1) and fiber length (Factor 2) [2]. Factor 1 and Factor 2 correlate well with Forgacs' S-and L-factors.

Ferritsius and Ferritsius [3,4,33] continued the work of Strand when applying the factors at some Stora Enso mills. On-line measurements were used for predicting the independent factors F1, fiber bonding, and F2, long fiber influence. In reference 4, it is reported how F1 and F2 were used for process control, with a more even pulp quality as the result. However, to predict F1 and F2 in the process, the sample position had to be known.

Ferritsius and Ferritsius also discovered that shives are not included in the F1 and F2 parameters and that therefore at least three independent parameters are needed to characterize the physical parameters of mechanical pulps. Recently developed methods for shive characterization [5,9] make characterization of this parameter possible.

With today's knowledge, mechanical fiber quality can be divided into five fundamental phenomena: fiber length, fiber bonding, resins, color, and shives. Figure 12 below shows the fundamental mechanical pulping quality star developed to illustrate this by Ferritsius.

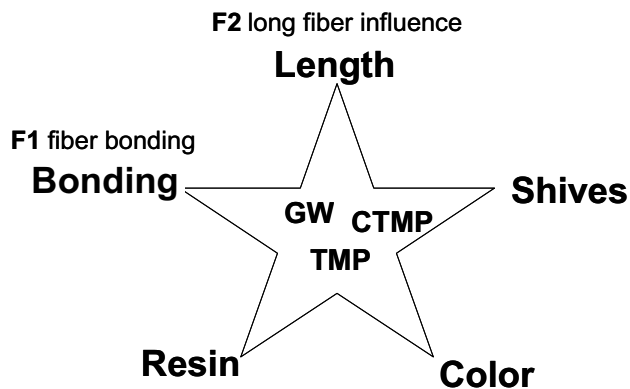


Figure 12. The Ferritsius fundamental mechanical fiber quality star - bonding ability, resins, color, shives, and length.

In an industrial perspective, fiber length is measured as a distribution by an optical analyzer. Shives content is usually displayed as a matrix of length and size of the shives, a type of distribution. Fiber bonding ability, on the other hand, is measured only as average values of tensile strength, density, or porosity of laboratory sheets of the entire pulp including fines. As was mentioned in Section 2.2.2, fines and fibers are very different in appearance and cannot be expected to obey the same bonding mechanisms. It may well be that the important influence of fiber bonding ability [e.g., 1, 6] on the printing paper is not evaluated thoroughly in the daily evaluation of the mechanical pulp.

One working hypothesis of this thesis is that average values of fiber bonding ability might not be enough to fully characterize a high-yield pulp, as the raw material is very inhomogeneous (cf. Section 2.1).

#### 2.4.2 Fibers in printing paper

Printing paper today is very thin, about 40 micrometers thick for thin, calandered journal paper and the trend is moving towards even lower grammages. It is therefore not unreasonable to conclude that the impact of the fiber quality of each individual fiber is increasing. Fibers with too low a fiber bonding ability might be the cause, if not of web breaks then at least insufficient paper structure and surface disturbances. If the fiber bonding ability of a fiber is higher than needed, the fiber has been subjected to an unnecessary level of mechanical treatment, that is, more refining energy is consumed than needed from a quality perspective. This, however, is an issue we will not have the answer to, until it is possible to measure the distribution of fiber bonding ability.

The raw materials, the fibers, are not homogeneous (Section 2.1). Therefore there will probably always be a distribution of fiber quality and fiber bonding ability in mechanical pulps. Every fiber has an inherent fiber bonding ability which can be affected by treatment in the refiners or grinders. Fiber properties such as flexibility, degree of external fibrillation, and collapsibility are also highly affected by the pulping process conditions.

For the thermomechanical pulping process, for example, the type of refiner (double/single disc), the refiner size, type and pattern of refining segments, specific energy input, plate gap, rotational speed, housing pressure, temperature, fiber retention time in the plate gap, chip moisture content, steam flow, breaker bar geometry, and chip feeding rate are some of the parameters affecting the pulp quality. After the first stage of defibration, it is common that a second refiner step is performed, to achieve a higher degree of fiber treatment. One or more reject steps are also common, where fibers that are not completely defibrated (*e.g.*, shives, two or more fibers not yet separated) or need further treatment go through a further refining stage.

To produce fibers of the right quality for the paper machine to produce the right paper quality, it is likely that fiber bonding ability needs to be evaluated more accurately than as average values of the entire pulp. The results of different fiber bonding abilities are sometimes visible in microscope, not only as numbers. Figure 13a below shows a long fiber laboratory sheet with a high fiber bonding ability (fibers interacting to a dense sheet) and Figure 13b fibers with low bonding ability that hardly interact with each other, making the sheet more open. Both Figures 13a and 13b are made from Bauer McNett fiber length fraction P16/R30.



Figure 13a. Long fiber laboratory sheet of fibers with high bonding ability (Bauer McNett fraction P16/R30).

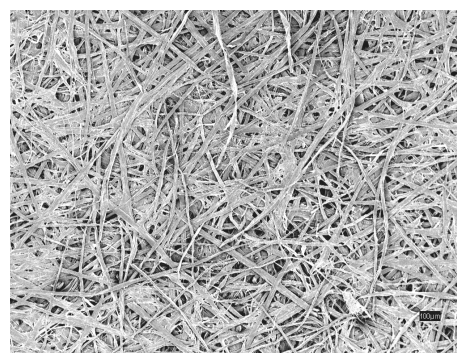


Figure 13b. Long fiber laboratory sheet of fibers with low bonding ability (Bauer McNett fraction P16/R30).

One important parameter proposed for fiber bonding ability is fiber collapsibility. A collapsed fiber is believed to provide for a smoother surface and a larger bonding area. As for all fiber geometry parameters, some fibers are more likely to collapse than others by inheritance, but the fiber collapsibility can be affected by treatment in the refining or in grinding processes.

Generally speaking, earlywood fibers are more likely to collapse than latewood fibers. As the fibers grow in the transition period between earlywood (grown in spring) and the latewood (grown in summer), transition wood fibers are formed. They typically have a large diameter and lumen, like the earlywood fibers, but also thick fiber walls like the latewood fibers. These transition wood properties make the fiber fairly easy to collapse, but also keen to spring back or decollapse [12, 13]. Decollapse occurs, for example, when exposed to moisture in coating, in the calander, or in the printing press.

Figures 14a-c show cross-sectional SEM micrographs of dry and rewetted printing paper. Some fibers that appeared collapsed in the dry paper have decollapsed, sprung back to its original shape when rewetted. Some shives are also visible in the rewetted paper that was not visible in the dry paper. The work of looking at cross-sections of printing paper in microscopy was inspired by Norman and Höglund [12].

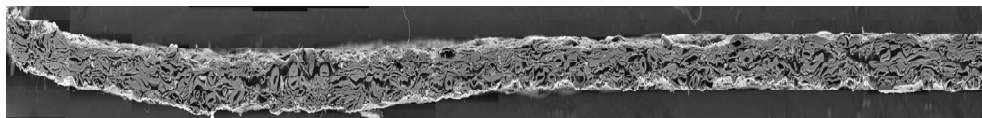


Figure 14a. Scanning electron micrograph of a cross-section of a dry, uncoated printing paper (Stora Enso Research Centre Falun).



Figure 14b. Scanning electron micrograph of a cross-section of a rewetted, uncoated printing paper (Stora Enso Research Centre Falun)

Figure 14c is a magnification of the same printing paper showed in Figures 14a and 14b. The upper image is the dry paper and the lower image the wet paper. In the magnified figure, individual fibers can be recognized.

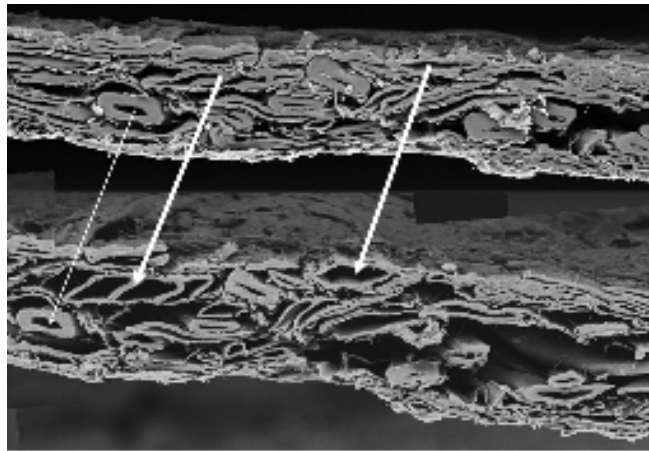


Figure 14c. Magnification of Figures 14a and 14b. The upper image shows the uncoated printing paper in dry conditions and the lower image the same paper rewetted. The wide arrows show how some of the fibers that appeared collapsed in the dry paper decollapsed when exposed to moisture. Some fibers that appeared large, thick-walled and disturbing in the dry paper did not change at all when wetted (thin arrow).

### 2.4.3 Distribution of fiber bonding ability

Given the inhomogeneity of wood fibers entering the pulp mill (Section 2.1) it is reasonable to assume that an average value of the fibers' bonding ability alone will not tell the whole truth about the fiber characteristic. With the continuously increasing demands on the mechanical pulp to be able to produce higher quality paper grades, average values of an entire pulp will probably not give sufficient information in the long run. With the trend moving towards lower and lower grammages in printing paper, the bonding ability of each individual fiber will become more and more important.

The fact that average values of fiber bonding ability alone are not sufficient to produce high quality printing papers, is one working hypotheses of this study. Another is that increased knowledge about the fundamental fiber behavior is needed to achieve improved long fiber bonding ability in mechanical pulps.

So far, there is no method to measure the distribution of fiber bonding ability in mechanical pulps. While fiber length and shives are displayed as distributions, usually average values of tensile index, density, or tear index of the entire pulp are used to mirror the bonding ability of a pulp. With a narrower distribution of fiber bonding ability (outline in Figure 15), the demand on the average value might even decrease, but with preserved or even improved fiber quality.

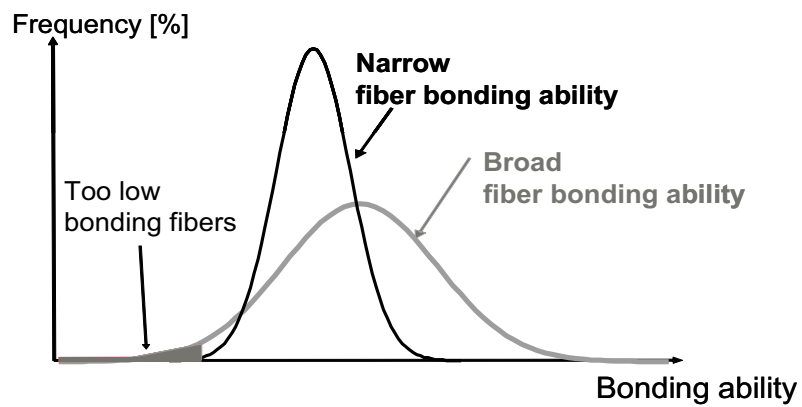


Figure 15. Outline of what the distribution of fiber bonding ability could look like. By reducing the fibers with too low a bonding ability, it is possible that a narrower bonding ability distribution can be achieved, also containing fewer over-refined fibers.

And now it is time to answer the question Stora Enso worker Luigi Alfonsetti asked two years ago: “How many of our fibers have too low bonding?”



### 3. MATERIALS AND METHODS

*The experimental section of this thesis deals mainly with the methodology of the study and explains why certain methods have been chosen rather than others.*

Five mechanical pulps (Pulps A-E), all produced from Norway spruce (*Picea Abies*) were fractionated in hydrocyclones with respect to the fiber bonding ability. The five industrial pulps were produced using different pulping processes, with different process conditions, and intended for different end products.

#### 3.1 Hydrocyclone fractionation

To get some idea of which fibers provide for a high and low fiber bonding ability respectively, hydrocyclone pilot trials were performed at Noss AB, Norrköping, Sweden.

Karnis and co-workers [7] used multi-stage hydrocyclone fractionation to evaluate the distribution of the specific surface of different mechanical pulps. Shagaev and Bergström presented in 2008 the use of hydrocyclones for fractionating fibers of different morphology [8]. Ferritsius and Ferritsius used Stand's independent factors F1 and F2 to show the different separation mechanisms of screens (separating by length) and hydrocyclones (separating by bonding ability) [3].

Hydrocyclones are designed to fractionate fibers with respect to specific surface and density. In a "forward cleaner", the most common hydrocyclone type, the feed stream is fed into the hydrocyclone's cylindrical part, with a flow concentration of about 0.5%. The flow inside the hydrocyclone makes the fibers of the highest specific surface, the accept-stream, leave the hydrocyclone at the base, the accept, which is usually positioned at the top of the hydrocyclone (Figure 16). The fibers of the lowest specific surface leave the hydrocyclone at the apex, the reject.

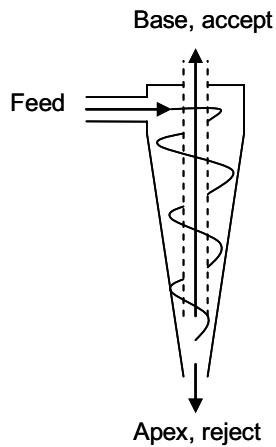


Figure16. Schematic hydrocyclone fractionation. The feed enters the hydrocyclone, which separates the fibers with respect to specific surface, the accept stream exits at the base and the reject stream at the apex.

As specific surface of the fibers is believed to strongly affect the fiber bonding ability, a hydrocyclone fractionation setup was used for the pilot trials. It was decided that a four-step fractionation would be best suited for the evaluation of fiber bonding ability. The fractionation trial setup is displayed in Figure 17 below.

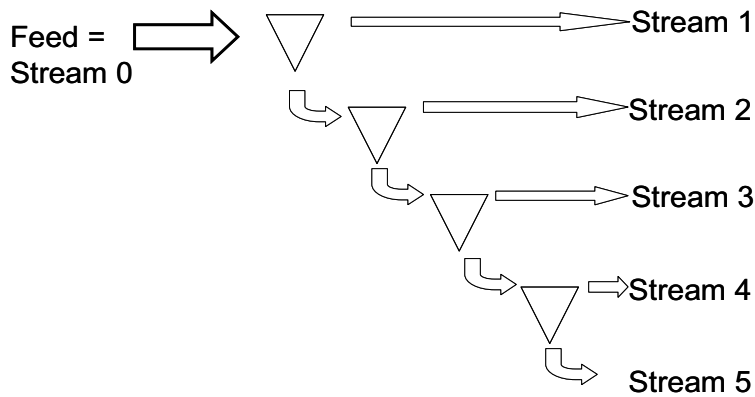


Figure 17. Fractionation trial setup at Noss AB, Norrköping, Sweden.

Pulp A was used as a reference pulp as the fiber bonding properties of Pulp A were believed to be in the middle range of the pulps to be tested. For Pulp A, all process parameters were set so that 20% of the R100 fibers (fibers too large to pass through a 100 mesh screen, further described in Section 3.2) in the reference pulp would exit with each hydrocyclone stream (cf. Figure 17).

With four hydrocyclone steps, five different streams were formed. The Pulp A fibers, believed to possess the highest bonding ability, went out with the first accept, Stream 1, and the reject-stream continued on to the second fractionation step. The second accept, Stream 2, contained the fibers believed to have the second highest bonding ability and so on. The fourth reject formed Stream 5.

For the four remaining pulps, Pulp B-E, the same process settings as for the reference pulp, Pulp A, were used. The fibers exited via one of the five streams depending on the bonding ability of the fiber. The amount of fibers going to each stream therefore functions as an indirect measure of the amount of high and low bonding fibers in each pulp. Pulps A-E represent a wide selection of different types of mechanical and chemimechanical pulps used for manufacturing of SC, news, and board qualities.

### **3.2 Bauer McNett fractionation**

Wakelin [36] has showed that the specific surface increases with reduced particle size, and how specific surface area therefore should be determined for a defined size fraction.

After having separated the fibers by bonding ability into five streams in the hydrocyclone fractionation setup, each stream was also fractionated by fiber length. The fiber length fractionation was performed in a Bauer McNett classifier with screens of 16, 30, 50, and 100 mesh, forming the fiber length groups R16 (retained fibers of a 16 mesh screen), P16/R30 (*i.e.* passed 16 mesh, retained 30 mesh), P30/R50, and P50/R100, see Figure 18 below. The Bauer McNett fractionation was performed in accordance to SCAN-CM 6:05 standard and “mesh” is explained in Table 2 below. The feed, Stream 0, was also fractionated by fiber length in the Bauer McNett classifier with the same Bauer McNett screens.

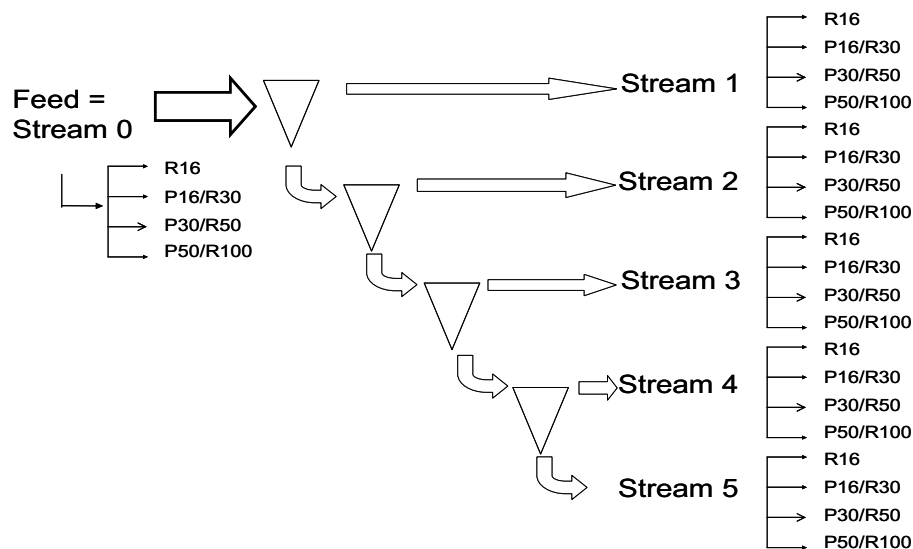


Figure 18. Bauer McNett classifier fractionation of the five hydrocyclone streams plus feed (Stream 0).

In the Taylor Equivalent series “mesh” is defined as the exact number of openings per linear inch of mesh. A screen of 16 mesh will have 4 openings per square inch and 16 openings per square inch. Higher numbers of wires per square inch result in smaller openings. The standard used for Bauer McNett mesh sizes in this study is the US standard. Table 2 below shows the conversion between Taylor and US standards for the Bauer McNett screens used in this study, and the approximate sieve size for each screen.

Table 2. Approximate sieve size of the Bauer McNett screen used in this study.

Sieve size (approx)	US standard	Taylor Standard
1.20 mm	16 mesh	14 mesh
0.599 mm	30 mesh	28 mesh
0.297 mm	50 mesh	48 mesh
0.152 mm	100 mesh	100 mesh

The reason for fractionating the fibers by fiber length after the bonding ability fractionation was to assure that the comparison of fiber bonding ability was performed at fairly similar fiber lengths. At the beginning of this study, the mechanisms of fiber bonding ability for fibers of different fiber lengths were not known. The fiber length groups from the Bauer McNett fractionations were therefore made as small as possible (R16, P16/R30, P30/R50, and P50/R100). Figure 19 below shows the Bauer McNett classifier fiber length fractionation setup. The

first vessel from the left contains the R16 fibers, the second the P16/R30 fibers, the third the P30/R50, and the fifth the P50/R100 fibers.



Figure 19. The wires separating the fibers by length are from the left 16 mesh (longest fibers), 30, 50 and 100 mesh (shortest fibers).

The R16 fiber length fraction tends to deviate a lot with respect to fiber length, as it is the first Bauer McNett fraction with no upper limit. Most evaluation of fiber properties has been done on the P16/R30 and P30/R50 fiber length fractions.

The Bauer McNett fractionations were performed at Stora Enso Research Centre Falun. Comparisons of amount R100 for each pulp were done using Bauer McNett fractionation at Noss AB. The amount R100 at Noss AB was consistently 2% higher than that at Stora Enso Research Centre Falun, emphasizing the uniqueness of each Bauer McNett classifier and that the levels of different Bauer McNett units might differ. However, given the consistent differences of the R100 fraction for the five pulps used in the investigation, it seems that the Bauer McNett fractionations were performed correctly.

### 3.3 Physical properties of laboratory sheets

From hydrocyclone Stream 0-5 and from each Bauer McNett fiber length fraction, long fiber laboratory sheets were formed (unorientated long fiber laboratory sheets, internal standard). These sheets were then tested for physical properties such as tensile strength and apparent density. Tensile strength was tested with ISO standard 1924-3 and apparent density was measured as STFI-density by SCAN-P 88:01.

To minimize deviation, all laboratory sheets were produced in the same laboratory, by the same technician. For the physical properties presented in Section 4, standard deviations with a 95% confidence interval are shown. However, it is known that

reported tensile strength testing can still deviate for the same pulp, when sheet forming is repeated. Klinga *et al* showed in 2007 how the method used in pressing and drying laboratory sheets can affect the result of the laboratory sheet testing [37]. It is therefore important to compare consistent and standardized methods in sheet preparation.

### 3.4 Fiber geometry by cross-sectional SEM-micrographs

Reme [9], Kure [10], Norman, [12], Dickson [13], and Mörseburg [14] are some of the researchers that have described the use of cross-sectional micrographs to measure fundamental fiber morphology. In this study, the Bauer McNett fractions P16/R30 of the feed, highest bonding stream (Stream 1) and lowest bonding stream (Stream 5) for each pulp was analyzed using such cross-sectional images.

The fibers to be analyzed are aligned, dry-frozen, and embedded in a polymer material. Figure 20 (photo: Olle Henningson, Örjan Sävborg, Stora Enso Research Centre Falun) shows how aligned fibers are embedded in a split straw before the polymer embedding.



Figure 20. Preparation of samples of orientated fibers for cross-sectional SEM analysis.

Small cross-sectional slices are cut from the polymer matrix and photographed in a scanning electron microscope (SEM). The cross-sections provide a view of the fibers' geometrical properties. Several fiber parameters such as fiber width, fiber wall thickness, shive and mini shive content [5] and collapsibility [13] can be measured in the micrograph image. Z-parameter, describing the presence of early- and latewood fibers [11], as well as fiber circularity, an indirect measure of the fiber collapse, can also be measured as average values and distributions with the cross-sectional micrograph method.

The cross-sectional image analysis method described above is accurate but time-consuming. The method is also to some extent influenced by the engineer analyzing the results. Experience is important when deciding how the image material should be interpreted. The image material is roughly divided into fibers, shives or fiber fragments, a division that was earlier performed manually. Although more automatic methods have been developed [9], some visual interpretation is still done and an experienced eye is vital for the proper use of the cross-sectional image analysis method.

SEM-images of long-fiber laboratory sheets were also taken and some of the images can be found in Appendix 4.

### **3.5 Acoustic emission**

Also old methods for new applications have been used to characterize the mechanical fibers. Acoustic emission has traditionally been used for steel characterization. Gradin *et. al.* and Isaksson *et. al.* [17,18] have used acoustic emission to characterize paper with respect to relevant physical parameters.

Pulps A and B have been analyzed for acoustic emission, where a tensile test is performed with a microphone attached to the test strip (Figure 21). During elongation, the microphone records the number of acoustic emissions, which is believed to be the breakage of fiber bonds. The test strips are 15\*100 mm as for a conventional tensile strength determination, but the speed of the elongation is ten times slower than normal (4 mm/min), to ensure the recording of all acoustic emissions. The test strips were made from orientated, calandered fiber laboratory sheets formed in a Formette dynamic sheet former from fiber length fraction P16/R30. The acoustic emission results were compared to values of fracture toughness and fracture toughness index, determined according to SCAN-P 77:95 standard.

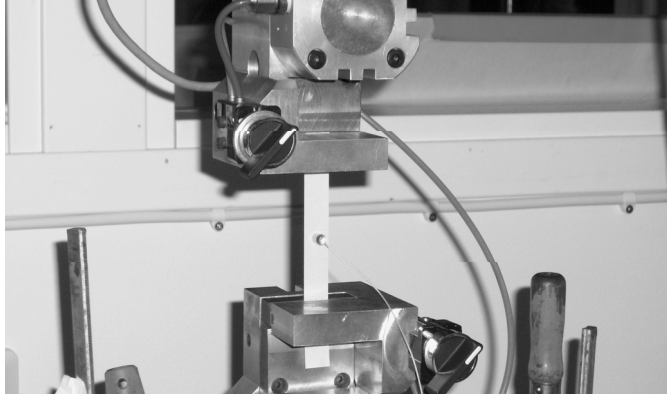


Figure 21a. The acoustic emission trial, showing the test strip and the microphone.

### 3.6 Measurement of fiber properties in FiberLab™

The recent development of optical analyzers has made it possible to measure a large amount of fibers in a short time, including the measurement of fiber morphology parameters such as fiber width, fiber wall thickness and external fibrillation. However, as more optical measurement devices come onto the market, the levels of the results might not always be calibrated to true values. Optical measurement devices are therefore recommended for use in comparing different pulps for relative values. The fiber morphology parameters fiber width and fiber wall thickness can be used to calculate the collapse resistance index (CRI), seen in Equation 1, that originates from Vesterlind and Höglund together with Gradin [16].

$$CRI = \frac{\text{fiberwall thickness}^2}{(\text{fiber width} - \text{fiberwall thickness})} \quad \text{Equation 1}$$

The fiber length fractions (P16/R30, P30/R50, and some P50/R100) as well as the whole pulp of each hydrocyclone stream of the five pulps plus the feed (Stream 0) were analyzed in a FiberLab™ device. Fiber geometry such as fiber length, external fibrillation, fiber wall thickness, fiber width, curl, straight segment, and cross-sectional area were analyzed optically. Also the fines content was measured. The measurements were made using two cameras that measure the fibers in a 50µm wide chamber and then deliver the data to the software. Figures 22 a-c below show some examples of these images that form the basis for calculating the fiber geometry.

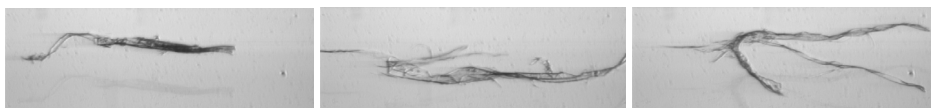


Figure 22a-c. Examples of FiberLab™ photos. From these photos, two cameras measure fiber geometry, e.g, fiber width, cross-sectional area, fiber wall thickness, fibrillation index, fiber length etc.

It is possible to save all the fiber images used for the fiber properties calculation. Attempts were made to use the images of the individual fibers for further image analysis but the image resolution proved too low. The unknown distance of the fiber from the camera (up to 50µm) is another reason why additional image analysis from FiberLab™ measurements has not yet succeeded.

The FiberLab™ measurement device measures a maximum of 100,000 fibers per run. For all pulps and fiber fractions, triple tests were run. For the P16/R30 fractions, about 5,000 fibers per run were measured (a total of at least 15,000 fibers), for the P30/R50 fractions about 10,000 fibers, making a total of at least 30,000 fibers.

The term “external fibrillation” is one of the parameters delivered from the FiberLab™ evaluation and is just what the name implies – external fibrillation of the fiber. It is measured in the FiberLab™ as total fiber area including fibrils, divided by fiber body area without fibrils.

For all average FiberLab™ device values in Section 4, standard deviations of 95% confidence interval are presented if nothing else is stated. Figure 23 shows the FiberLab™ device with sampling carousel, software display and measuring chamber in the box under the shelf.



Figure 23. FiberLab™ device – sample carousel, measuring device, and computer.

FiberLab™ is probably one of the best optical devices on the market for characterizing the fiber geometry of mechanical pulps. However, as the device is one of the first of its kind to measure external fibrillation, for example, there are still several maintenance issues to be solved. If the device is to be used continuously, unannounced recalibrations connected to software updates are unacceptable. It was also discovered that the average values from FiberLab™ are not exactly the same as average values calculated from the raw data. The reason for this is that the software divides the raw data into pixel groups before calculating the average values on “traditional” grounds, from a time when optical equipment was not as well-developed as it is now. It must also be remembered that the values delivered from the FiberLab™, raw data or average values delivered from the software, are relative and not absolute. Kauppinen [15] provides further information about the measurement principles of the FiberLab™ measurement.

Before using the FiberLab™ raw data, “zero”-fibers need to be excluded. In this study, when calculating average values or distributions, all fibers showing a fibrillation index, fiber wall thickness, cross-sectional area, or fiber width that equal zero have been excluded. It is also important to ensure that all parts of the FiberLab™ device are working properly and that calibration is accurate at all times.

### 3.7 Bonding Indicator - BIN

In Section 4, the parameter Bonding Indicator, BIN, is presented and discussed. As shown in Figure 41, predicted BIN for fibers (fines not included) correlate well with tensile strength. As discussed in Section 2.2, the long fiber bonding ability in mechanical pulps may be influenced by several parameters, including contact area and fiber flexibility. Equation 2 below shows the principle equation that was used to predict the Bonding Indicator (BIN).

$$\text{Bonding Indicator (BIN)} = A + B * CRI + C * \text{Fibrillation} \quad \text{Equation 2}$$

Today, Bonding Indicator is predicted by the raw data for each individual fiber, delivered by the FiberLab™ device. Linear regressions of collapse resistance index (calculated from fiber width and fiber wall thickness), and external fibrillation are behind the denotation Bonding Indicator (Equation 2). Which arithmetic fiber length interval that is the most correct to predict the BIN-distribution within, needs to be further investigated. This method of predicting the Bonding Indicator in mechanical pulps is hoped to be of industrial, possible eventually industrial online use. Hopefully it will also be able to replace the use of laboratory fiber sheets to predict fiber bonding ability.

## 4. RESULTS AND DISCUSSION

*Results of the hydrocyclone fractionation and evaluation of fiber properties in Streams 0-5 for Pulp A and Pulp B are reported in Paper I. Paper II also includes Pulp C, Pulp D, and Pulp E and reports about the definition of Bonding Indicator, BIN, as well as the method used to calculate it. In this section, the results leading to the Bonding Indicator method are also presented and discussed.*

The results of the Bauer McNett fiber length fractionation for Pulps A - E are presented in Figure 24 below, showing the weight percent of fibers in each Bauer McNett fraction. The total amount of R100 fibers (fibers too large to pass through a screen of 100 mesh) is the height of each bar respectively. Remaining pulp is material small enough to pass through a 100 mesh screen (P100).

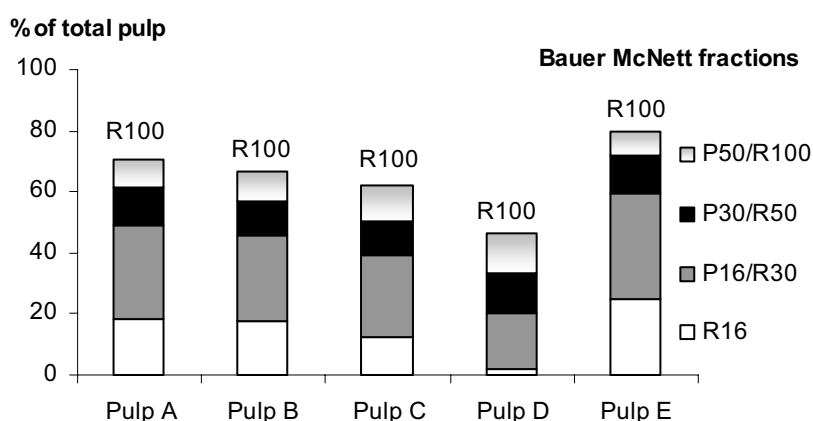


Figure 24. Bauer McNett fractions R16, P16/R30, P30/R50, and P50/R100 for the feed of Pulps A - E. The total amount of R100 (fibers not passing through a 100 mesh screen) is the height of the bar, remaining is P100 (material passing through a 100 mesh screen).

### 4.1 Hydrocyclone fractionation – weight percent per stream

The way the fibers divide into the five hydrocyclone streams is in itself one measure of the distribution of fiber bonding ability in the pulp. As Stream 1 contains the fibers of highest bonding ability and Stream 5 the fibers of lowest bonding ability with a consecutively falling scale in between, a high amount of fibers in Stream 1 suggests a high amount of high bonding fibers.

Pulp A, which was used as a reference pulp, was controlled so that about 20% of the R100 fibers went with each stream (Figures 25a and b). For the four remaining

pulps, the same process settings were used and the fibers could fractionate freely with respect to bonding ability. In this way, the amount of fibers per hydrocyclone stream became an indicator of pulp's fiber bonding ability. Pulp B, for example, shows a higher amount of fibers in Stream 1 than Pulp A (Figure 25a and b), suggesting a higher amount of high bonding fibers for both the P16/R30 and the P30/R50 fractions.

For all the five tested pulps, the way the P16/R30 fraction divided in the hydrocyclone fractionation (weight percent per stream) was very similar to the way the total R100 fibers divided. The reason for this has not yet been established. Examples of the how the amounts of fibers going to each hydrocyclone stream were calculated can be followed in reference 21. The way the P30/R50 fraction divided in the hydrocyclone setup was similar to the results for the P16/R30 fraction, Figures 25a and 25b.

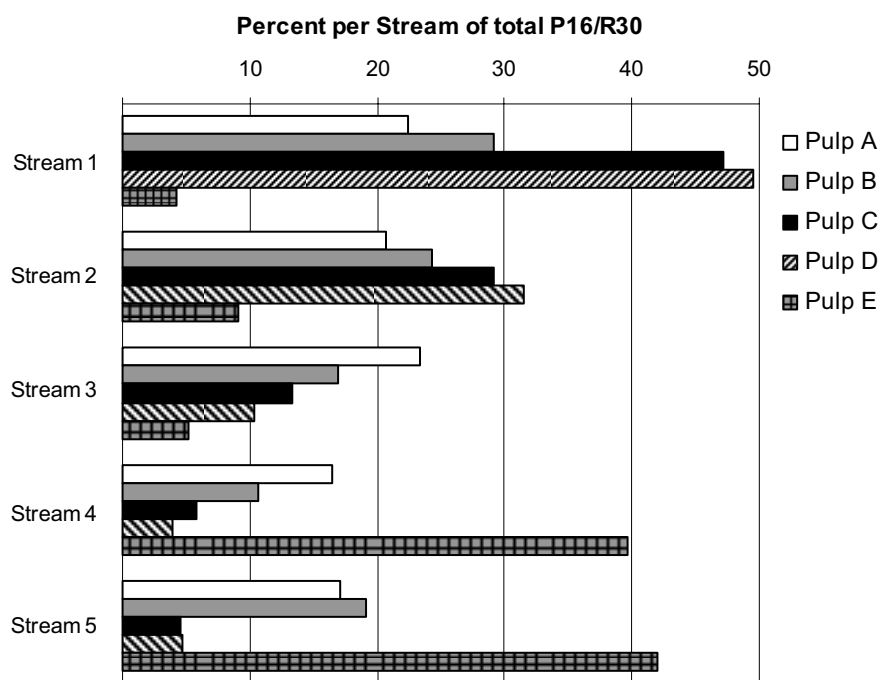


Figure 25a. Amount of fibers per hydrocyclone stream of the P16/R30 fraction. Stream 1 is the first accept stream and Stream 5 the last reject stream.

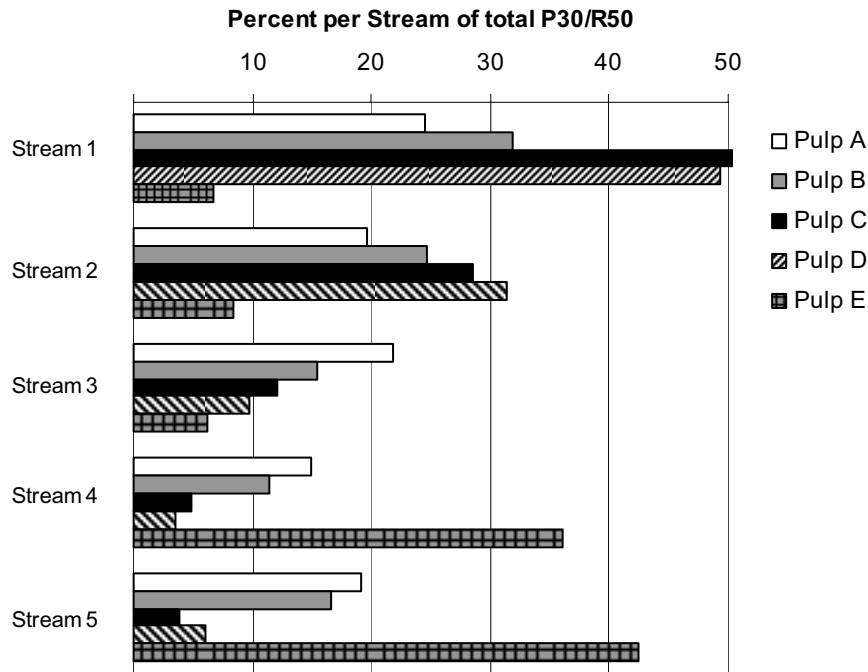


Figure 25b. Amount of fibers per hydrocyclone stream of the P30/R50 fraction. Stream 1 is the first accept stream and Stream 5 the last reject stream.

Before the second hydrocyclone fractionation of Pulp B took place, it was proposed that the level of bonding ability, evaluated as tensile strength, for example, of each stream would be the same for all pulps. This was not the case; the level of bonding ability in each stream is dependent on the feed pulp's bonding ability.

#### 4.2 Fractionation by fiber length in the Bauer McNett classifier

The result of the Bauer McNett fractionation of the feed pulps can be seen in Figure 24 above. The height of each bar is the amount of R100 fibers, that is, the amount of fibers retained inside a screen of 100 mesh. As mentioned in the experimental part (Section 3), the focus in this study is on fibers exclusively, not on fines.

Clark [38] suggested that Bauer McNett fractionated fibers not only by fiber length but also by coarseness. Petit-Conil *et al* [39] reported findings that it was fiber length together with flexibility that decided which Bauer McNett fraction the fibers end up in. According to Petit-Conil, comparing average fiber length in the specific Bauer McNett fraction with theoretical fiber length of that fraction, flexibility could

be measured. Comparing different pulps for the same Bauer McNett screens, longer average fiber length would suggest higher fiber flexibility.

Differences in average fiber length within the pulps can be seen for both the P16/R30 and the P30/R50 fractions (Figure 26a and 26b). Generally, Streams 1 - 5 show a “smiling” profile, with highest average fiber length in Stream 1, decreasing for Streams 2, 3, and 4, and increasing again for Stream 5. The outlying point, Pulp E, Stream 3, shows the same values after repeated measurements and has yet to be explained.

The overall lowest average fiber length is found in Pulp C, one of the pulps with the highest expected and evaluated bonding ability (Section 4.3). The overall highest average fiber length was found for Pulp E, containing the fibers evaluated to have the lowest bonding ability. Pulp E is also the pulp where the difference in average fiber length is the largest between the streams. It is clear, however, that the fiberlength of each Bauer McNett fraction is not, as Figures 26a and 26b show, absolute for all pulps.

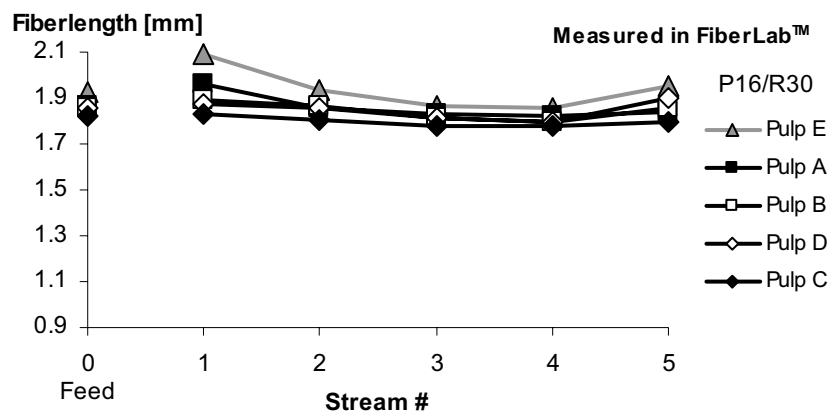


Figure 26a. Average fiber length of each hydrocyclone stream, P16/R30 fraction.

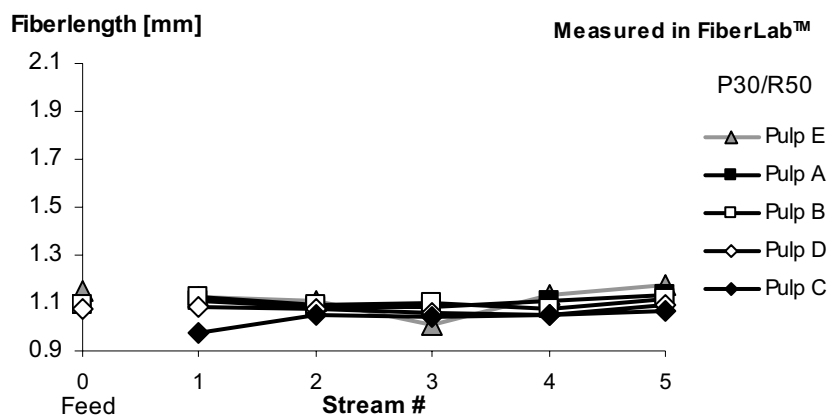


Figure 26b. Average fiber length of each hydrocyclone stream, P30/R50 fraction.

The hydrocyclone fractionation works by fluid mechanisms so that the smallest particle material (fine material or fines) exits the hydrocyclones with the accept stream. The amount of fines is therefore the highest in Stream 1. The Bauer McNett fractionation procedure might prove inefficient in removing all fines and the fear that high contents of fines in Stream 1 would increase tensile strength of the laboratory sheets of the long fiber fraction is therefore motivated.

However, if there were fines in Stream 1 after the Bauer McNett fractionation, average fiber length would be the lowest in Stream 1 and increasing, which, according to Figure 26a, is not the case for the P16/R30, nor for the P30/R50 fraction (Figure 26b).

The fines measurements in FiberLab™ for the P16/R30 and P30/R50 fractions also suggest that the amount of fines (measured as length-weighted fines) is very low, about 0.1% for the P16/R30 fraction and about 0.6% and for the P30/R50 fraction, Table 3. The fines content should therefore not be affecting the strength properties in fiber laboratory sheets to any decisive extent. Table 3 shows the amount of fines as measured in the FiberLab™ device. It has to be remembered, however, that the FiberLab™ device shows relative values. For the P30/R50 fraction, the fines content is the highest in Stream 1 and decreasing.

Table 3. Length-weighted fines for Stream 0-5, Pulp A (P16/R30 and P30/R50 fractions).

Pulp A	Fines(l) P16/R30	Fines(l) P30/R50
Feed	0.09% std 0.01	0.59% std 0.04
Stream 1	0.08% std 0.01	0.94% std 0.05
Stream 2	0.10% std 0.01	0.73% std 0.03
Stream 3	0.06% std 0.01	0.39% std 0.04
Stream 4	0.06% std 0.01	0.25% std 0.01
Stream 5	0.06% std 0.01	0.14% std 0.02

### 4.3 Physical properties of laboratory sheets

The five pulps were tested for physical properties of long fiber laboratory sheets. The long fiber fractions P16/R30, P30/R50 and for most pulps also the fiber length fractions R16 (longest fibers) and P50/100 (shortest fibers) were used in the evaluation. Each stream was tested, as well as the feed.

For all pulps, the highest tensile strength was that of Stream 1 and the lowest that of Stream 5, with a consecutively falling scale in between, Figures 27a and 27b. The exceptions to the consecutively falling scale are Streams 1 and 2, Pulp A, and Streams 2 and 3, Pulp B, which show the same tensile strength (Figure 27a).

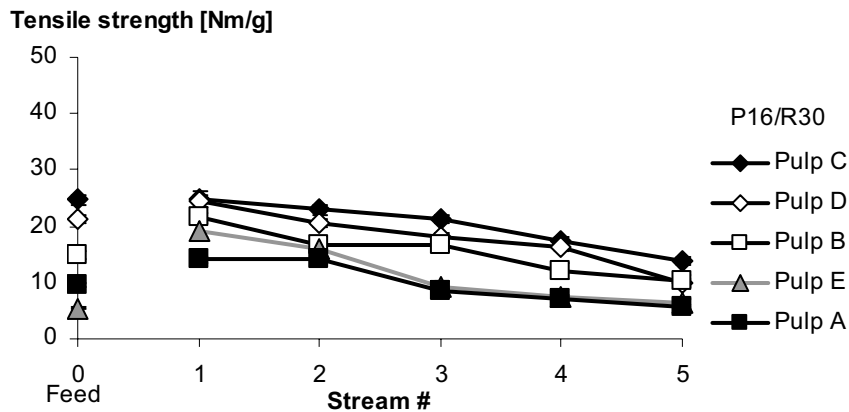


Figure 27a. Tensile strength for each hydrocyclone stream for Bauer McNett fraction P16/R30.

Figure 27b shows how the pattern is the same for the P30/R50 fraction as for the P16/R30 fraction (Figure 27a). The differences in tensile strength between Stream 1 and Stream 5 for the fiber laboratory sheets appear to be larger for the P30/R50 fraction than for the P16/R30 fractions, cf. Figures 27a and 27b, for all five pulps.

This might suggest either that the hydrocyclones are more effective at fractionating shorter fibers, or that the differences in fiber bonding ability are larger within the shorter P30/R50 fiber length fraction.

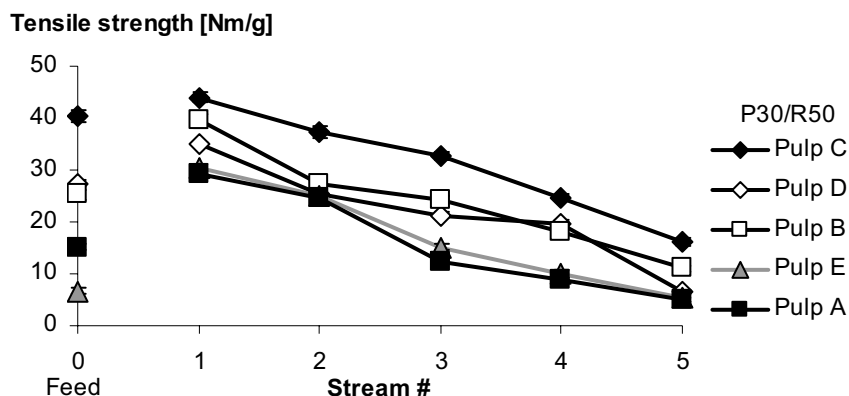


Figure 27b. Tensile strength for each hydrocyclone stream for Bauer McNett fraction P30/R50.

An unpredicted pattern appeared when evaluating the tensile strength of the laboratory sheets. It turned out that the tensile strength in Stream 5 was the same for all Bauer McNett fractions in each specific pulp. Figure 28 show this behavior for Pulp E. The same behavior can be seen for Pulps A-D in Appendix 1.

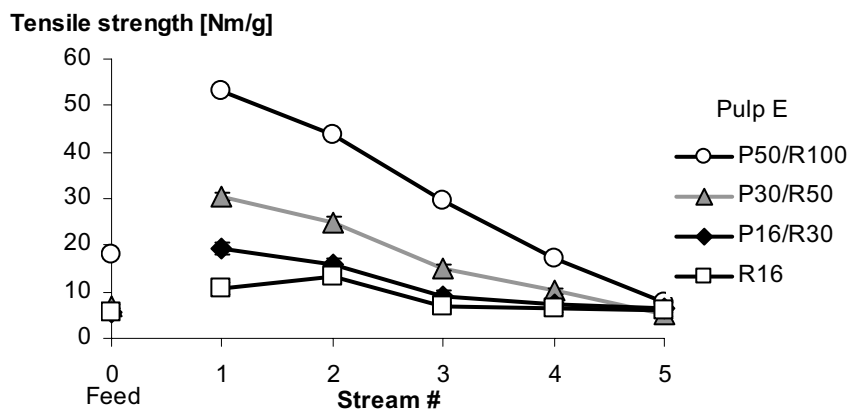


Figure 28. Tensile strength per stream (Pulp E), for the fiber length fractions R16, P16/R30, P30/R50, and P50/R100.

For the apparent density (measured as STFI-density, further explained in Section 3.3), as for tensile strength of the P16/R30 and P30/R50 fractions (Figures 27a and b), there is also a trend that the highest apparent density values are found in

Stream 1 and lowest in Stream 5. The trend, however, is not as clear as for the tensile strength, see Figures 29a and 29b.

The trend of larger differences between Stream 1 and Stream 5 for the P30/R50 fraction than for the P16/R30 fraction can also be seen in Figures 29a and 29b below, that show the apparent density per stream.

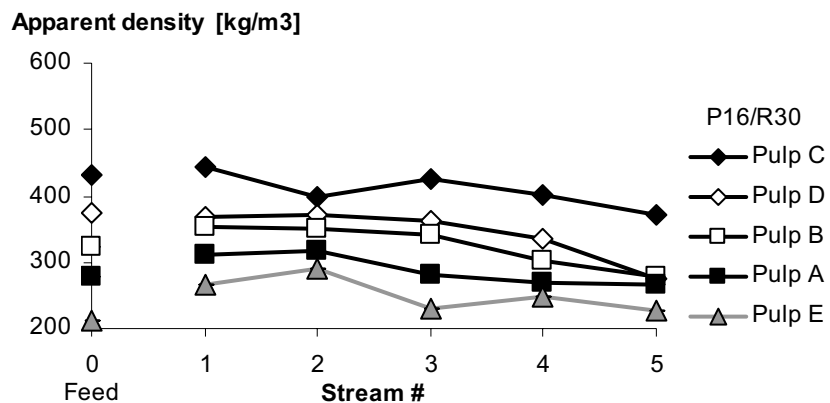


Figure 29a. Apparent density per stream for each hydrocyclone stream for Bauer McNett fraction P16/R30.

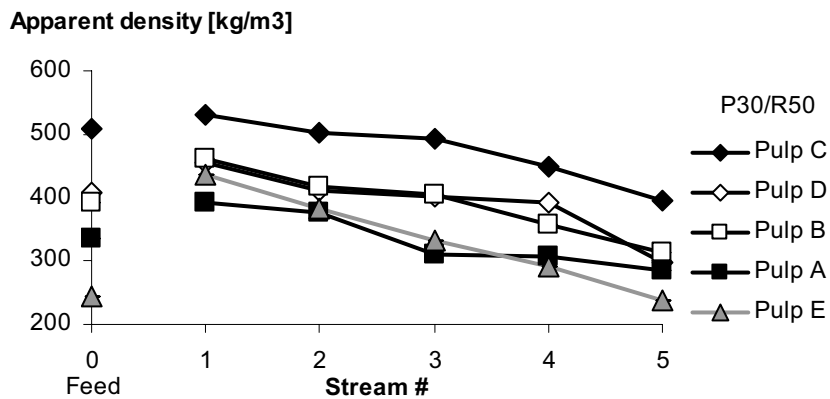


Figure 29b. Apparent density per stream for each hydrocyclone stream for Bauer McNett fraction P30/R50.

The apparent density shows a similar pattern of values converging towards a lowest value in Stream 5, as for tensile strength (Figures 28). The trend for the apparent density, however, is not as consistent as for tensile strength. Figure 30 below shows apparent density for the P16/R30, P30/R50, and P50/R100 fiber length

fractions for Pulp D. The same figure can be found in Appendix 2, where also the apparent density for all pulps is presented.

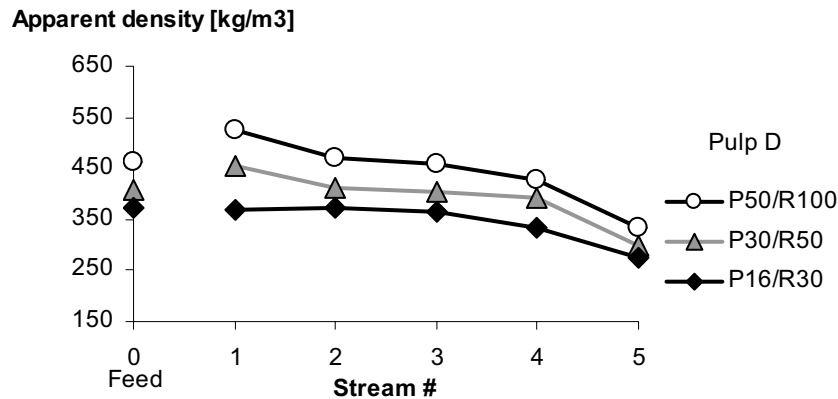


Figure 30. Apparent density per stream for Bauer McNett fractions P16/R30, P30/R30, and P50/R100.

Apparent density is believed to mirror the sheet structure [31] and it is also believed that the fiber's collapsibility is to some extent mirrored by apparent density. When tensile strength is used as an assumed measure of the fiber bonding ability, it is suggested that it is not only fiber collapsibility that provides for fiber bonding ability.

#### 4.4 Fiber geometry by cross-sectional SEM-micrographs

Cross-sectional SEM micrographs were used to measure geometrical properties of the fibers. The highest bonding fibers, Stream 1, Figure 31a, have thinner fiber walls, larger lumens and appear more collapsed. These fibers are typical earlywood fibers. Figure 31b shows Stream 5 fibers with thicker fiber walls, smaller lumens, and not as collapsed an appearance as the Stream 1 fibers. The Stream 5 fibers appear to contain a large proportion of latewood fibers. Among the Stream 5 fibers, some shives can also be detected.



Figure 31a. Cross-sectional micrograph of Pulp A Stream 1, highest bonding fibers, P16/R30 fraction.



Figure 31b. Cross-sectional micrograph of Pulp A, Stream 5, lowest bonding fibers, P16/R30 fraction.

As the FiberLab™ device does not measure absolute values as discussed in Section 3.6, cross-sectional analysis was performed to get a reference for the FiberLab™ measurements. Figure 32 below shows the distribution of the fiber wall thickness of the feed to Pulps A-E. Figure 32 can also be compared to the distribution of fiber wall thickness from the FiberLab™ measurements, Figure 38 in Section 4.6, where the large differences in fiber wall thickness from cross-sectional SEM images and FiberLab™ measurements are discussed. The trends, however not absolute values, in the fiber wall thickness distribution are similar for the two methods, especially with Pulp D towards the higher values. The resolution of the histograms of both methods, however, is too low in this specific case to draw any valid conclusions.

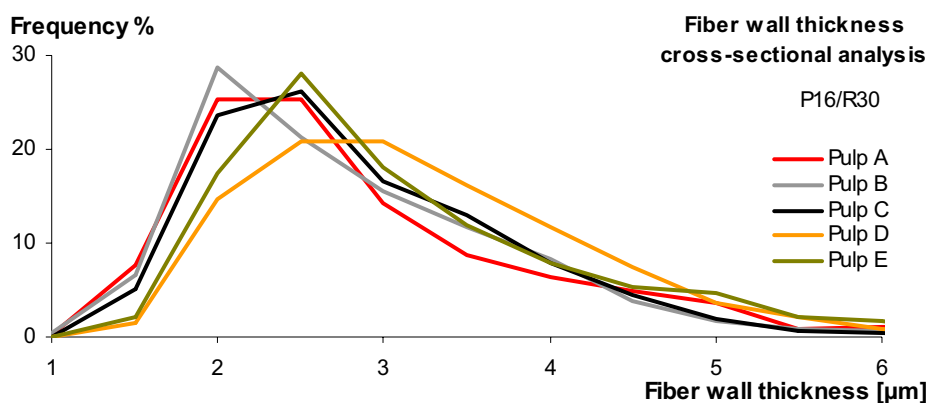


Figure 32. Fiber wall thickness measured from the cross-sectional micrographs, Pulp A-E, P16/R30.

## 4.5 Acoustic emission

Acoustic emission (AE) monitoring was performed on calandered Formette sheets from the P16/R30 Bauer McNett fraction of Pulps A and B. The purpose, was to see whether some AE parameter could be identified that would reflect any anticipated difference in fiber bonding ability.

The load and total number of acoustic hits (acoustic events recorded by the piezo electric transducer) versus time for Pulps A and B are shown in Figures 33a and 33b below. The black stapled curves are the load curves (scale to the left) and the grey curves show the total number of acoustic hits (scale to the right). For reasons of clarity, only the results from Stream 1 and 5 are shown. It should be noted that since the straining rate is constant, time and elongation are directly proportional.

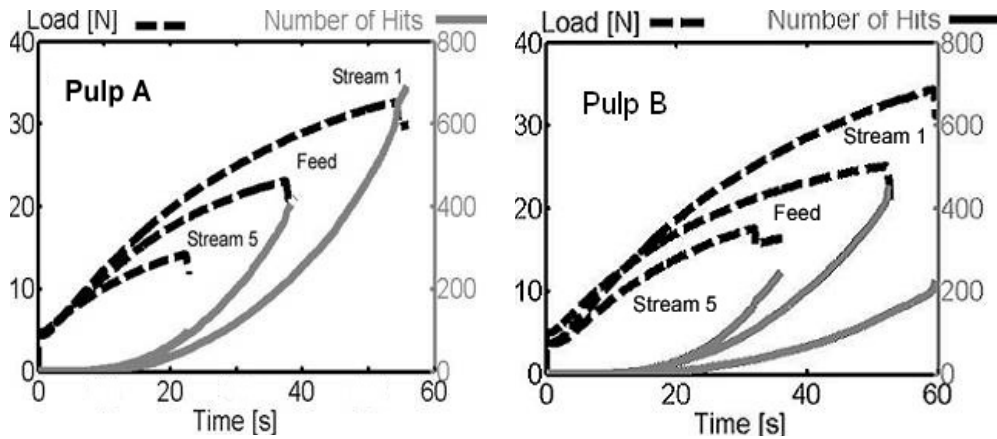


Figure 33a. Load - elongation curves (black) and total number of acoustic hits (grey), Pulp A.

Figure 33b. Load - elongation curves (black) and total number of acoustic hits (grey), Pulp B.

Comparing Stream 1 Pulp A (Figure 33a) and Stream 1 Pulp B (Figure 33b) in the figures above, one main difference appears. Maximum load are not very different between the two (33.2 N for Pulp A and 37.9 N for Pulp B). However, the number of hits is different for the two pulps. For Pulp A, the registered number of recorded acoustic emissions is about three times higher than for Pulp B, to the same load. If the numbers of acoustic events reflect the number of broken fiber bonds, it might suggest that each fiber bond in Stream 1 Pulp B is stronger than Stream 1 Pulp A. This is also discussed in Paper I.

From the acoustic emission curves shown in Figures 33a and 33b, two parameters can be defined. The first one which represents the elastic energy density at onset of

damage (bond failure in this case) is termed  $W_c$  and can be calculated from the results in Figures 33a and 33b according to:

$$W_c = \frac{\sigma_c}{2 * E} \quad \text{Equation 3}$$

In equation 3,  $\sigma_c$  is the load at 10% of the total number of acoustic events at fracture, divided by the product of specimen width and grammage of the paper. E is the E – modulus calculated from the initial slope of the load – elongation curve. For further details regarding  $W_c$  cf. reference 18.

Another parameter which might be of importance when trying to define some quality measure for paper, is the S – index defined according to:

$$S - index = \sigma_f^* * (\varepsilon_f - \varepsilon_c) \quad \text{Equation 4}$$

where  $\sigma_f^*$  is the load at fracture divided by the product of specimen width and grammage of the paper.  $\varepsilon_f$  is the strain at fracture and  $\varepsilon_c$  the strain at 10% of the total number of acoustic events at fracture.

In Figures 34a and 34b, the  $W_c$  and the S – index for both Pulps A and B and for all streams is shown. Both parameters ranked the pulps and the streams in the same way.

The correlation of  $W_c$  from the acoustic emission with traditionally measured fracture toughness is shown in Figure 35a below. The correlation of S-index from acoustic emission with traditionally measured fracture toughness index is shown in Figure 35b below.

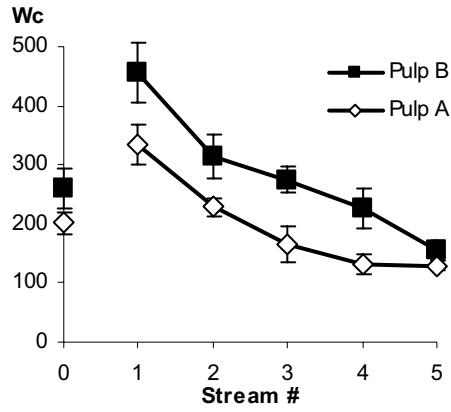


Figure 34a. Wc from acoustic emission measurements for Pulp A and Pulp B, for each stream.

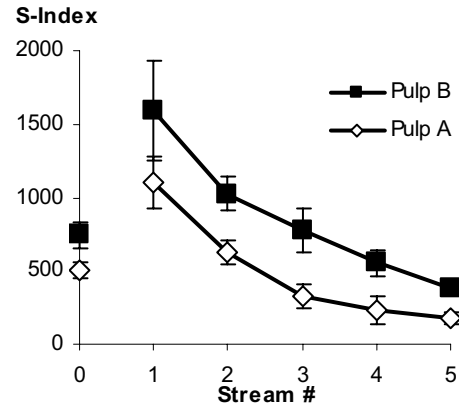


Figure 34b. S-index from acoustic emission measurements for Pulp A and Pulp B, for each stream.

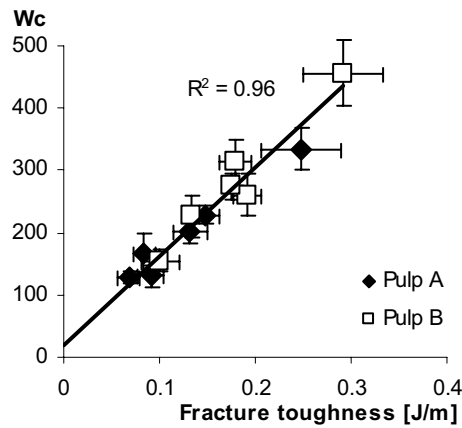


Figure 35a. Correlation between Wc and fracture toughness for Pulp A and Pulp B.

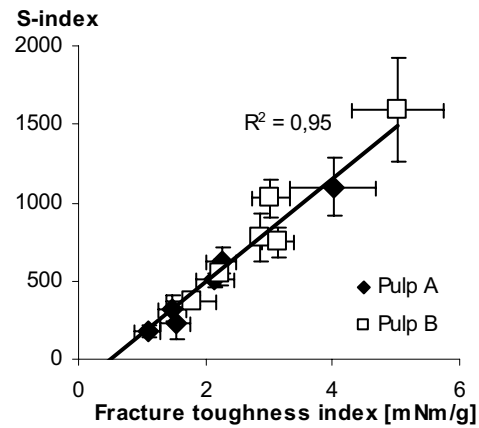


Figure 35b. Correlation between S-index and fracture toughness index for Pulp A and Pulp B.

The acoustic emission results are promising. A lot of information about the fiber behavior under strain is hidden within the cumulative curves of acoustic events and load (Figures 33a and 33b). However more work is needed to conclude what the differences in number of acoustic events, shapes of curves, and other physical parameters withdrawn from the curves really mean for the fiber properties.

## 4.6 Measurement of fiber properties in FiberLab™

Measurements of fibers of the P16/R30 and the P30/R50 fiber length fractions in FiberLab™ give a good idea of the fiber properties, based on a large number of fibers.

### 4.6.1 External fibrillation

External fibrillation was found to be the highest in Stream 1 and lowest in Stream 5 for all measured pulps and for the fiber length fractions P16/R30 and P30/R50, Figures 36a and 36b.

**Fibrillation index [%]**

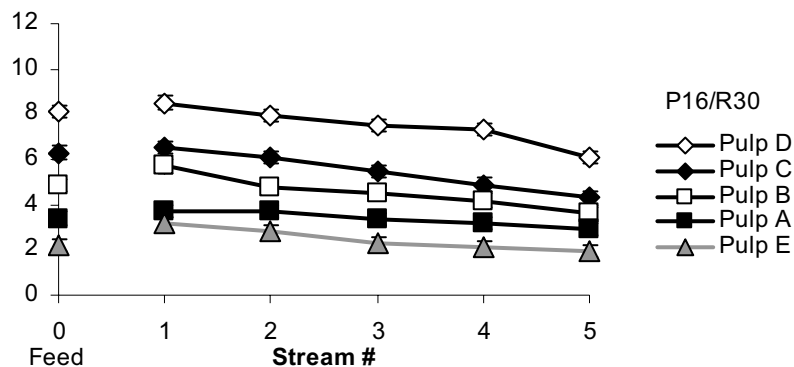


Figure 36a. External fibrillation measured as fibrillation index per stream, fraction P16/R30.

**Fibrillation index [%]**

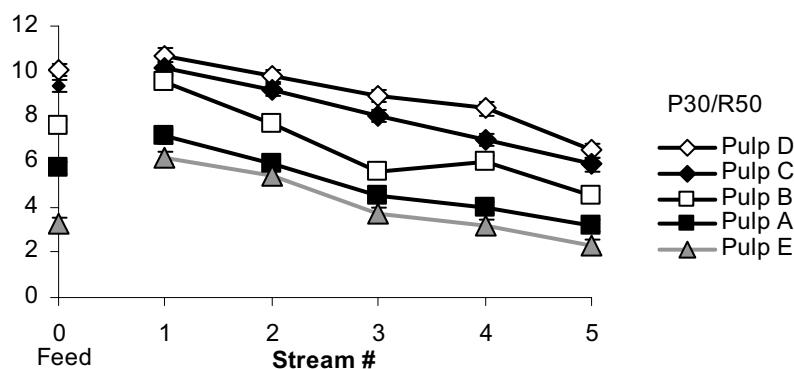


Figure 36b. External fibrillation measured as fibrillation index per stream, fraction P30/R50.

For some pulps, the differences in fibrillation index between Stream 1 and Stream 5 are numerically very small, for example for Pulp A P16/R30, Figure 36a. These differences, however, are larger than they appear from the numerical values. When measuring the fibers, the differences in external fibrillation are even visible in

microscope, with more fibrils on the Stream 1 fibers and basically no fibrils for the lowest bonding fibers in Stream 5. Not knowing the small numerical differences between the levels of external fibrillation, this might be rejected as measuring spreading and the importance of constant and careful up-to-date calibration is thus emphasized. The 95% standard deviations from the triplicate testing are shown in all the figures of FiberLab™ averages.

Although the average values of external fibrillation are very close, the shapes of the distributions for the five tested pulps are different (Figures 2.1 and 2.2 in Appendix 2). The extremes are Pulp D with a fairly level curve and Pulp E with a narrow distribution curve.

#### 4.6.2 Fiber wall thickness

Fiber wall thickness was measured both as distributions and as average values from FiberLab™. For all five pulps and for fiber length fractions P16/R30 and P30/R50, the lowest fiber wall thickness was found in Stream 1 and the highest in Stream 5, Figures 37a and 37b. For both fiber length fractions, Pulp C shows the overall lowest cell wall thickness. The overall highest fiber wall thickness, on the other hand, is Pulp D for the P16/R30 fiber length fraction, and Pulp A for the P30/R50 fiber length fraction.

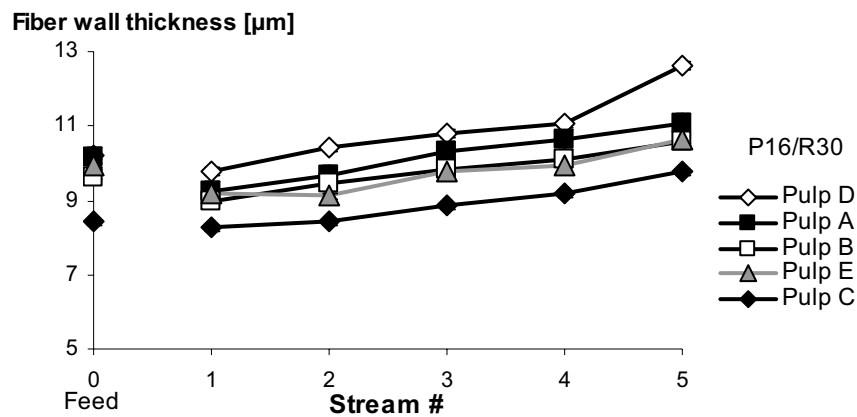


Figure 37a. Fiber wall thickness per stream, fraction P16/R30.

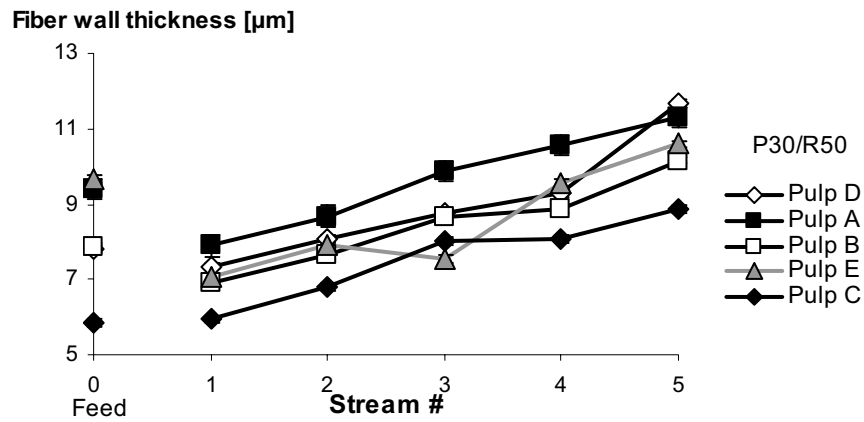


Figure 37b. Fiber wall thickness per stream, fraction P30/R50.

Distributions of fiber wall thickness were forced to be made with wide histogram boxes due to FiberLab™ settings. Figure 38 shows the distribution of fiber wall thickness for the P16/R30 fraction.

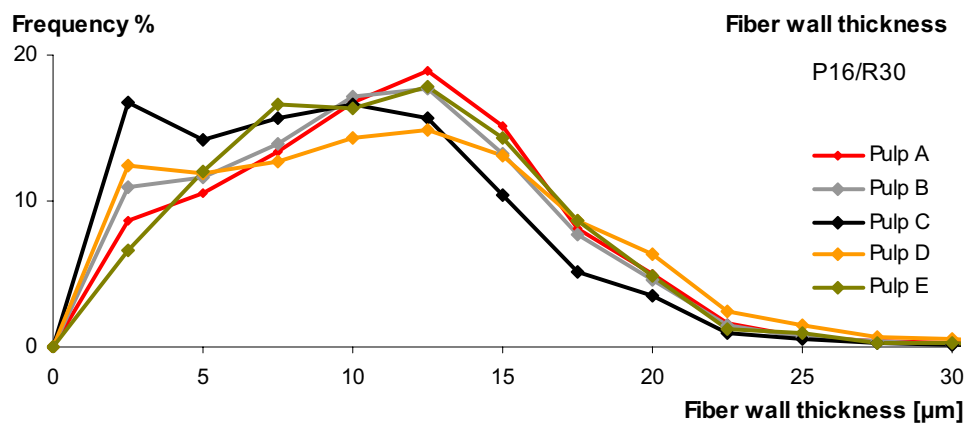


Figure 38. Distribution of fiber wall thickness from FiberLab™ measurements.

As discussed in Section 3.6, the level of the fiber wall thickness measurements from FiberLab™ is not calibrated to real values of fiber wall thickness. Table 4 below shows some average fiber wall thickness from the cross-sectional analysis, and from the FiberLab™ measurements. The differences are large, and FiberLab™ values are used as ranking.

Table 4. Fiber wall thickness from cross-sectional SEM analysis and the FiberLab™ device, Feed pulps, P16/R30 fraction.

Pulp B	Average Fiber wall thickness [μm] Cross-sectional SEM analysis	Average Fiber wall thickness [μm] FiberLab™
Feed (Stream 0)	2.5	9.6
Stream 1	2.3	9.0
Stream 5	2.8	10.6

#### 4.6.3 Fiber width

Fiber width from FiberLab™ was also measured both as average values per stream and as distributions. For both the P16/R30 and P30/R50 fractions, Figures 39a and 39b respectively, average fiber width is lowest in the highest bonding stream, Stream 1, and highest for the lowest bonding stream, Stream 5. For the P16/R30 fiber length fraction, Figure 39a, Pulp D shows the overall highest fiber width and Pulp C the lowest. For the P30/R50 fraction, Figure 39b, Pulp A has the highest fiber width overall, while Pulp C is still the pulp containing the overall thinnest fibers.

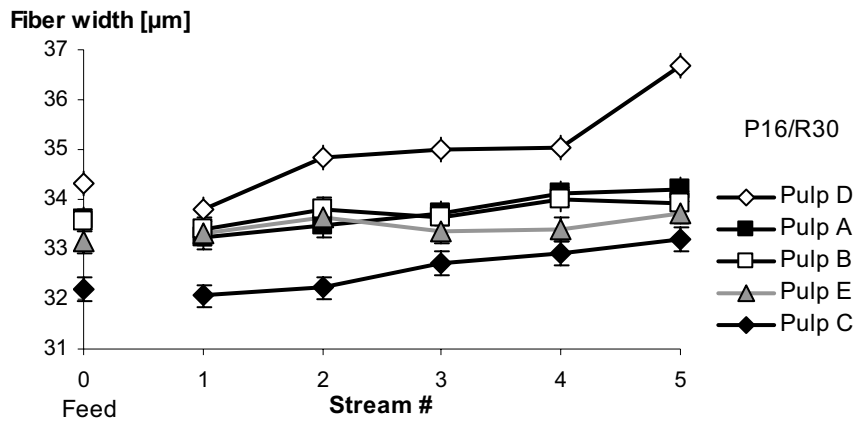


Figure 39a. Fiber width per stream for the P16/R30 fraction.

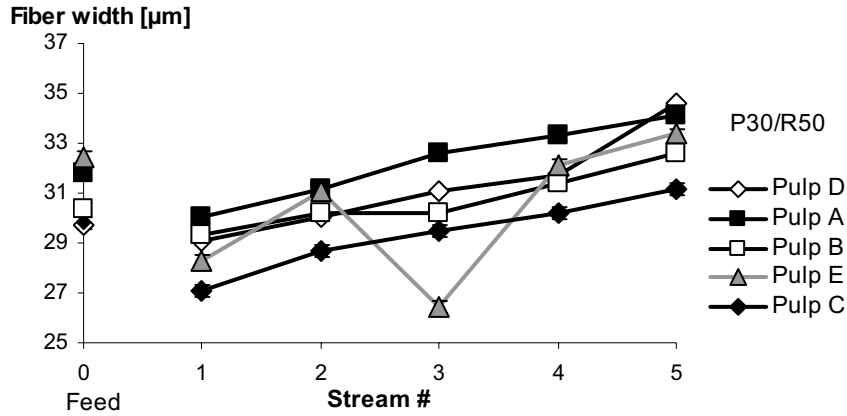


Figure 39b. Fiber width per stream for the P30/R50 fraction.

As for Pulp E Stream 5, P30/R50 fiber length fraction, no explanation has yet been found for the deviant measurement.

The distributions of fiber width of the P16/R30 and P30/R50 fractions are shown in Appendix 2. In the fiber width distributions, Pulp C stands out with the highest amount of thin fibers.

#### 4.6.4 Collapse resistance index (CRI)

Vesterlind and Höglund [16] suggested, together with Gradin at Mid Sweden University, in 2005 that fiber width and fiber wall thickness could be used to calculate collapse resistance index, CRI. As the name implies, a high CRI means that the fiber is more difficult to collapse. In printing paper, where strength and surface are important, a low collapse resistance index is preferable.

After the formula suggested by Vesterlind and Höglund [16], Collapse Resistance Index is calculated as;

$$CRI = \frac{\text{fiberwall thickness}^2}{(\text{fiberwidth} - \text{fiberwall thickness})} \quad \text{Equation 1 by [16, 29]}$$

Average values of Collapse Resistance Index of fiber length fractions P16/R30 and P30/R50, Figure 40a and 40b, show that Pulp C has the overall lowest collapse resistance index of both fiber length fractions. For the P16/R30 fiber length fraction, Pulp D shows the overall highest collapse resistance index and for the P30/R50 fiber length fraction, Pulp A shows the overall highest.

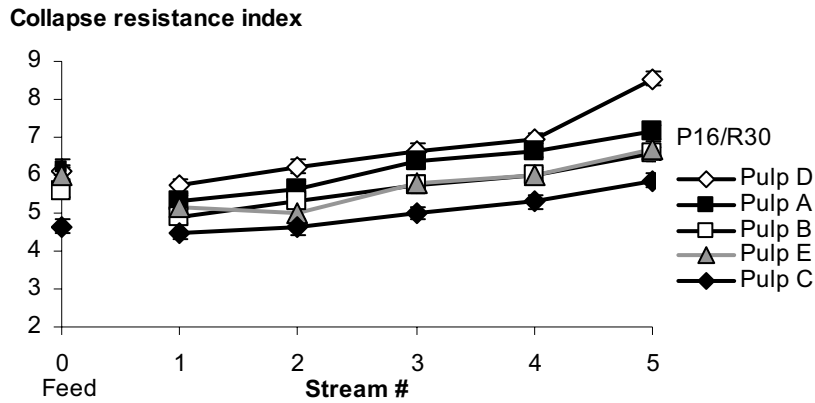


Figure 40a. Collapse resistance index for each stream, P16/R30 fraction.

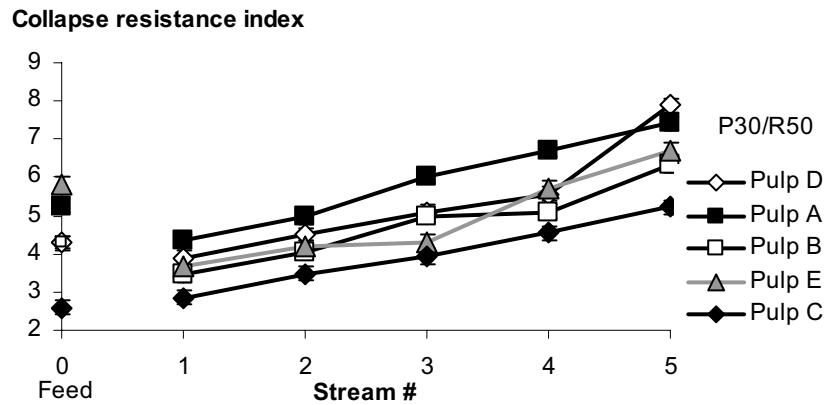


Figure 40b. Collapse resistance index for each stream, P30/R50 fraction.

Distributions of collapse resistance index can be found in Appendix 2 and show that Pulp C has the overall highest amount of low collapse resistance index fibers, for the P16/R30 and the P30/R50 fiber length fractions, Figures 2.7 and 2.8 respectively. For both the fiber length fractions shown, Pulp E has the overall lowest amount of fibers with low collapse resistance index, and a higher amount of fibers with high collapse resistance index.

## 4.7 Bonding Indicator – BIN

### 4.7.1 Prediction of average Bonding Indicator

To be able to determine the importance of various fiber parameters in providing high and low fiber bonding ability, several fiber parameters were evaluated. In Paper I, it is shown how none of the parameters fiber wall thickness, fiber width,

external fibrillation or collapse resistance index (CRI) alone correlates with long fiber tensile strength.

As this study refers to the fundamental fiber properties that affect printing paper surface and strength, fiber bonding ability is believed to be mirrored by long fiber tensile strength [1, 6], further discussed in Section 2.2.1.

It was discovered that linear regression of collapse resistance index and external fibrillation can be combined into one factor, Bonding Indicator or BIN, which correlates with long fiber tensile strength. Figure 41 below shows the correlation of Bonding Indicator and tensile strength of long fiber laboratory sheets.

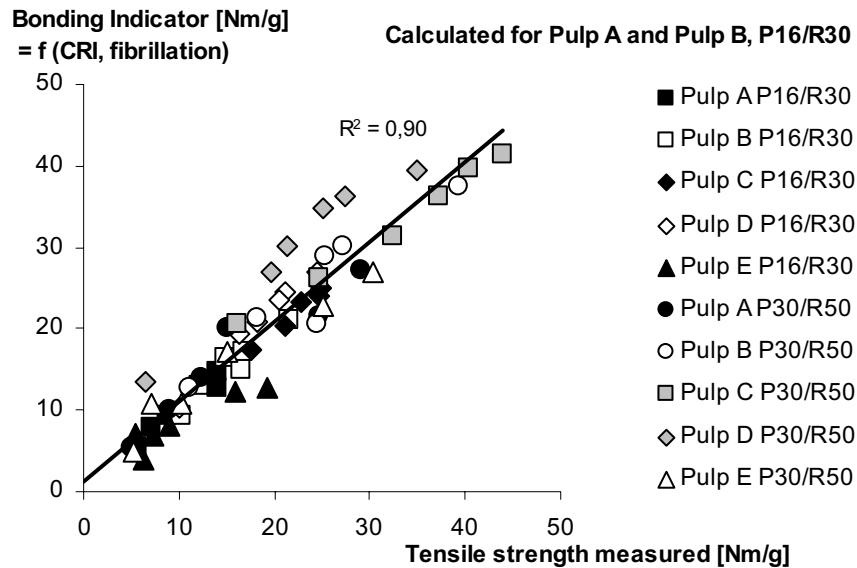


Figure 41. Correlation between measured tensile strength of long fiber laboratory sheets and Bonding Indicator (BIN).

The linear regression used to predict the Bonding Indicator was performed for the P16/R30 fractions of Pulp A and Pulp B. Remaining pulps were then added to the formula of prediction. Interestingly, not only Pulp C, Pulp D, and Pulp E P16/R30 fiber length fraction, but also the pulps of shorter fiber length, P30/R50, adapted this prediction well. This strengthens the results presented by Forgacs [1], Strand [2], and Ferritsius and Ferritsius [3] that fiber length and fiber bonding are independent factors. The basic principle for predicting Bonding Indicator is shown in Equation 2.

$$\text{Bonding Indicator (BIN)} = A + B * \text{CRI} + C * \text{Fibrillation} \quad \text{Equation 2}$$

Collapse Resistance Index, CRI, is calculated by the use of Equation 1 (Section 4.6.4) [16, 29]. Fibrillation index, that is, external fibrillation, is measured in the FiberLab™ device, further explained in Section 3.6.

For Pulp D P30/R50 long fiber fraction, the correlation of predicted and measured tensile strength is not complete; measured Pulp D P30/R50 fraction gave a slightly weaker result than predicted. The reason for this has not yet been established. It is possible that yet another fiber geometry parameter is needed to be able fully to predict the Bonding Indicator of all types of mechanical pulps.

#### **4.7.2 Distributions of Bonding Indicator**

By predicting the Bonding Indicator for each individual fiber, a BIN-distribution can be obtained containing fibers with both positive and negative values. It is believed that the amount of negative BIN fibers and the shape of the BIN-curve characterize the distribution in fiber quality.

It has now been established that the fibers from the hydrocyclone fractionation trials have high, Stream 1, and low, Stream 5, bonding ability, with a consecutively falling scale in between (Sections 4.3 – 4.6). Using these thoroughly evaluated fibers from the different streams in BIN-distributions may therefore help to show whether the method of BIN-distributions is logical or not.

As seen in Figure 42 (magnified in Figures 43a-d), the BIN-distributions arranged themselves in "stream-order". The Stream 1 distribution shows the highest amount of high-BIN fibers (fibers with high BIN on the x-axis) and the lowest amount of low-BIN fibers. Stream 2 has the second lowest amount of low-BIN fibers and so on. The BIN-distribution of the feed is situated in the middle of the streams, between Stream 2 and Stream 3.

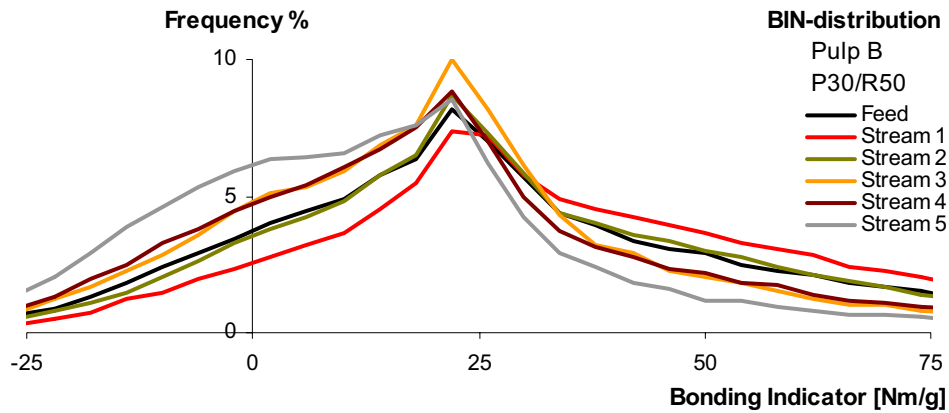
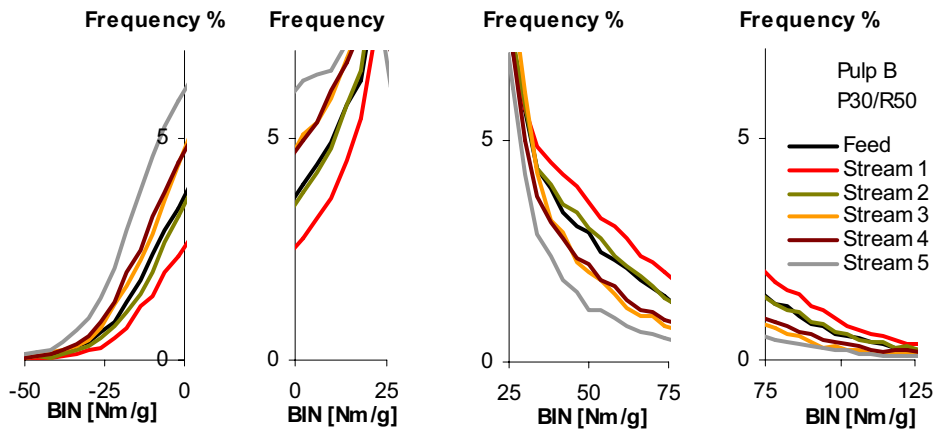


Figure 42. BIN-distribution for each Stream and Feed, Pulp B, P30/R50 fiber length fraction.

The arrangement in stream-order is further displayed in Figures 43a-43d. Some BIN-intervals have been magnified to further illustrate the following relationships:

Stream 5 has the highest amount of low-BIN-fibers and  
Stream 1 has the lowest amount of low-BIN fibers (Figures 43a and 43b).

Stream 5 has the lowest amount of high-BIN fibers and  
Stream 1 has the highest amount of high-BIN fibers (Figures 43c and 43d).



Figures 43a-d. Magnification of Figure 42. BIN-distributions for Stream 0-5, Pulp B, P30/R50 fraction, for different BIN-intervals. High BIN suggests high bonding ability and low BIN suggests low bonding ability. The streams have arranged themselves in "stream-order".

The reason for the feed BIN-distribution being closer to the BIN-distribution of Stream 2 than Stream 3 is found in Figure 25b in Section 4.1. The feed of Pulp B P30/R50 fractionated in the hydrocyclone pilot plant setup so that 56.4 % of all P30/R50 fibers went with Streams 1 and 2, which is why the feed stream is displaced towards Stream 1 and 2, but still fairly central.

The pattern of streams arranged in the BIN-curves by stream-order is valid for all tested pulps, Pulps A - E, for the P16/R30 and P30/R50 fiber length fractions. Distributions for these pulps, together with tables of the amounts of positive and negative BIN can be found in Appendix 3.

The BIN-distributions of Pulps A - E for fiber length fractions P16/R30 (Figure 44a) and P30/R50 (Figure 44b) are shown below. Different pulps give different BIN-distributions. The amount of fibers per stream, Figures 25a and 25b, can be used as a comparison, to get an idea of the amount of high and low bonding fibers respectively.

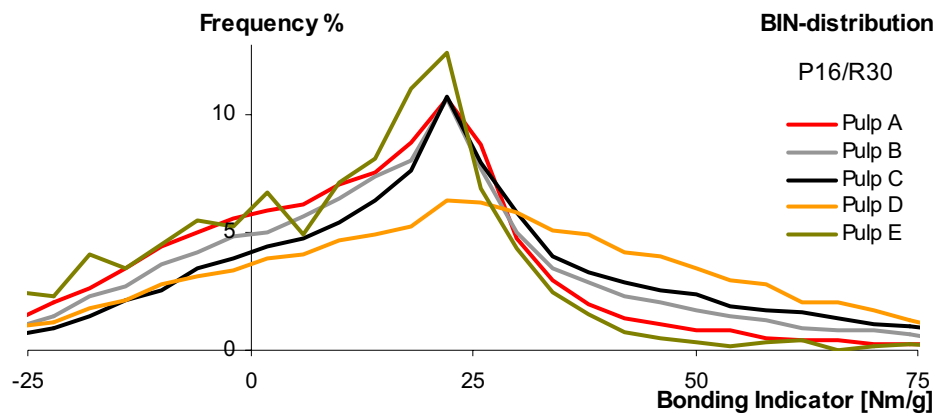


Figure 44a. Distribution of Bonding Indicator for the P16/R30 fraction. The area under each curve is one, and high BIN suggests fibers of high bonding ability.

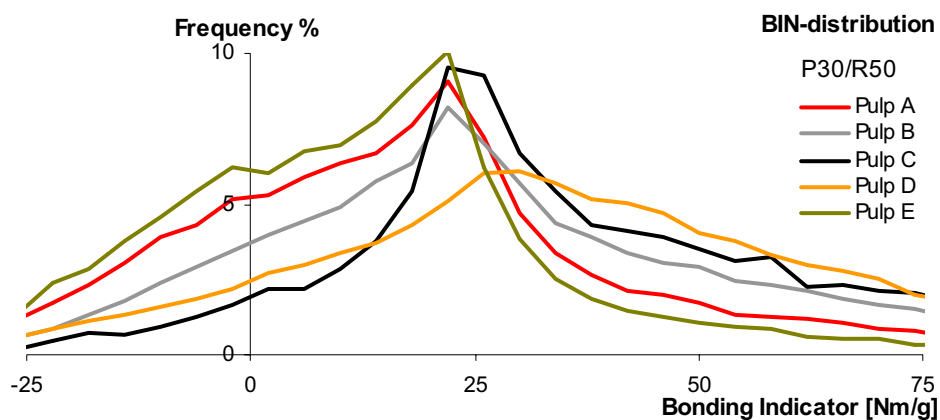


Figure 44b. Distribution of Bonding Indicator for the P30/R50 fraction. The area under each curve is one, and high BIN suggests fibers of high bonding ability.

Figures 44a and b above show that although average BIN is very similar for Feed Pulp C and Pulp D for the P16/R30 fraction (23.9 and 24.5 Nm/g respectively, Figure 41), the BIN-distributions for these pulps are fairly different. Pulp D has a higher amount of high-BIN fibers than Pulp C, but also a slightly higher amount of fibers with negative BIN fibers.

#### 4.7.4 Identifying all fibers in the BIN-distributions

The fibers in the five hydrocyclone streams all originate from the feed. Therefore, it should be possible to identify the fibers from the feed to the five streams. The BIN-distributions of each stream were weighted with the amount of fibers going with each hydrocyclone stream (Figures 25a and 25b). The weighted streams, Streams 1-5 were added and compared with the feed stream. This was done within each of the fiber length fractions, P16/R30 and P30/R50.

An example may clarify how the weighting was performed for Pulp B fraction P30/R50. The Pulp B, P30/R50 feed is a total of 100% and the feed was divided into five streams: 24.5% of all P30/R50 fibers went with Stream 1, 19.7% with Stream 2, 21.8% with Stream 3, 14.9% with Stream 4 and 19.1% with Stream 5. The BIN-distribution of Stream 1 was weighted by 0.245; the BIN-distribution of Stream 2 by 0.197 and so on. These weighted streams were added and compared with the BIN-distribution of the feed for Pulp B, P30/R50 fiber length fraction.

Figure 45 below shows an example of the distributions obtained when the hydrocyclone stream is weighted by amount of fibers.

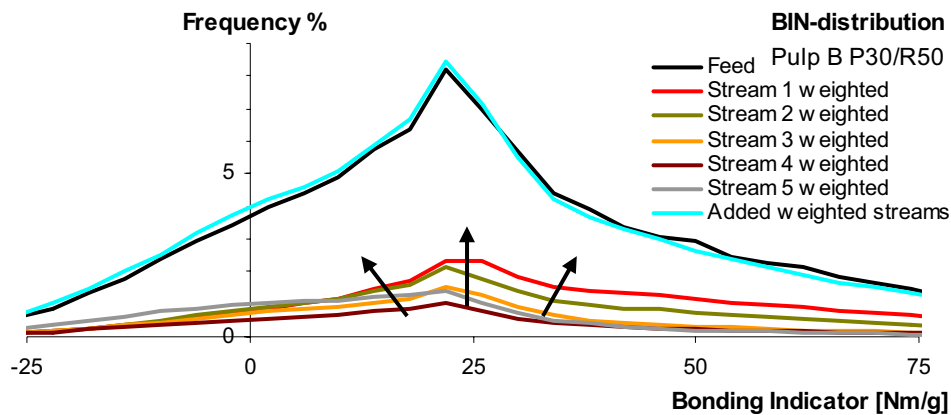


Figure 45. Each stream was weighted by the amount of fibers of that stream from the hydrocyclone fractionation. The added streams formed a curve correlating well with the BIN-distribution of the feed, suggesting that all fibers from the hydrocyclone fractionation were identified.

Figure 45 above suggests that by adding the BIN-distributions of all streams in a pulp, weighted by the amount of fibers that went with that stream, the BIN-distribution of the feed is obtained. This is valid for all five pulps, for both fiber length fractions P16/R30 and P30/R50. It suggests that all ingoing fibers to the hydrocyclones have been identified. It also strengthens the validity of Bonding Indicator (BIN).

#### 4.7.5 BIN-distributions for fibers – without fiber length fractionation

All distributions of Bonding Indicator that have been shown were done for fiber length fractions P16/R30 and P16/R50 respectively. So far, in order to predict average BIN or the BIN-distribution, fractionation of the fibers by fiber length in a Bauer McNett classifier has been performed. This is time consuming as well as requiring a fair amount of material.

Looking at the fiber length distribution of the total pulp, P16/R30, and P30/R50 fractions for one of the pulps, Pulp A (Figure 46), it can be seen that the P16/R30 and the P30/R50 fractions overlap. The main parts of the fibers of both these fiber length fractions are included in the fiber length interval of 0.7-3.2 mm (measured in FiberLab™). Since the BIN prediction works for both the P16/R30 and the P30/R50 fiber length fractions (Figure 41), the fiber bonding mechanisms of these two fiber length fractions should be compatible.

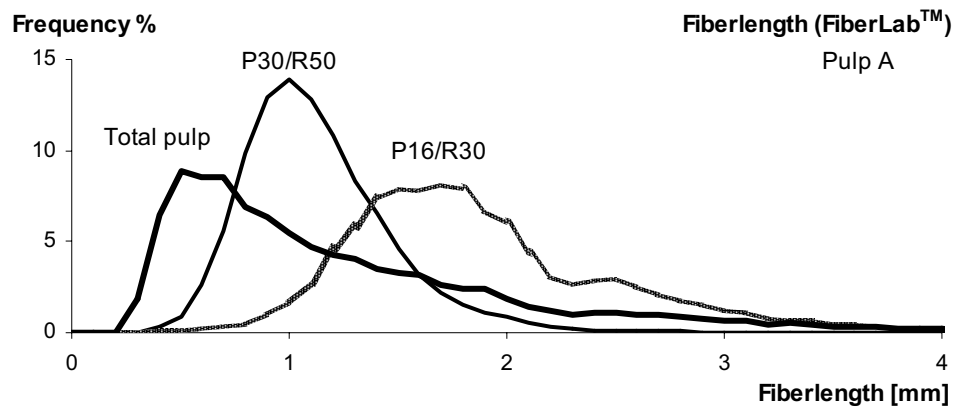


Figure 46. As the prediction of Bonding Indicator works for both the P16/R30 and P30/R50 fiber length fractions, it should be possible to isolate the fiber length interval of the P30/R50 and the P16/R50 fractions and derive the Bonding Indicator from the fiber of this specific interval from the whole pulp.

Fiber length fractionation of the BIN-measured fibers can be performed in the computer. By isolating fibers of a certain lengths from measurements on an entire pulp including fines, the long fiber quality, BIN, can be measured without prior fiber length fractionation.

Figure 47 shows the long fiber Bonding Indicator, calculated from whole pulps, not fiber length fractionated mechanically, only digitally. Comparing Figure 47 below with Figures 44a and 44b, the BIN-distributions for the P16/R50 and P30/R50 fiber length fractions, it can be seen that the distributions are fairly similar. This suggests that it is possible to derive the Bonding Indicator of fibers from the whole pulp without fractionating by fiber length for example in a Bauer McNett classifier, first.

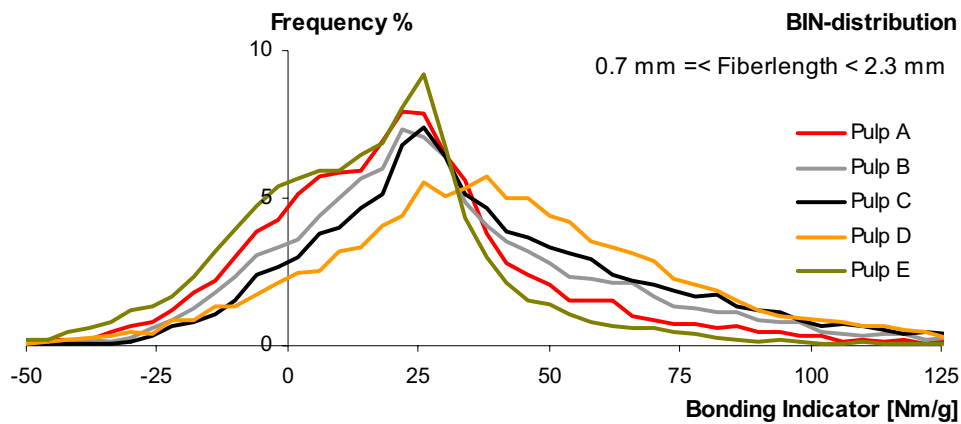


Figure 47. BIN-distribution of fibers, calculated from the entire pulp, for fibers of isolated fiber length 0.7-2.3 mm.

Table 5 below shows the amount of negative BIN fibers for Pulp A-E for different fiber length intervals (isolated from entire pulps) and for the P16/R30 and P30/R50 fiber length fractions. It is believed, that the amount of negative-BIN fibers might be one of the BIN-measures (besides the shape of the BIN-curve) on the fiber characteristic. The amount of negative-BIN fibers, as well as the shapes of the BIN-curve, should of course be expected to be different for different pulping grades.

By comparing the amount of negative BIN-fibers for selected isolated fiber lengths, it should be possible to get an idea of which fiber lengths can be used for the BIN-distributions from an entire pulp.

Pulp E shows the largest difference between amounts of negative BIN for different fiber lengths. For the fiber lengths interval 0.5-1.5 mm, Pulp E shows 13.6% negative BIN, whereas for remaining fiber length fractions, the amount of negative BIN-fibers is significantly higher (Table 5). For remaining pulps, Pulp A-D, the differences in amount of negative BIN-fibers between the different fiber lengths are smaller. However, more work is needed to conclude between which fiber length intervals the BIN-distributions should be calculated. More tables showing the amount of negative BIN fibers for different streams and pulps can be found in Appendix 3.

Table 5. Amount of negative BIN fibers for BIN-distributions from five different fiber lengths intervals and the Bauer McNett fractions P16/R30 and P30/R50.

Amount negative BIN [%]	Pulp A	Pulp B	Pulp C	Pulp D	Pulp E
P16/R30	28.1	22.5	16.3	18.7	30.7
P30/R50	24.3	14.6	6.5	11.2	29.2
0.5-1.5 mm	15.5	11.1	7.7	8.6	13.6
1.5-2.5 mm	20.1	17.1	12.3	12.3	40.7
2.5-4.0 mm	19.4	19.5	13.0	9.8	46.0
0.7-2.3 mm	19.1	14.4	9.9	10.4	26.5
0.7-3.5 mm	18.6	14.5	9.9	10.2	28.9

For all the BIN-distributions created so far, either for the P16/R30 or P30/R50 fiber length fractions or for isolated fiber lengths from the entire pulp, the top of the distributions has constantly been at BIN about 25 Nm/g. The reason for this has not yet been established, but will be investigated in work to be carried out in the near future.

To sum up the result section, it seems that a distribution of Bonding Indicator of fibers in mechanical pulp furnishes (with “bonding” as defined in Section 2.2.1) can be predicted by optical analyzing methods. Also the prediction of BIN for fibers from entire pulps is of importance, as this method is hoped to be of industrial use.

## 5. FINAL DISCUSSION

This study presented a method of measuring the distribution of fiber bonding ability in mechanical pulps. As discussed in Section 2.2.1, the term fiber bonding is somewhat cunning, as it refers to different kinds of bonding. When discussed from a mechanical pulping point of view, fiber bonding ability in this work is used to describe how the fiber properties will contribute to surface properties and structure and strength of the printing paper. This is influenced by the ability of the mechanical fibers to form contact areas. Without fiber-fiber or fiber-fibril contact area, no fiber-fiber interactions of any kind will be formed.

The optical measurements of the FiberLab™ device showed that it was possible to predict the tensile strength of long fiber laboratory sheets, using linear regressions of collapse resistance index and external fibrillation. The parameter obtained, that correlates with the tensile strength of laboratory sheets of the P16/R30 and P30/R50 fiber length fractions, is named Bonding Indicator or BIN. The linear regressions that were used for the prediction of Bonding Indicator were performed for the five hydrocyclone streams and feed of Pulp A and Pulp B Bauer McNett fractions P16/R30 only. Pulp C-E P16/R30 fraction, Pulp A-C, and Pulp E P30/R50 fraction also adapted well when inserted into the equation, and correlated just as well with tensile strength as the pulps used for the linear regression. For one pulp, Pulp D, P30/R50 fraction, the prediction did not work as well as for the other types of fibers, as it was weaker than predicted. It is possible that yet another parameter is needed to fully understand the mechanisms of fiber bonding ability in all mechanical pulps, or that the assumption that the fiber is circular (used for predicting CRI, [16]) did not work for this particular fiber fraction.

The variations in inherent fiber properties of the raw material that enters the mill are, and will always be, considerable in a northern climate. One working hypothesis of this study was that since there is a distribution in, among other things, fiber wall thickness and diameter inherent in the wood fibers, there might be a distribution also of fiber bonding ability in the pulp produced by this raw material. Average values, as used today, might not be sufficient to characterize the mechanical pulp fibers. By using the Bonding Indicator formula for each individual fiber from the raw data delivered from the optical measurements, a distribution of Bonding Indicator, BIN, was predicted (raw data for each fiber containing information about the fiber length, width, wall thickness, external fibrillation etc). As there is now a tool available, to measure the distribution of fiber bonding ability, several new questions arise – How is the distribution of Bonding Indicator changing over different process steps? How is the BIN-distribution

affected by specific process changes? Are there any clear correlations between different BIN-distributions and specific printing paper quality parameters?

The principle formula for predicting Bonding Indicator is shown in the thesis. However, with different levels of calibrations for different FiberLab™ devices, the constants may differ from FiberLab™ to FiberLab™ and are therefore not published. In this study, collapse resistance index (CRI), as calculated from reference 16, was one fiber parameter used for predicting the Bonding Indicator. It is not impossible that collapse resistance index calculated in this specific way can be replaced with another measure of contact area, to predict the Bonding Indicator.

This method is intended for industrial use and to predict the BIN-distribution for mechanically fractionated fiber length intervals was interesting enough. However to also be able to predict the BIN-distributions of fibers from raw data of the entire pulp much increased the prospects of an online method.

As mentioned above, a tool for measuring the bonding ability distribution in mechanical pulp furnishes is now available and there are several questions to be answered. One of them, asked by dear Luigi mentioned in Section 1, was “How many of our fibers have too low bonding?” Hopefully, the BIN-method will give the answer shortly.

## 6. CONCLUSIONS

*In this study concerning fiber bonding ability in mechanical pulp furnishes, it has been concluded that:*

- It is possible to predict Bonding Indicator (BIN) from collapse resistance index and external fibrillation from optical measurements. Bonding Indicator correlates with tensile strength of laboratory sheets from long fiber fractions.
- It is possible to measure the distribution of fiber bonding ability in mechanical pulps. The BIN-distribution indicates the amount of fiber with low and high predicted Bonding Indicator.
- BIN-distributions of fibers of selected fiber lengths can be obtained from measurements on the whole pulp, without prior fiber length fractionation. This is of great value as the method is intended as an industrial and possibly on-line method.

## 7. FUTURE WORK

*Future work in this study will include:*

Further evaluation of the BIN-method in different process steps.

Investigations of which BIN-distributions are characteristic for different pulp- and paper qualities.

Investigations of which fiber lengths are the most representable for isolation of certain fiber lengths when predicting the BIN-distributions of fibers from entire pulps.



## 8. ACKNOWLEDGEMENTS

This study was carried out at Stora Enso Kvarnsveden Mill, Borlänge, Sweden and at Stora Enso Research Centre Falun, Falun, Sweden, in cooperation with Mid Sweden University, FSCN, Mechanical Pulping Industrial Research College, from May 2006 to May 2008. Financial support has been provided by the Swedish Knowledge Foundation (KK-stiftelsen). Pilot trials were performed at Noss AB, Norrköping.

Industrial supervisor in the project was Olof Ferritsius, M.Sc., Research Manager Mechanical Fibers at Stora Enso Research Center Falun. University supervisors were Professor Hans Höglund, Mid Sweden University and Professor Per Engstrand, Mid Sweden University. The extended supervisory group also included Hans Ersson, Development Manager at Stora Enso Kvarnsveden Mill, Rita Ferritsius, Senior Specialist at Stora Enso Research Centre Falun and Per Gradin, Professor of Solid Mechanics, Mid Sweden University.

*I would like to pay all of the following people special thanks for their various and valued contributions to the project.*

Olof Ferritsius, Stora Enso Research Center, Falun, Sweden. Together with Rita Ferritsius and Hans Ersson the creator of this project, which started out as a master's thesis study. The project could never have been carried out without the insight and inventiveness of Olof who has been a compass for this whole investigation. Thanks for sharing your knowledge, for new ideas, for a mind more open than the Vasaloppet start field the night before the ski-race, for not only thinking outside the box, but actually creating new boxes and for never-failing support and encouragement. You are the Karl Popper of mechanical pulping!

Hans Ersson, Stora Enso Kvarnsveden Mill, for letting a "master student crazy enough to be interested in mechanical fibers" into the department, for foresight of the mill's future needs, for recognizing the demands of increased fiber knowledge, for never-ending sport stories and above all, for total support and encouragement.

Rita Ferritsius, Stora Enso Research Center, Falun, Sweden, for sharing your fiber- and refining process expertise, for always sticking to what you know is right, for your intoxicating curiosity to find out more about fundamental fiber properties and for your contribution in bringing the FiberLab™ to Stora Enso Research Centre Falun, which has been of the greatest importance both to this study and to

continued research in the area. Thanks also for coming up with the name of BIN designation, Bonding Indicator.

Professor Hans Höglund, Mid Sweden University FSCN, the initial academic supervisor of the project. For creating the foundation stones for the project's university establishment, and for solid support when needed most.

Professor Per Engstrand, Mid Sweden University, for continuing the work started by Hans Höglund and trying to bring the academic world closer to the industry (or the other way around).

Professor Per Gradin, solid mechanics, Mid Sweden University for bringing a physicist's view on pulp and paper into the discussion and thereby opening up new worlds.

The Swedish Knowledge Foundation for financial support and genuine interest in the topics of research

Oleg Shagaev, Annika Bjärestrand, Bernt Bergström, Martin Gustavsson, Elisabeth Kurula and all the staff involved at Noss AB – for inspiring cooperation, co-authoring (Oleg), excellently performed pilot trials, text reviewing, enthusiasm, good company during long pilot trial nights and for introducing me to Norrköping's best pizza.

The members of Mid Sweden University FSCN Industrial Research College for relevant and inspiring discussions, technical input and lots of fun. Special thanks to Magnus Paulsson for valuable help with the report.

Luigi Alfonsetti, Stora Enso, for asking the question that we are now trying to answer – “How many of our fibers have too low bonding?”

Anders Hansson and Mikael Rautio, Stora Enso Research Center Falun, for trustworthy programming help, bad Star Wars jokes, encouraging Dilbert-cartoons, fun trips together and for enduring my constant need of carbohydrates and coffee.

Tomas Larsson, Stora Enso Kvarnsveden, for insightful technical input, for bringing the consumer aspect into quality thinking, for a national and global overall view of the demands on pulp and paper, and also for motivating me to find something we can really use.

Tomas Haglund, Kurt Sundstedt, Martin Jansson, Tobias Åslund, Jens Erkers, Mats Tanse, Kvarnsveden Mill, for process consulting.

Örjan Sävborg and Olle Henningson, Stora Enso Research Center Falun, for excellent fiber microscopy and sample preparation, for cross-sectional micrographs analysis and a much appreciated will to share your knowledge

Mats Hiertner, Stora Enso Research Center, for support worthy a dictionary about standard deviation philosophy.

All laboratory personnel at Stora Enso Research Center Falun for help in producing and testing the lab sheets and your amazingly well fulfilled ambition to always performing 100%, no matter what the situation. Thanks also for good company during these years.

Development engineers, operators and laboratory personnel at Kvarnsveden Mill – for good discussions, good input, support in every possible way and good company. A special thanks to Fredrik Lundström, development engineer, TMP, who has been involved in this project from the beginning, for good process discussions and for enhancing quality thinking throughout the mill. One day we will get rid of the “f-word” (f-ness).

Julia Netrval and Hanna Sohlén, for well performed work during the summer.

Andrew Casson and Naomi Little, for linguistic help with the report.

Professor Mikael Lindström, Pulp Technology, Royal Institute of Technology, Sweden – for being the first to suggest that the master thesis that started this project should continue as a licentiate study.

Jacob Stångmyr, Stora Enso Kvarnsveden, for Excel consulting and for help with creating the data base.

Pethra Nordlund, Stora Enso Kvarnsveden, and Anna Häggström, Mid Sweden University FSCN, for arranging, organizing and reminding.

Mats Tanse and Jan-Erik Nordström, for company during way too late nights at the mill office. Last one locks the doors, first one serves the coffee.

Matts Bjerneby, Kvarnsveden Mill, for ensuring me that no matter the outlook, there is still hope. And also that it is never too late to give in :=)

Ylva, Hajer, Susanna, Lina, Christina, Anna, Linda for lots of fun during our student years and more fun to come.

The brain works best at above 175 heartbeats per minute (empirically concluded) – thanks to Coach and training friends.

Mum and dad, Henk and Jonte, for 100% support throughout the years, regardless of my particular interest at the moment.

Robban, for listening to all my fiber thoughts, for input from the world outside the pulp and paper industry bowl, for cooking, encouraging, complementing and advising, for being you.

## 9. REFERENCES

- [1] **Forgacs, O.L.** (1963): "The characterization of Mechanical Pulps", Pulp Paper Mag. Can., 64: 89-116.
- [2] **Strand, B.** (1987): "Factor Analysis as Applied to the Characterization of High Yield Pulps", TAPPI Pulping Conf. Washington D.C., USA, November 1-5, 1987, 61-66.
- [3] **Ferritsius, O. and Ferritsius, R.** (2001): "Experiences from Stora Enso mills of Using Factor Analysis for Control of Pulp and Paper Quality.", Int. Mechanical Pulping Conf., Helsinki, Finland, June 4-8, 2001, 495-504.
- [4] **Ferritsius, O. and Ferritsius, R.** (1997), "Improved Quality Control and Process Design in Production of Mechanical Pulp by the Use of Factor Analysis", Int. Mechanical Pulping Conf., Stockholm, Sweden, 1997, 111-126.
- [5] **Ferritsius, R. and Rautio, M.** (2007): "Differences on fibre level between GW and TMP for magazine grades", Proceedings, Int. Mechanical Pulping Conf., Minneapolis, USA, May 6-9, 2007, CD-ROM.
- [6] **Mohlin, U.-B.** (1989): "Fiber Bonding Ability – a Key Pulp Quality Parameter for Mechanical Pulps to Be Used in Printing Papers." Proceedings Int. Mechanical Pulping Conf., Helsinki, June 6-8 1989, Finland, 49-57.
- [7] **Karnis, A.** (1981): "Refining of Mechanical Pulp Rejects", Proceedings, Int. Mechanical Pulping Conf., Oslo, Norway, June, 16-19, 1981.
- [8] **Shagaev, O. and Bergström, B.** (2005): "Advanced Process for Production of High Quality Mechanical Pulps for Value-Added Paper Grades." Proceedings, Int. Mechanical Pulping Conf., Oslo, Norway, June 7-9, 2005, 169-179.
- [9] **Reme, P. A.** (2000): "Some effects of wood characteristics and the pulping process on mechanical pulp fibres", Doktor ingeniør degree, Norwegian University of Science and Technology, Trondheim, Norway.
- [10] **Kure, K.-A.** (1997): "The Alteration of the Wood Fibres in Refining", Proceedings, Int. Mechanical Pulping Conf., Stockholm, Sweden, June 9-13, 1997, 137-150.
- [11] **Reme, P. A., Johnsen, P. O., and Helle, T.** (1999): "Changes induced in early-and latewood fibres by mechanical pulp refining", Nord. Pulp Paper Res. J. 14(3), 256-262.

- [12] **Norman, F., and Höglund H.** (2003): "Moisture-induced Surface Roughness in TMP-based Paper – The Influence of Fiber Cross-section Dimensions" Proceedings, 23rd Int. Mechanical Pulping Conf., Quebec, Que., Canada, June 2-5, 2003, 409-414.
- [13] **Dickson, A.R., Corson, S.R., Dooley, N.J.** (2005): "Fibre collapse and de-collapse determined by cross-sectional geometry", Proceedings, 24th Int. Mechanical Pulping Conf., Oslo, Norway, June 7-9, 2005.
- [14] **Mörseburg, K.** (2000): "Development and characterization of Norway spruce pressure groundwood pulp fibres", Academic dissertation, Åbo Akademi University, Turku, Finland.
- [15] **Kauppinen, M.** (1998): "Prediction and Control of Paper Properties by Fiber Width and Cell Wall Thickness Measurement with Fast Image Analysis", PTS Symposium: Image analysis for Quality and Enhanced productivity.
- [16] **Vesterlind, E.-L. and Höglund, H.** (2005): "Chemi-mechanical pulp made from birch at high temperature", Proceedings, SPCI International Conference, June 14-16 2005, Stockholm, Sweden.
- [17] **Gradin, P.A., Nyström, S., Flink, P., Forsberg, S., Stollmeier, F.** (1997): "Acoustic Emission Monitoring of Light-Weight Coated Paper". J. Pulp Paper Sci. 23(3), 113-118.
- [18] **Isaksson, P., Gradin, P.A. and Kulachenko, A.** (2006): "The onset and progression of damage in isotropic paper sheets", International Journal of Solids and Structures 43, pp 713-726.
- [19] **Salmén, L.** (1985): "Mechanical properties of wood fibers and paper in Cellulose Chemistry and its Applications" eds. T.P. Nevell and S.H. Zeronian Ellis Horwood Ltd., 505-530.
- [20] **Ilvessalo-Pfäffli, M.-S.** (1995): "Fiber Atlas, Identification of Papermaking Fibers", Springer-Verlag, Berlin, Heidelberg.
- [21] **Reyier, S.** (2006): "Fractionation of mechanical fibers with respect to bonding", Masters thesis, Royal Institute of technology, Stockholm, Sweden.
- [22] **Panshin, A. J. and DeZeeuw, C.** (1970): Textbook of wood technology. "Vol. I: Structure, identification, uses and properties of the commercial woods of the United States and Canada". 3rd edition, McGraw-Hill, New York.

- [23] **Sundholm, J.** (1999): Papermaking Science and Technology, Chapter 4 "Fundamentals of mechanical pulping", Gummerus Printing, Jyväskylä, Finland, 35- 65.
- [24] **Daniel, G.**, (2004): The Ljungberg Textbook Chapter 3: "Wood and Fibre Morphology", Royal Institute of Technology, Stockholm, Sweden.
- [25] **Ezpleta, L.B., and Simon, JLS.** (1970): "Atlas de fibres para pasta de celulosa II parte, Vol 1., Ministerio de Agricultura", Madrid.
- [26] **Huusari, E.** (1999): "Refining of shives and coarse fibers", Chapter 10, Papermaking Science and technology Mechanical Pulping, Gummerus printing, Jyväskylä, Finland, 289-310.
- [27] **Henriksson, G., Lennholm, H., Brännvall, E.** (2004): The Ljungberg Textbook, Wood Chemistry and Wood Biotechnology, Chapter 2: "The Trees", Royal Institute of Technology, Stockholm, Sweden.
- [28] **Lennholm, H., Blomqvist, K.** (2004): The Ljungberg Textbook, Wood Chemistry and Wood Biotechnology, Chapter 4 "Cellulose", Royal Institute of Technology, Stockholm, Sweden.
- [29] **Vesterlind, E.-L.** (2006): "High temperature CTMP from birch", Licentiate of Philosophy thesis, Mid Sweden University, Sundsvall, Sweden.
- [30] **Höglund, H., Sohlén, U., and Tistad, G.** (1976): "Physical properties of wood in relation to chip refining", Tappi; 59(6): 144-147.
- [31] **Fellers, C., Norman, B.** (1998): "Pappersteknik", Institutionen för Pappersteknik, Kungl Tekniska Högskolan, Stockholm, Sweden.
- [32] **Sundholm, J.** (1999): Papermaking Science and Technology, Chapter 3: "History of mechanical Pulping", Gummerus Printing, Jyväskylä, Finland, 23-33.
- [33] **Ferritsius, O.** (1996): "Control of Fundamental pulp properties in TMP and SGW production by the use of factor analysis", Proceedings, SPCI, World Pulp and Paper week, June 4-7, 1996, Stockholm, Sweden, Part I, 245-255.
- [34] **Torgnysdotter, A., Kulachenko, A., Gradin P. and Wågberg, L.** (2007): "The link between the fibre contact zone properties and the physical properties of paper: A way to control paper properties.", Journal of Composite Materials, 41(13), 1619.
- [35] **Wågberg, L., Forsberg, S., Johansson, A., Juntti, P.** (2002): "Engineering of Fibre Surface Properties by application of the Multilayer Concept. Part I: Modification of Paper Strength", J. Pulp Paper Sci., 28 (7), 222-227.

- [36] **Wakelin, R.F.** (2004): "Evaluation of pulp quality through sedimentation measurements", 58th Appita annual conference and exhibition, Canberra, ACT, Australia, 19-21 April, 2004, Paper 3A41, 9.
- [37] **Klinga, N.** (2007): "The influence of Fibre Characteristics on Bulk and Strength Properties of TMP and CTMP from Spruce", Licentiate of technology thesis, Mid Sweden University, Sundsvall, Sweden.
- [38] **Clark, J. d'A.** (1985): "Some thoughts on fiber classification and length", Tappi J. 68(8), 119-120.
- [39] **Petit-Conil, M., Cocheaux, A., and de Choudens, C.** (2004): "Mechanical pulp characterisation: a new and rapid method to evaluate fibre flexibility", Pap. Puu 76(10), 657-662.
- [40] **Sjöström, E.** (1993): "Wood chemistry Fundamentals and Applications", Academic press Inc., San Diego, California.
- [41] **Teleman, A.** (2004): The Ljungberg Textbook, Wood Chemistry and Wood Biotechnology, Chapter 5 "Hemicelluloses and Pectins", Royal Institute of Technology, Stockholm, Sweden.

## APPENDIX

The appendix contains figures of interest for this study that for space matters had to be excluded from Section 4. The figures in the appendix are denoted after the appendix chapters.

### Appendix 1. Physical parameters of long fiber laboratory sheets

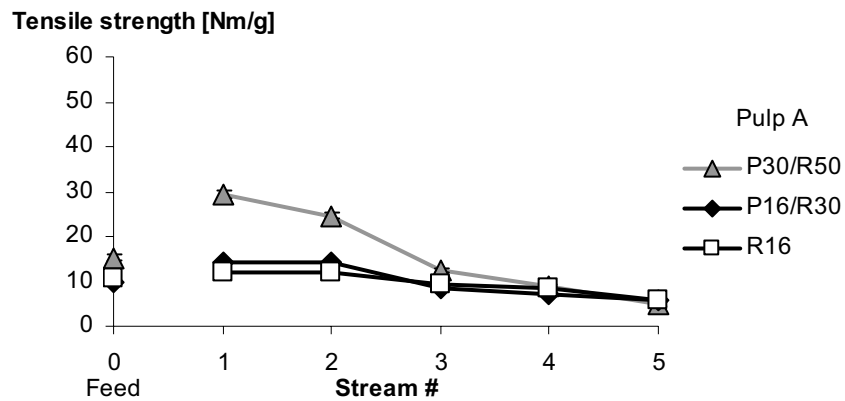


Figure 1.1. Tensile strength per stream, fractions R16, P16/R30, and P30/R50, Pulp A.

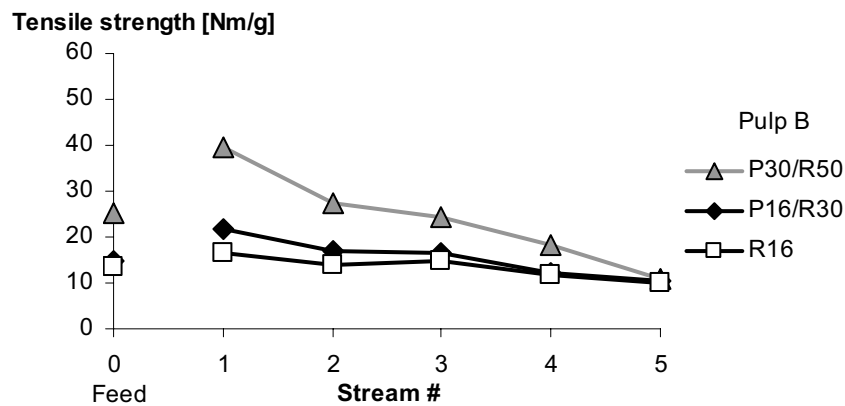


Figure 1.2. Tensile strength per stream, fractions R16, P16/R30, and P30/R50, Pulp B.

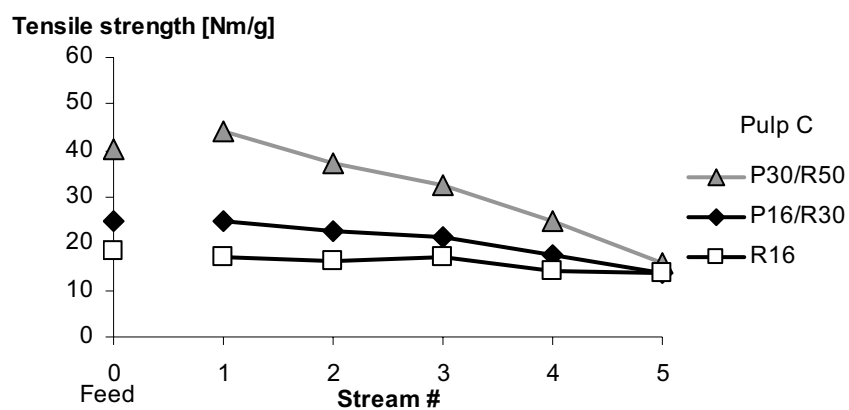


Figure 1.3. Tensile strength per stream, fractions R16, P16/R30, and P30/R50, Pulp C.

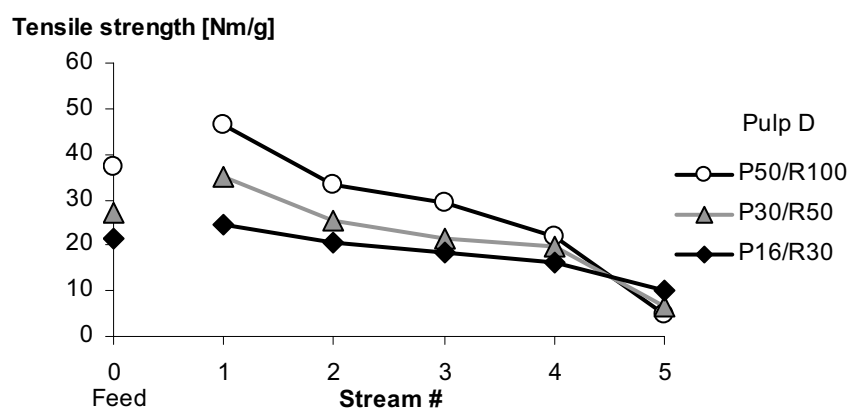


Figure 1.4. Tensile strength per stream, fractions P16/R30 and P30/R50, and P50/R100, Pulp D.

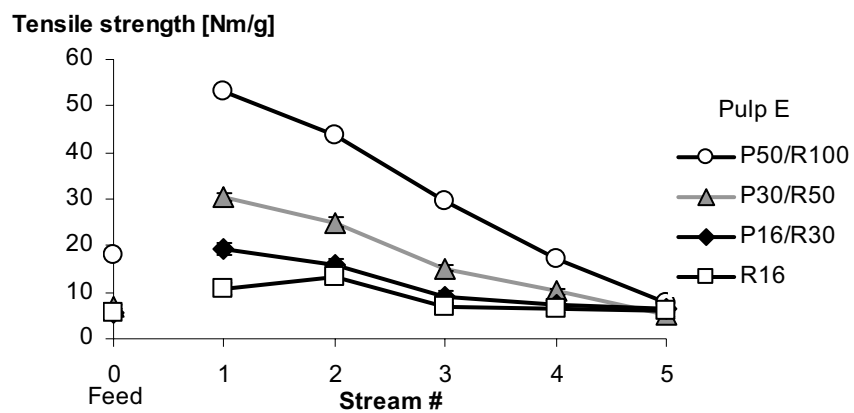


Figure 1.5. Tensile strength per stream, fractions R16, P16/R30, P30/R50, and P50/R100, Pulp E.

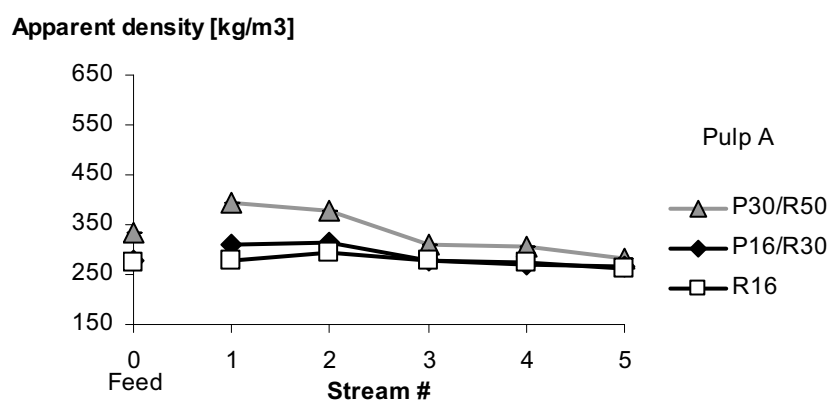


Figure 1.6. Apparent density per stream, fractions R16, P16/R30, P30/R50, Pulp A.

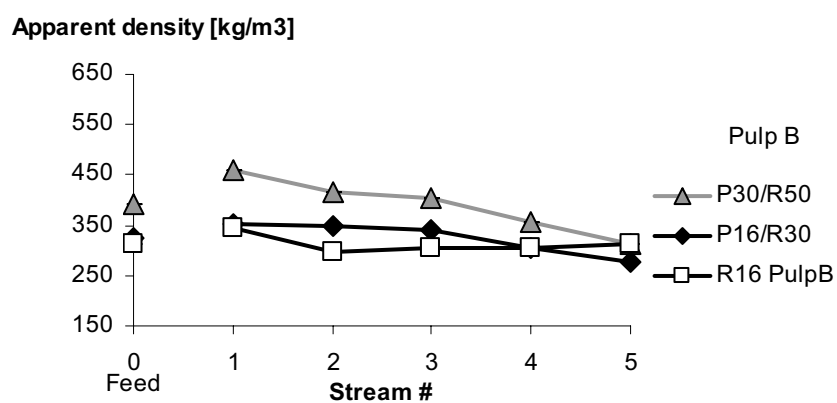


Figure 1.7. Apparent density per stream, fractions P16, P16/R30, P30/R50, Pulp B.

**Apparent density [kg/m<sup>3</sup>]**

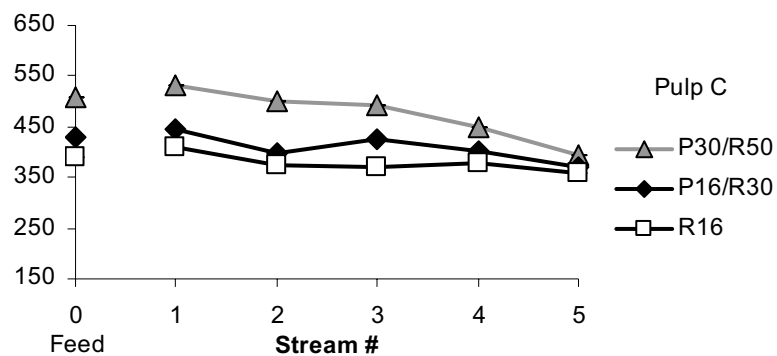


Figure 1.8 Apparent density per stream, fractions P16, P16/R30, P30/R50, Pulp C.

**Apparent density [kg/m<sup>3</sup>]**

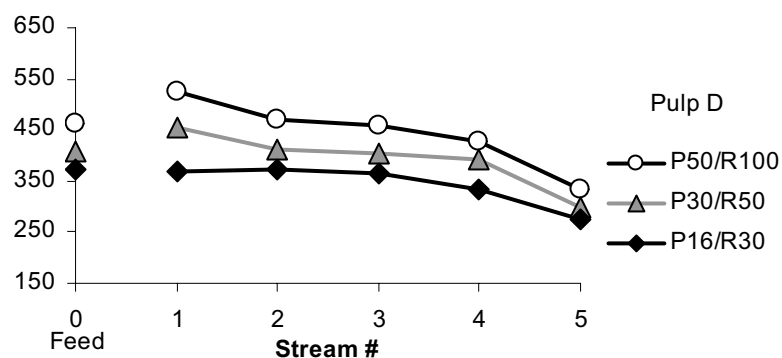


Figure 1.9. Apparent density per stream, fractions P16/R30, P30/R50, P50/R100, Pulp D.

**Apparent density [kg/m<sup>3</sup>]**

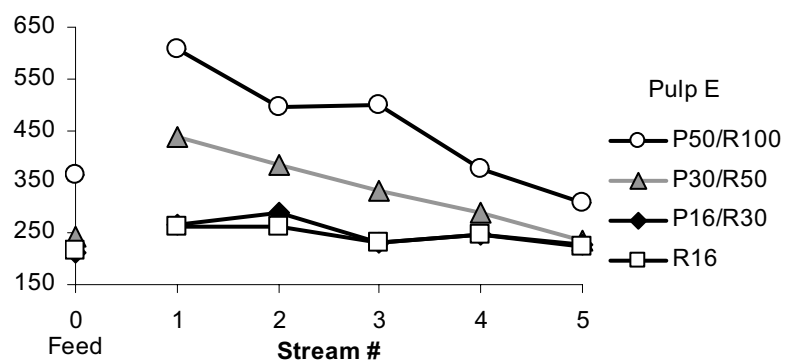


Figure 1.10. Apparent density pre stream, fractions P16, P16/R30, P30/R50, P50/R100, Pulp E.

## Appendix 2. Distributions of fiber properties from FiberLab™

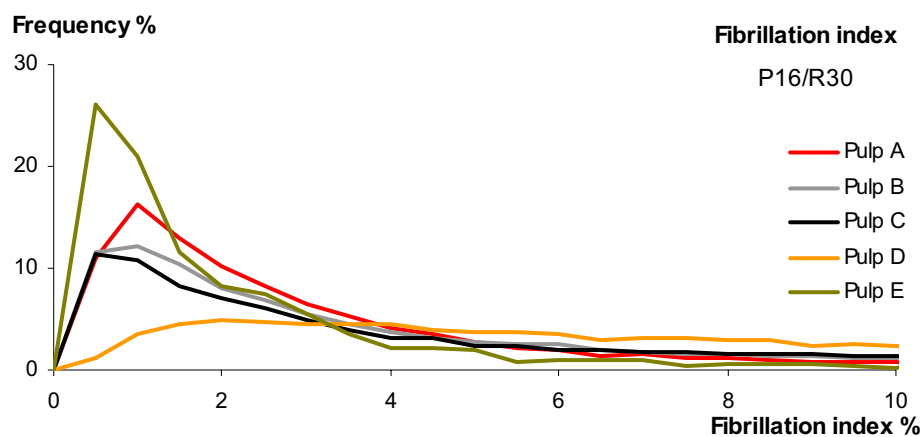


Figure 2.1. Fibrillation index distribution P16/R30 fraction.

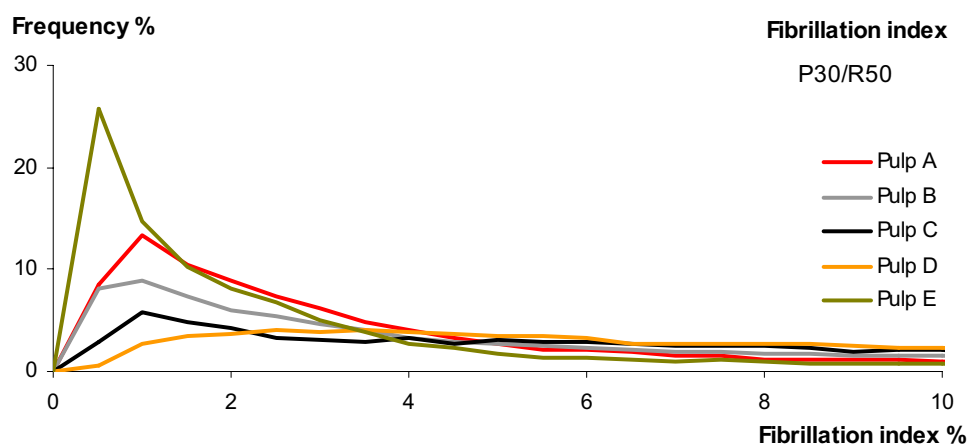


Figure 2.2. Fibrillation index distribution, P30/R50 fraction.

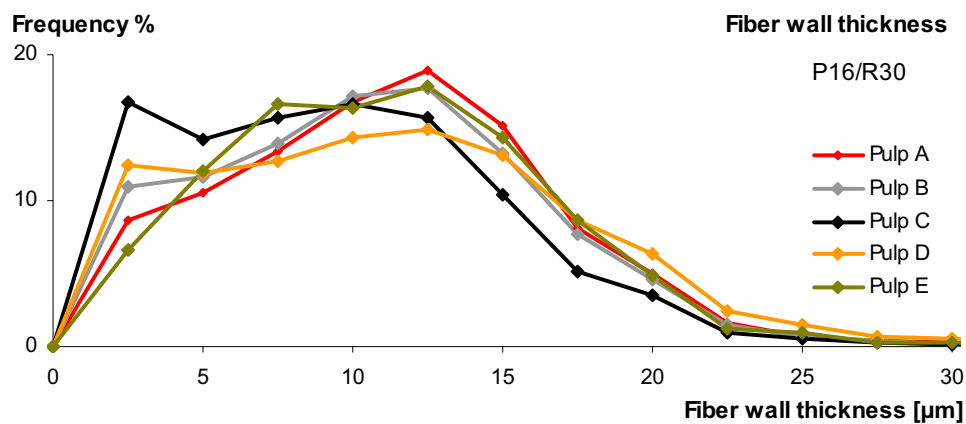


Figure 2.3. Distribution of fiber wall thickness, P16/R30 fraction.

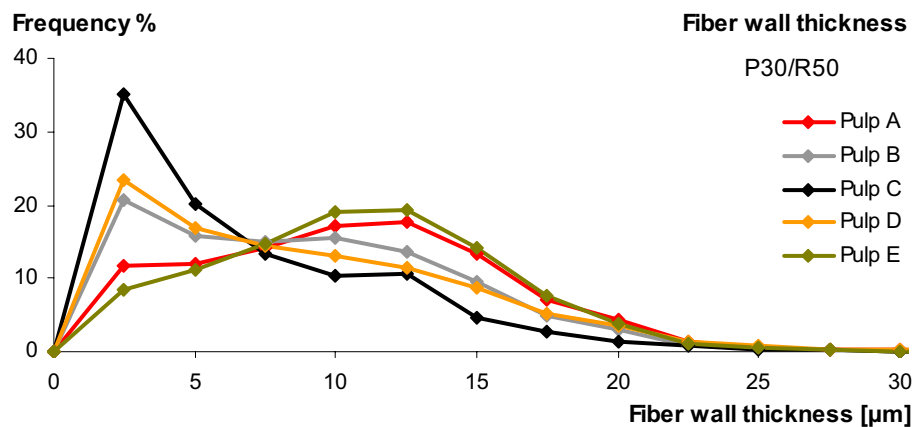


Figure 2.4. Distribution of fiber wall thickness, P30/R50 fraction.

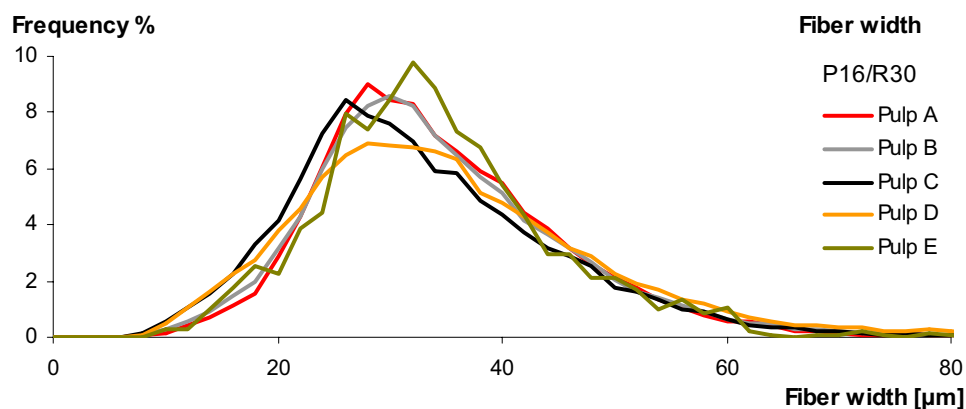


Figure 2.5. Distribution of fiber width, P16/R30 fraction.

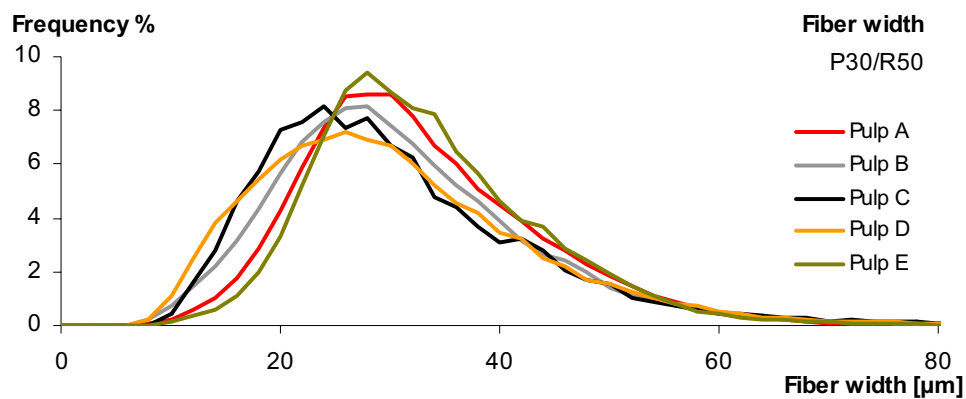


Figure 2.6. Distribution of fiber width, P16/R30 fraction.

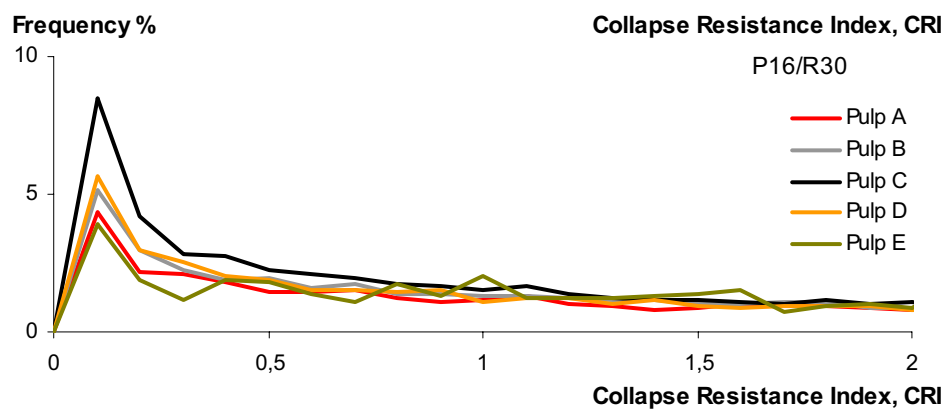


Figure 2.7. Distribution of Collapse Resistance Index, CRI, P16/R30 fraction.

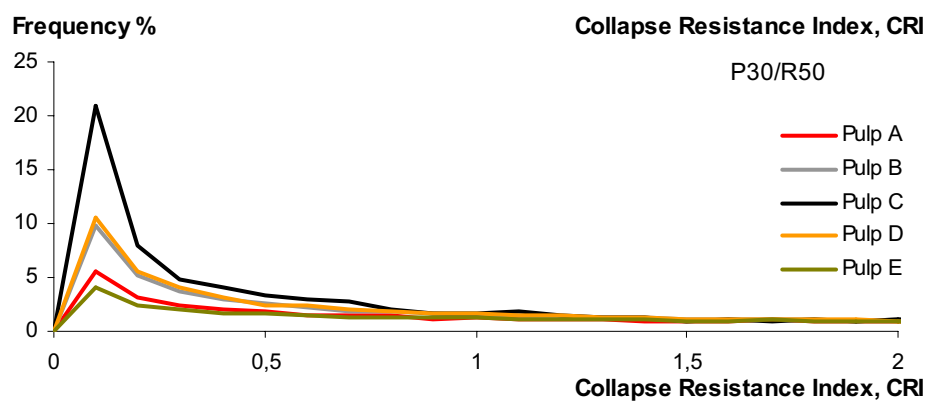


Figure 2.8. Distribution of Collapse Resistance Index, CRI, P30/R50 fraction.

### Appendix 3. BIN-distributions (Bonding Indicator)

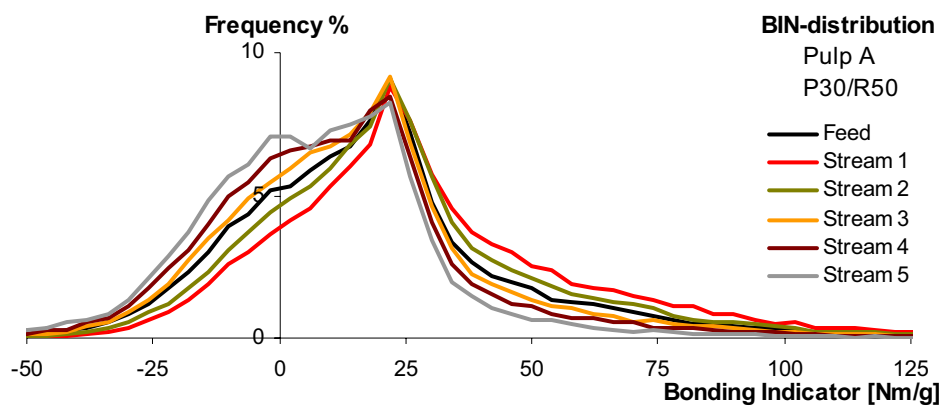


Figure 3.1. BIN-distribution Pulp A, P30/R50, Stream 1-5 and Feed.

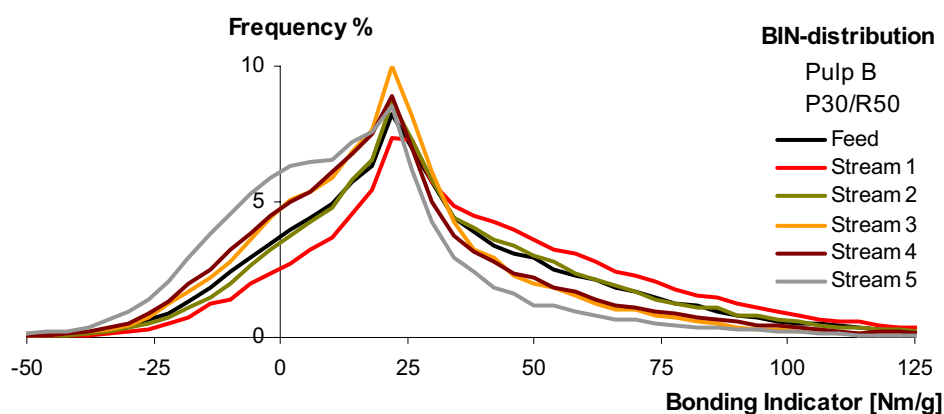


Figure 3.2. BIN-distribution Pulp B, P30/R50, Stream 1-5 and Feed.

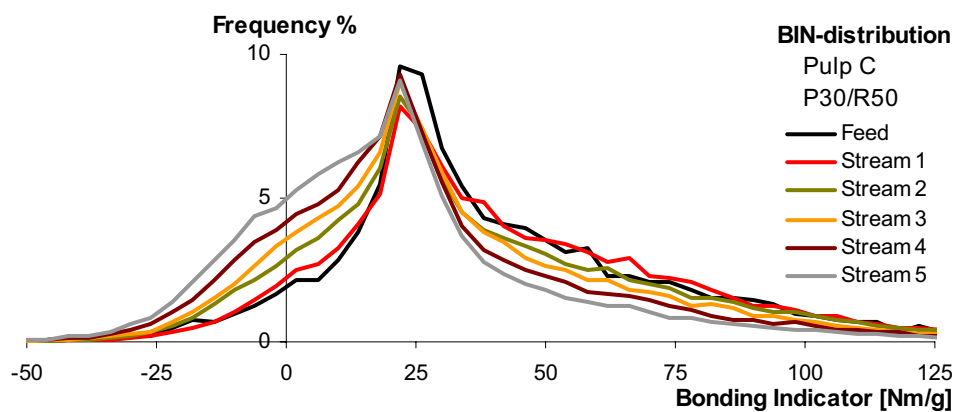


Figure 3.3. BIN-distribution Pulp C, P30/R50, Stream 1-5 and Feed.

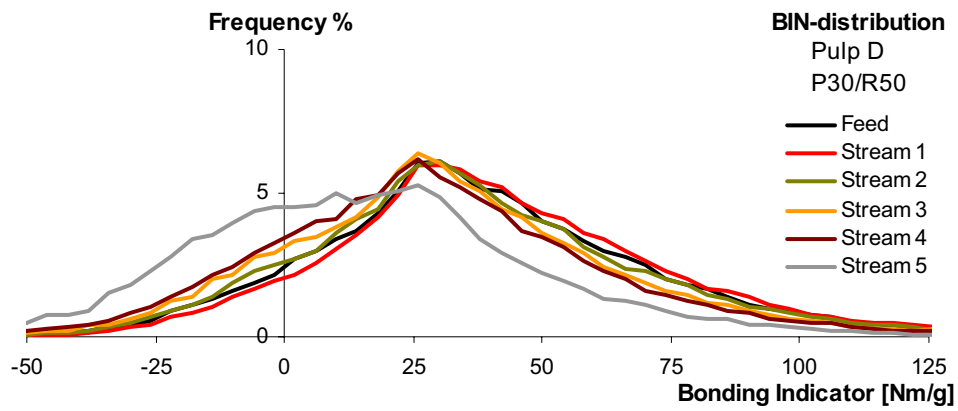


Figure 3.4. BIN-distribution Pulp D, P30/R50 Stream 1-5 and Feed.

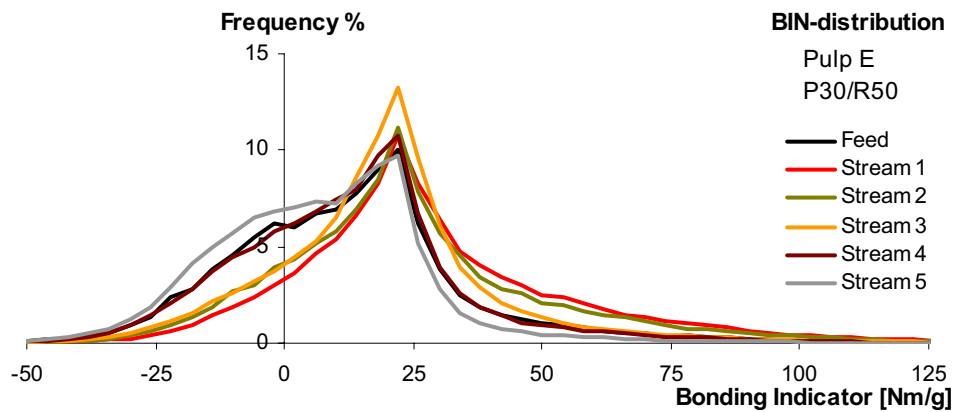


Figure 3.5. BIN-distribution Pulp E, P30/R50, Stream 1-5 and Feed.

#### BIN-distributions from whole pulps for fiber length intervals

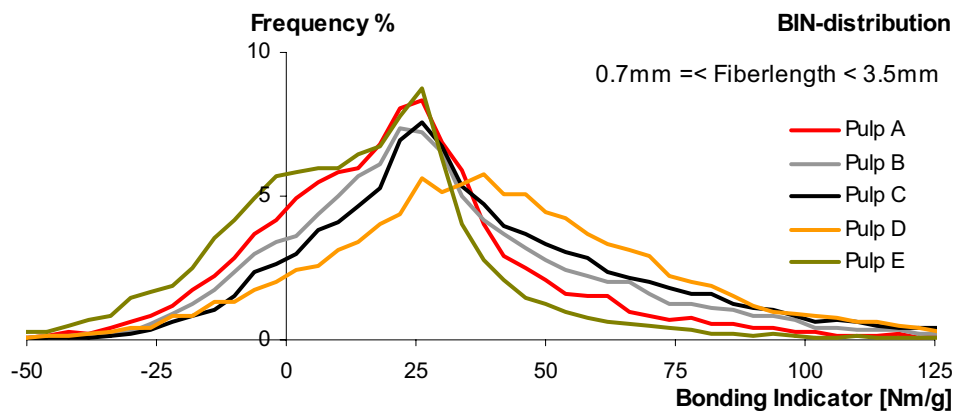


Figure 3.6. BIN-distribution for fibers from total pulp, isolated fiber length 0.7 - 3.5 mm.

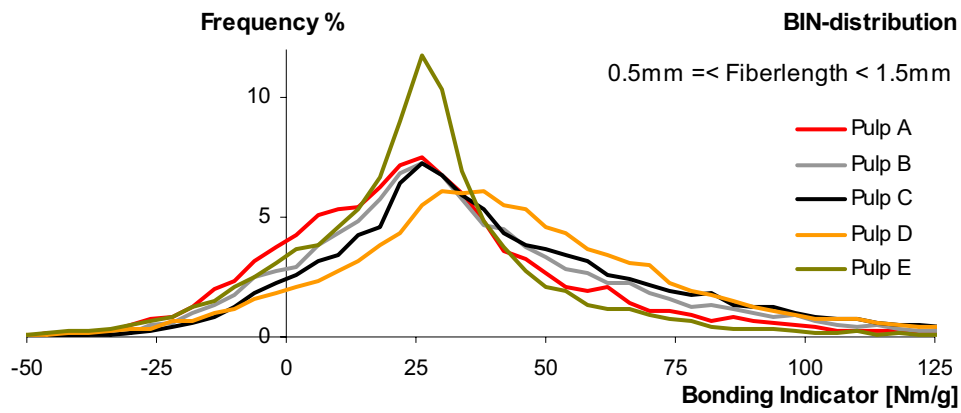


Figure 3.7. BIN-distribution for fibers from total pulp, isolated fiber length 0.5 - 1.5 mm.

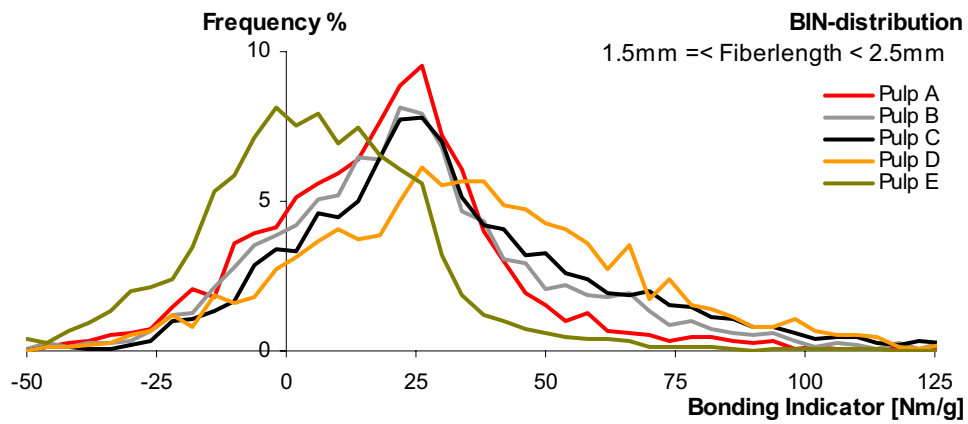


Figure 3.8. BIN-distribution for fibers of total pulp, isolated fiber length 1.5 - 2.5 mm.

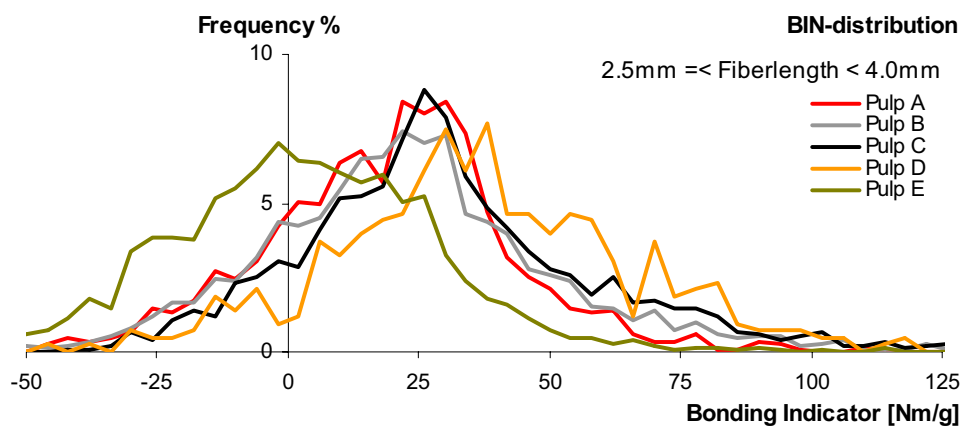


Figure 3.9. BIN-distribution for fibers of total pulp, isolated fiber length 2.5 – 4.0 mm.

### Average BIN for fiber length intervals

Table 3.1. Average BIN fiber length fraction.

Average BIN [Nm/g]	Pulp A	Pulp B	Pulp C	Pulp D	Pulp E
P16/R30	9.9	16.4	23.9	24.5	7.0
P30/R50	16.8	28.9	39.8	36.2	10.9
0.5-1.5 mm	25.4	33.3	39.8	40.5	23.1
1.5-2.5 mm	16.8	23.4	29.9	33.0	3.3
2.5-4.0 mm	17.3	21.1	28.5	34.7	0.57
0.7-2.3 mm	20.5	29.4	36.4	38.9	13.2
0.7-3.5 mm	20.5	28.8	35.7	38.8	11.5

### Amount negative BIN-fibers (low bonding fibers) for fiber length intervals

Table 3.2. Amount of negative BIN fibers. different fiber length fractions.

Amount negative BIN [%]	Pulp A	Pulp B	Pulp C	Pulp D	Pulp E
P16/R30	28.1	22.5	16.3	18.7	30.7
P30/R50	24.3	14.6	6.5	11.2	29.2
0.5-1.5 mm	15.5	11.1	7.7	8.6	13.6
1.5-2.5 mm	20.1	17.1	12.3	12.3	40.7
2.5-4.0 mm	19.4	19.5	13.0	9.8	46.0
0.7-2.3 mm	19.1	14.4	9.9	10.4	26.5
0.7-3.5 mm	18.6	14.5	9.9	10.2	28.9

Table 3.3. Amount of negative BIN fibers. P16/R30 fraction.

Amount negative BIN [%] P16/R30	Pulp A	Pulp B	Pulp C	Pulp D	Pulp E
Feed	28.1	22.5	16.3	18.7	30.7
Stream 1	21.5	17.1	15.1	16.4	22.5
Stream 2	23.9	20.0	16.2	19.0	22.2
Stream 3	28.9	22.8	18.6	21.9	28.5
Stream 4	31.0	25.1	21.0	23.5	30.2
Stream 5	34.3	29.7	24.9	33.3	34.6

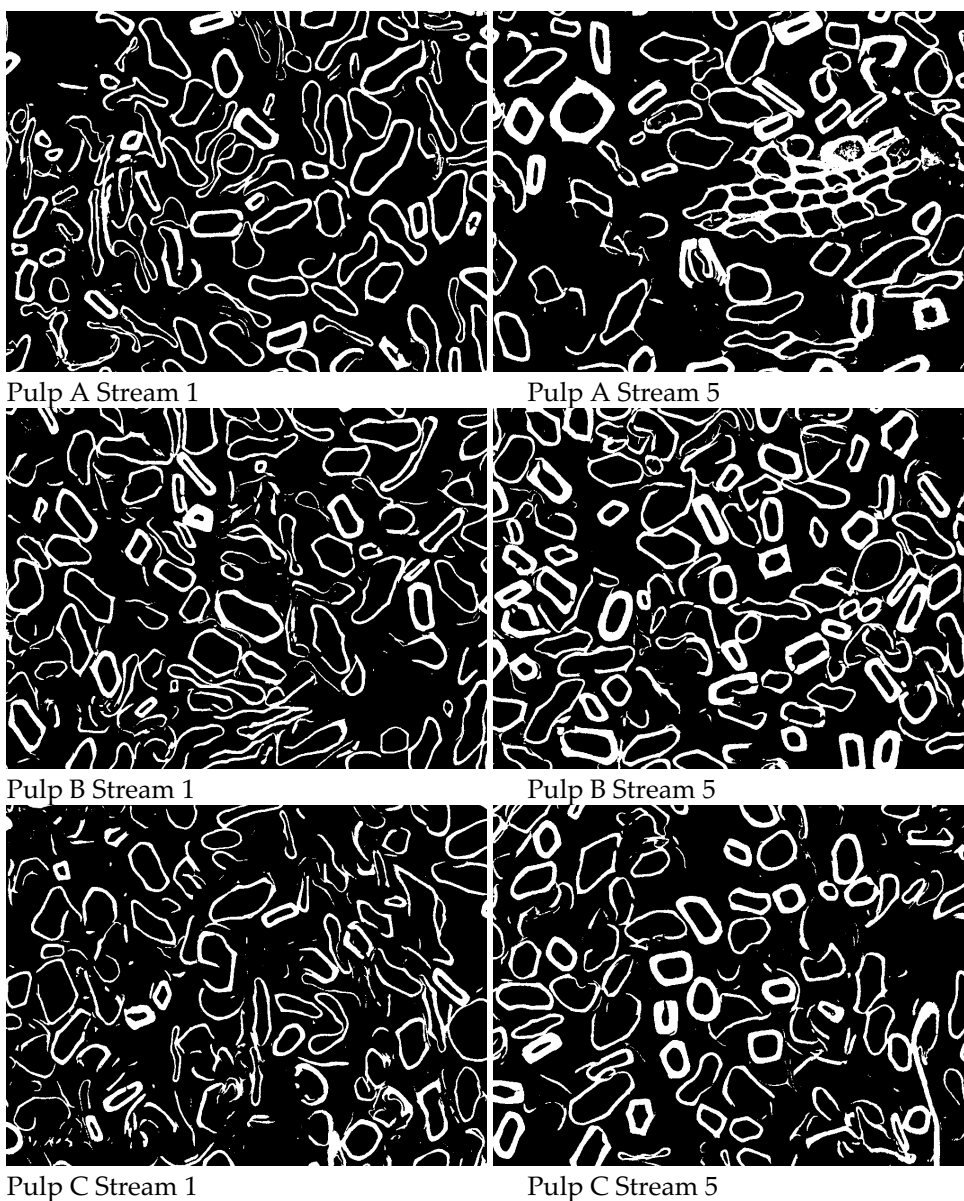
Table 3.4. Amount of negative BIN fibers. P30R50 fraction.

Amount negative BIN [%] P30/R50	Pulp A	Pulp B	Pulp C	Pulp D	Pulp E
Feed	24.3	14.6	6.5	11.2	29.2
Stream 1	14.9	9.2	6.5	9.2	11.4
Stream 2	18.9	12.8	10.1	12.5	15.3
Stream 3	26.6	18.2	12.4	15.7	16.7
Stream 4	31.6	19.8	16.6	18.3	27.6
Stream 5	37.1	28.8	21.3	33.0	36.4

## Appendix 4. SEM-images

### Cross-sectional micrographs from fiberlength fraction P16/R30

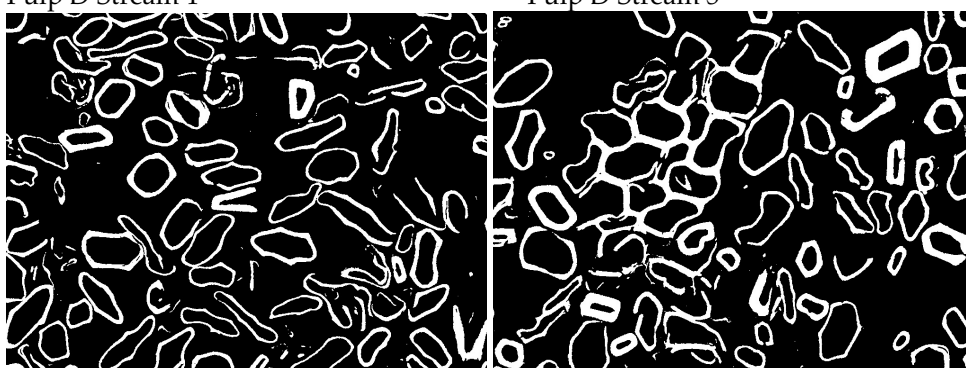
*Photos: Olle Henningsson, Örjan Sävborg, Stora Enso Research Centre Falun, Sweden*





Pulp D Stream 1

Pulp D Stream 5

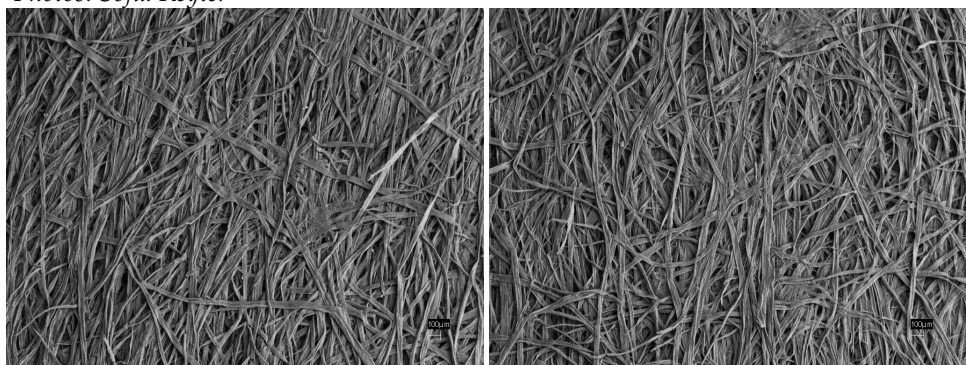


Pulp E Stream 1

Pulp E Stream 5

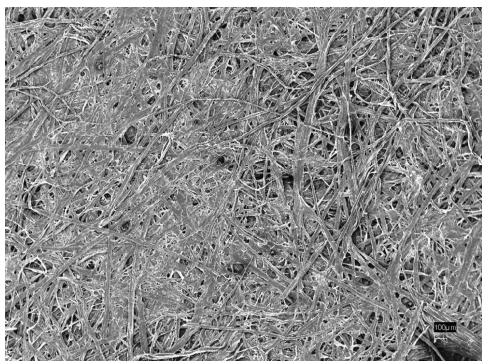
**Long fiber laboratory sheets, fiberlength fraction P16/R30.**

*Photos: Sofia Reyier*

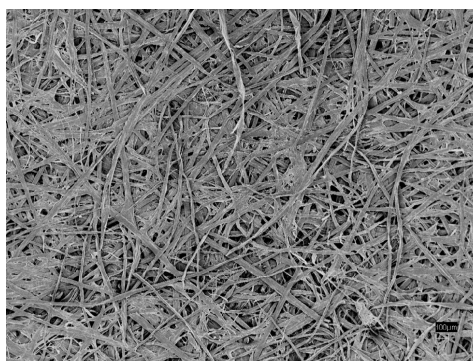


Pulp B Stream 1

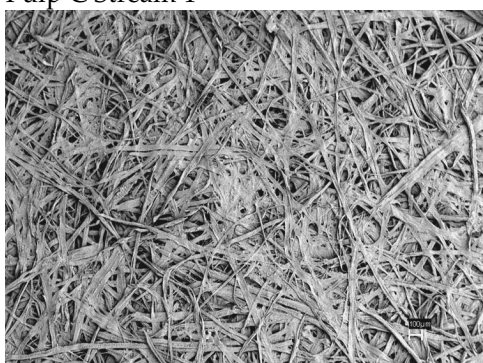
Pulp B Stream 5



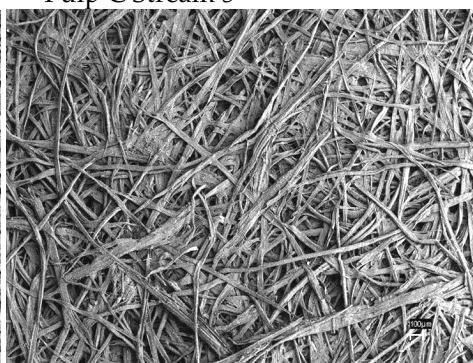
Pulp C Stream 1



Pulp C Stream 5



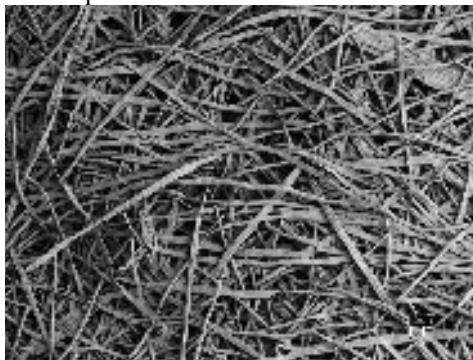
Pulp D Stream 1



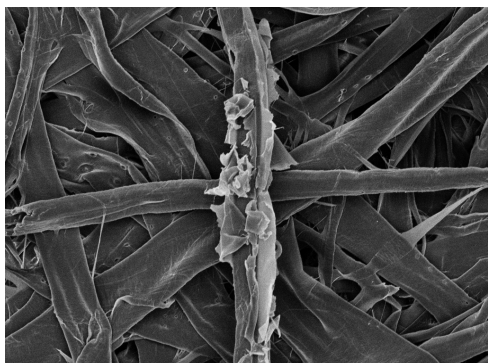
Pulp D Stream 5



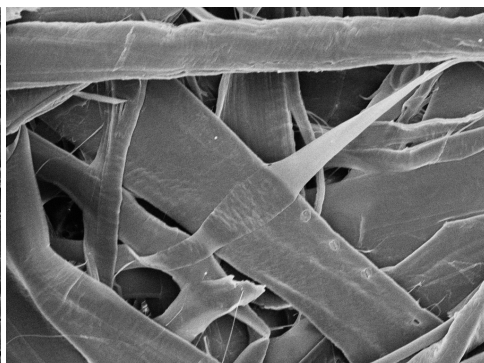
Pulp E Stream 1



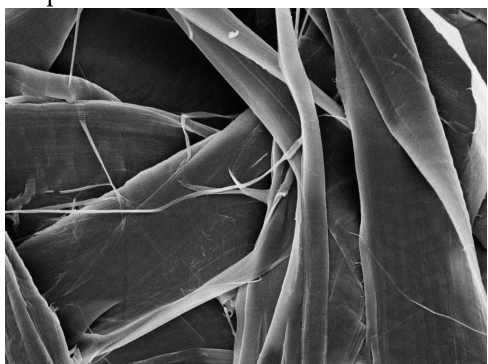
Pulp E Stream 5



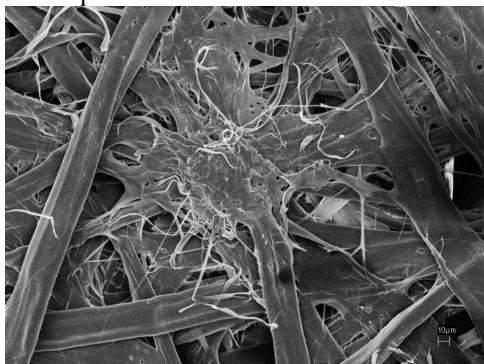
Pulp C Stream 0



Pulp C Stream 0



Pulp C Stream 1



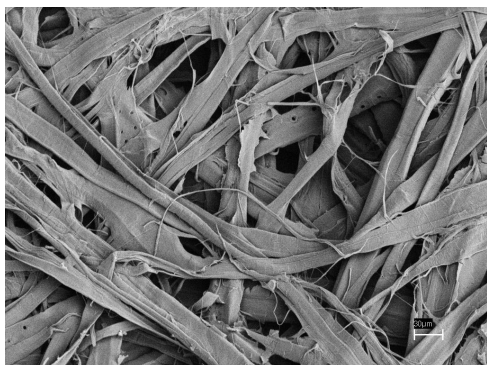
Pulp C Stream 5



Pulp D Stream 0



Pulp D Stream 1



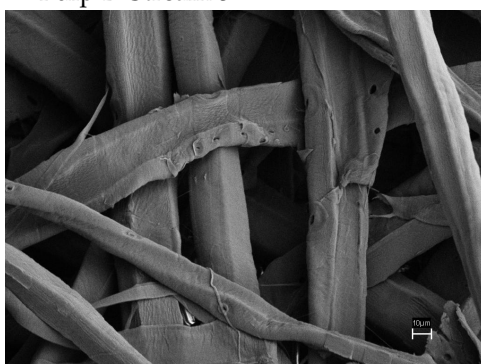
Pulp D Stream 1



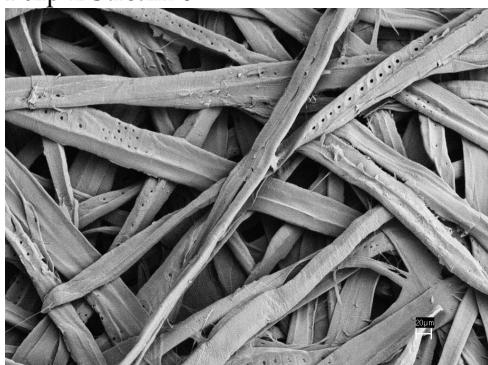
Pulp D Stream 5



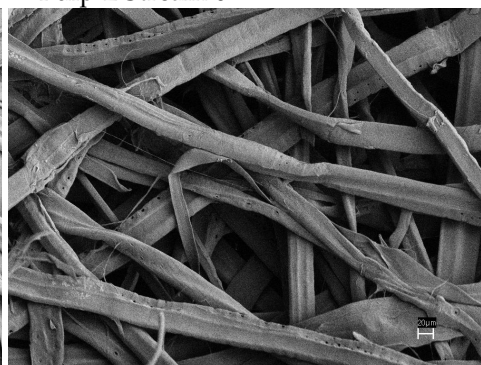
Pulp E Stream 0



Pulp E Stream 0



Pulp E Stream 1



Pulp E Stream 5